Deanship of Graduate Studies
Al-Quds University

An Advanced Deep Learning Framework for Real-Time Breast Cancer Lesion Analysis in Clinical Ultrasound

Suliman Imad Suliman Thwib

M.Sc. Thesis

Jerusalem – Palestine

1446/2025

An Advanced Deep Learning Framework for Real-Time Breast Cancer Lesion Analysis in Clinical Ultrasound

Prepared By:

Suliman Imad Suliman Thwib

Supervisor: **Prof. Radwan Qasrawi**

This Thesis submitted in partial fulfillment of requirements for the degree of Master of Computer Science

Faculty of Graduate studies—Al-Quds University

1446/2025

Al-Quds University
Deanship of Graduate Studies
Computer Science

Thesis Approval

An Advanced Deep Learning Framework for Real-Time Breast Cancer Lesion Analysis in Clinical Ultrasound

Prepared by: **Suliman Imad Suliman Thwib**

Registration No: **22212270**

Supervisor: **Prof. Radwan Qasrawi**

The master's thesis was submitted and accepted, Date: 20/05/2025.

The names and signatures of the examining committee members are as follows:

1- Head of Committee: Prof. Radwan Qasrawi Signature:

2- Internal Examiner: Dr. Nael Abu Halawa Signature: _____

3- External Examiner: Dr. Hussein Al Masri Signature: ___ Hussein AL Masri

Jerusalem – Palestine

1446/2025

Dedication

I dedicate this work to my family who stood by me throughout this journey. Your love and support gave me strength when I needed it most.

To my parents, thank you for your endless encouragement and for teaching me to work hard and never give up. Your belief in me made all the difference.

To my teachers who shared their knowledge and guided me along the way. Your wisdom and patience helped shape not just this research, but who I am as a scholar.

To my friends who offered laughter during difficult times and understanding during long absences. Your friendship made this path brighter.

This achievement belongs to all of you as much as it belongs to me.

Declaration

I certify that this thesis submitted for the degree of Master is the result of my own research, except where otherwise acknowledged, and that this study (or any part of the same) has not been submitted for a higher degree to any other university or Institution.

Signed: 

Suliman Imad Thwib

Date: 28 / 05 / 2025

Abstract

Breast cancer represents the most common malignancy among Palestinian women, accounting for 32.1% of all female cancers with a concerning 52% of cases diagnosed at advanced stages. Early detection is hindered by multiple challenges, including limited access to specialized radiologists, inadequate digital infrastructure, and socioeconomic barriers. This research develops and validates an advanced deep learning framework for real-time breast cancer lesion analysis in clinical ultrasound videos, specifically designed to address these challenges within the Palestinian healthcare context.

The research encompasses the entire analytical pipeline from contrast enhancement through detection to tracking. A comprehensive dataset of 17,903 ultrasound cases was curated from two Palestinian healthcare facilities, including 11,383 images from the Dunya Women's Cancer Center (2018-2023) and 6,520 video frames from Augusta Victoria Hospital (2024-2025). This locally representative dataset, including cases with confirmatory biopsy results, ensured the clinical relevance and cultural appropriateness of the developed system.

The framework integrates three key technical innovations. First, a systematic evaluation of contrast enhancement techniques identified Contrast-Limited Adaptive Histogram Equalization (CLAHE) with a clip limit of 1 as optimal for breast ultrasound preprocessing, achieving superior Enhancement Measure Estimation (23.670) and Peak Signal-to-Noise Ratio (24.359) with minimal computational overhead (0.536ms). Second, comprehensive comparison of You Only Look Once (YOLO) architectures established YOLOv11-L as the most effective model for lesion detection, achieving mean Average Precision of 0.93 and sensitivity of 0.88 while maintaining real-time performance (4.6ms). Transfer learning further improved performance, with the TL12 approach achieving mAP of 0.955 and sensitivity of 0.938. Third, a novel hybrid Detection-Based Tracking (DBT) approach combining Kernelized Correlation Filter (KCF) tracking with YOLO verification demonstrated superior performance for lesion tracking, achieving success rates of 0.976 for benign and 0.984 for malignant lesions when combined with CLAHE preprocessing.

Performance evaluation using ultrasound video sequences with confirmatory biopsy results validated the framework's clinical applicability. The combined pipeline maintained real-time processing capability (approximately 54 frames per second) while achieving high accuracy in lesion detection and tracking. These results demonstrate that deep learning approaches can effectively enhance breast ultrasound interpretation capabilities in resource-constrained healthcare environments.

This research represents a significant contribution to addressing breast cancer detection challenges in Palestine by providing a computationally efficient, clinically applicable framework that complements limited specialized expertise. The methodology established for developing context-specific AI systems for medical imaging offers a blueprint for similar initiatives in other resource-constrained healthcare environments. Future work should focus on implementing multiple object tracking capabilities, extending to 3D ultrasound analysis, and conducting larger multi-center clinical validation studies.

Table of Contents

List of Figures

List of Tables

Chapter One : Introduction

This chapter establishes the foundation for research on advanced deep learning approaches to breast cancer detection through ultrasound imaging in the Palestinian healthcare context. Beginning with an examination of breast cancer's prevalence and impact in Palestine, the chapter explores the unique challenges facing the Palestinian healthcare system in implementing effective screening and detection programs. The discussion progresses through an analysis of current detection methods and their limitations, culminating in a clearly defined problem statement that addresses the paradoxical situation where ultrasound has emerged as a widely available imaging modality yet remains constrained by limited specialized interpretation expertise. Building on this contextual foundation, the chapter presents the research questions, objectives, and hypotheses that guide this study, focusing on how artificial intelligence can enhance breast ultrasound interpretation while accommodating local resource constraints. The scope, limitations, and organizational structure of the thesis are then outlined, providing a comprehensive roadmap for the investigation of technological solutions tailored to the specific needs of breast cancer detection in Palestine.

1.1 Overview

Breast cancer represents a significant global health challenge, with an estimated 2.3 million new cases and over 685,000 deaths reported worldwide annually (World Health Organization, 2022). The disease burden is particularly concerning in resource-constrained regions where healthcare infrastructure and specialized medical expertise are limited, leading to delays in diagnosis and poorer outcomes (Mimi, 2015).

In the Palestinian territories, breast cancer is the most common malignancy among women, accounting for 32.1% of all female cancers and ranking as the third leading cause of cancer-related deaths in the West Bank (Palestinian Ministry of Health, 2022; Saadah et al., 2024). The disease's prevalence and impact in this region are shaped by a complex interplay of socioeconomic, political, and healthcare system factors that create unique challenges for detection and treatment. Despite its significance as a public health concern, the Palestinian healthcare system faces numerous obstacles in breast cancer screening, detection, and diagnosis, stemming from limited resources,

restricted healthcare access, and a shortage of specialized medical professionals (Giacaman et al., 2009; Hamdan & Defever, 2003).

The early detection of breast cancer is crucial for improving survival rates and treatment outcomes. Traditional screening methods include mammography, ultrasound imaging, and clinical breast examinations. While mammography remains the gold standard for breast cancer screening in many developed countries, ultrasound presents distinct advantages in resource-limited settings like Palestine. Ultrasound technology is more accessible, cost-effective, and particularly valuable for examining dense breast tissue, which is more common among younger women and those of Middle Eastern descent (Berg et al., 2008; Brem et al., 2015).

In recent years, artificial intelligence (AI) has emerged as a transformative force in medical imaging, demonstrating remarkable potential to enhance diagnostic accuracy, reduce interpretation variability, and address the shortage of specialized radiologists (Hosny et al., 2018; Y. Shen et al., 2021). Deep learning algorithms, a subset of AI techniques, have shown particular promise in analyzing medical images, including ultrasound, to detect abnormalities with performance comparable to or exceeding that of human experts (J. Z. Cheng et al., 2016; Teuwen et al., 2021). The integration of AI with ultrasound imaging could potentially democratize access to high-quality breast cancer detection by enabling less specialized healthcare providers to deliver more consistent and accurate diagnostic services, even in settings with limited resources and expertise.

This research investigates the intersection of these elements: breast cancer's prevalence in Palestine, the advantages of ultrasound imaging in resource-constrained environments, and the potential of AI to enhance diagnostic capabilities to develop technological solutions tailored to the specific healthcare challenges of the region. The subsequent sections of this chapter explore the Palestinian breast cancer landscape in greater depth, analyze current detection methods and their limitations, define the specific research problem addressed by this study, and outline the questions, objectives, and hypotheses that guide the investigation.

1.2 Breast Cancer in Palestine

Breast cancer represents the most common malignancy among Palestinian women, with incidence rates showing concerning upward trends. According to data from the Palestinian Ministry of Health, breast cancer accounts for approximately one-third of all female cancer cases in the occupied Palestinian territories (State of Palestine Palestinian Central Bureau of Statistics Palestine in Figures, 2023). Saadeh et al. reported that breast cancer ranks as the third leading cause of cancer-related deaths in the West Bank, highlighting its substantial impact on women's health (Saadah et al., 2024).

The incidence of breast cancer in Palestine has fluctuated over the years, rising from 78.9 per 100,000 women in 2014 to 83.9 per 100,000 in 2015 (Kariri et al., 2017). More recent data from 2023 shows 546 new breast cancer cases in the West Bank, with an incidence rate of 18.6 cases per 100,000 total population, making it the most common cancer diagnosis (Palestinian Ministry of Health, 2022). By comparison, colorectal cancer ranked second with 468 new cases (15.9 per 100,000 population), followed by bronchus and lung cancer in third place (316 cases, 10.8 per 100,000 population). This persistent prevalence is particularly concerning given the younger age

profile of Palestinian breast cancer patients compared to Western populations. Research indicates that Arab women tend to develop breast cancer at younger ages than their Western counterparts (Najjar & Easson, 2010). According to (Najjar & Easson, 2010), Arab women are diagnosed with breast cancer at an average age of 48 years (SD 2.8), approximately ten years earlier than women in Western countries. Research has also revealed notable differences between ethnic groups within the region, with Arab Palestinian women receiving diagnoses at a mean age of 51.5 years, while Jewish women are diagnosed at a mean age of 55.9 years (Nissan et al., 2004). These age differences significantly impact screening strategies, as younger women typically have denser breast tissue, which reduces the effectiveness of mammography as a primary screening tool. Breast cancer in Palestine is frequently diagnosed at advanced stages, resulting in poorer prognosis and increased treatment complexity. According to a 2024 study by Shaymaa AlWaheidi on breast cancer in women in Gaza, the stage distribution at diagnosis reveals concerning patterns. The data indicates that only 6% of breast cancer cases are diagnosed at Stage I, while 35% are detected at Stage II, 33% at Stage III, and 19% at Stage IV (AlWaheidi et al., 2024). This represents a combined 52% of cases detected at advanced stages. This stage distribution indicates significant challenges in early detection efforts compared to developed countries where advanced-stage diagnoses typically account for 30-35% of cases. The low percentage of Stage I diagnoses suggests substantial limitations stem from various factors, including limited awareness, cultural barriers, cost constraints, and restricted mobility due to political instability (AL-Tell, 2019; Daoud et al., 2018).

The economic burden of breast cancer is substantial, straining already resource-limited healthcare systems worldwide. According to a systematic review by Li Sun et al. on global treatment costs of breast cancer by stage, the weighted means of cumulative treatment costs were $29,724 at stage I, $39,322 at stage II, $57,827 at stage III, and $62,108 at stage IV in 2015 US dollars (Sun et al., 2018). On average, costs at stage II, III and IV were 32%, 95%, and 109% higher than costs at stage I. This dramatic escalation in treatment costs with advancing disease stages underscores the economic importance of early detection strategies, particularly in resource-constrained settings like Palestine.

Beyond direct healthcare costs, breast cancer imposes considerable societal and economic burdens. A study by Daoud et al. documented that breast cancer patients in Palestine experience an average of 16 weeks of productivity loss, with ripple effects on household economics and family welfare (Daoud et al., 2018). These findings emphasize the multidimensional impact of breast cancer in Palestinian society and the importance of effective early detection strategies.

The Palestinian healthcare system operates within a complex political and economic landscape, characterized by fragmentation, resource limitations, and persistent access challenges. The system comprises multiple provider sectors, including the Ministry of Health, UNRWA (United Nations Relief and Works Agency for Palestine Refugees), non-governmental organizations, and private providers, often with overlapping responsibilities and inconsistent coordination (Mimi, 2015; World Health Organization. Regional Office for the Eastern Mediterranean, 2023).

Healthcare financing in Palestine faces chronic constraints, with public health expenditure amounting to approximately 11% of the total government budget, which is significantly lower than regional and international benchmarks for healthcare systems with similar disease burdens (Falah

et al., 2020). This limited financing translates to inadequate infrastructure, outdated equipment, and insufficient human resources for comprehensive health services, including breast cancer detection programs.

Geographic and political barriers severely impact healthcare access in Palestine. The separation wall, military checkpoints, and restricted mobility significantly impede patient movement, particularly for Gaza residents seeking specialized care (Khatib et al., 2017). Al-Tell et al. documented that 48.5% of Palestinian women reported missing at least one scheduled mammography appointment due to movement restrictions (AL-Tell, 2019). These barriers disproportionately affect rural and marginalized communities, exacerbating healthcare disparities.

Human resource constraints represent another significant challenge. The Palestinian healthcare system faces critical shortages of specialized professionals, including radiologists, oncologists, and trained technicians essential for breast cancer detection and treatment. Saadeh et al. emphasized the "lack of skilled experts able to accurately interpret mammograms" as a major challenge (Saadah et al., 2024).

The healthcare workforce situation is further complicated by limited training opportunities, professional migration, and uneven distribution of healthcare facilities. As indicated in the annual health report, there is significant variation in primary healthcare center distribution across governorates, with Hebron having the highest concentration (128 centers) in the West Bank, while other areas like Tubas and Jericho & Al Aghwar have only 12 centers each. Similarly, in Gaza Strip, Deir Al Balah (15) and Gaza (14) governorates have the highest number of centers, while Rafah has only 4. Additionally, the report shows specialized services are unevenly distributed, with mammography provided in only 14 clinics and X-ray services in 16 centers in the West Bank, contributing to expertise gaps in critical healthcare domains (Palestinian Ministry of Health, 2022).

Digital health infrastructure in Palestine shows uneven development, affecting the potential for technological interventions like AI-based systems. While approximately 64% of district and tertiary hospitals maintain electronic health records, smaller facilities and primary care centers often rely on paper-based systems (Mimi, 2015). Mimi (2015) also reported significant disparities in technical infrastructure, with only a small fraction of healthcare facilities having reliable high-speed internet connections and 70.5% maintaining continuous electricity supply (Mimi, 2015).

Despite these challenges, several promising healthcare initiatives have emerged in recent years. The Palestinian National Cancer Registry, established in 2018, has improved data collection on cancer incidence and outcomes (Yarney et al., 2020). As illustrated in the UNFPA breast cancer report in Palestine, some NGOs also run mobile mammography clinics that outreach rural areas. These initiatives are crucial considering that annually around 180,000 Palestinian women should undergo mammography screening (Juan Jubran, 2018).

1.3 Detection Methods and Challenges

Clinical breast examination (CBE) and breast self-examination (BSE) represent essential components of breast cancer detection in Palestine, particularly in areas with limited access to imaging services. These methods are promoted through community health programs and primary

healthcare initiatives (UNRWA, 2022). However, adoption of regular breast self-examination (BSE) remains suboptimal. Research conducted at Beit Jala Governmental Hospital in 2016 revealed that 59% of breast cancer patients didn't know how to perform BSE (Juan Jubran, 2018).

Mammography serves as the primary screening tool for breast cancer in Palestine, with most diagnostic centers located in major cities like Ramallah, Nablus, and Gaza City (Palestinian Ministry of Health, 2022). The Palestinian Ministry of Health has established several mammography units, though their distribution is uneven and favors urban areas (Palestinian Ministry of Health, 2022).

The utilization of mammography screening in Palestine remains suboptimal. While in Israel, screening for breast cancer is common, with 70 percent of women aged 50-69 receiving mammogram screenings, rates in the occupied Palestinian territory are very low. Studies of Palestinian women from the West Bank found that over 60 percent of women over the age of 50 have never attended a mammography session (World Health Organization, 2022). This low utilization stems from various factors, including limited awareness, cultural barriers, cost constraints, and restricted mobility due to political instability (AL-Tell, 2019; Daoud et al., 2018). Almuhtaseb et al. identified specific sociocultural barriers, including modesty concerns, fear of diagnosis, and family dynamics that influence women's decisions to seek mammographic screening (Almuhtaseb & Alby, 2021).

Quality and consistency of mammography services present additional challenges. For example, image interpretation delays are common, with patients waiting an average of 6 days to receive their results. While about 69% of organizations provide test results in less than 6 days, 31% take more than 7 days, with some facilities requiring 10 to 14 days. These delays not only increase anxiety among patients but also potentially impact timely treatment initiation for suspicious findings (Juan Jubran, 2018).

The shortage of specialized breast radiologists significantly affects mammography interpretation quality. Saadeh et al. highlighted the "challenge in the lack of skilled experts able to accurately interpret mammograms" as a significant limitation (Saadah et al., 2024). This expertise gap leads to interpretation variability and potential diagnostic errors.

Ultrasound imaging has emerged as an increasingly important modality for breast cancer detection in Palestine. Compared to mammography, ultrasound equipment is more widely available, with units present in most district hospitals and many primary healthcare centers (Juan Jubran, 2018). The affordability, portability, and absence of radiation exposure make ultrasound particularly suitable for the resource-constrained Palestinian healthcare system.

Ultrasound proves especially valuable for examining dense breast tissue, which is more common among younger women and those of Middle Eastern descent. According to the annual health report (2023), ultrasound detected 31.8% more breast abnormalities than mammography alone in Palestinian women under 50 years of age (Palestinian Ministry of Health, 2022). This finding is particularly relevant given the younger age profile of breast cancer patients in Palestine.

In clinical practice, ultrasound serves multiple roles in the Palestinian breast cancer detection pathway. For symptomatic women, it often represents the initial imaging modality due to greater accessibility compared to mammography. For screening purposes, ultrasound frequently complements mammography, particularly for women with dense breast tissue or those with inconclusive mammographic findings (Juan Jubran, 2018; Palestinian Ministry of Health, 2022).

However, ultrasound interpretation remains highly operator-dependent, requiring considerable expertise for accurate diagnosis. Hong et al. noted significant variation in diagnostic accuracy among different radiologists interpreting breast ultrasound images, with mean accuracy of 73.5% (Hong et al., 2025). This variability highlights the potential benefit of standardized interpretation approaches, potentially through AI assistance.

Training in breast ultrasound techniques presents another challenge. According to UNFPA, many radiologists in Palestine lack specialized training in breast ultrasound interpretation (Juan Jubran, 2018). This significant training gap contributes to the variability in examination quality and diagnostic accuracy.

The integration of advanced breast cancer detection technologies in Palestine continues to be at an early developmental phase. Magnetic resonance imaging (MRI) capabilities for breast cancer assessment remain limited to a select few specialized medical centers across the region. Due to significant cost constraints and resource limitations, these sophisticated imaging services are typically reserved exclusively for patients categorized as high-risk cases or those requiring specialized diagnostic evaluation. This restricted availability of cutting-edge detection methods creates substantial disparities in comprehensive care, particularly affecting patients in rural or underserved areas who face additional barriers to accessing these specialized diagnostic services. (Falah et al., 2020; Juan Jubran, 2018; Mimi, 2015).

Community-based screening initiatives have also emerged as an important approach to improving breast cancer detection in Palestinian communities with limited healthcare access. Mobile screening units equipped with ultrasound and staffed by trained healthcare workers have reached underserved populations in rural areas and refugee camps (Juan Jubran, 2018). These initiatives demonstrate the potential of innovative delivery models to overcome access barriers inherent in the fragmented Palestinian healthcare system.

Several key limitations affect breast cancer detection in Palestine. The fragmented nature of the healthcare system complicates coordinated detection efforts, with Jubran et al. describing a complex landscape divided between multiple providers with overlapping responsibilities and inefficient resource allocation (Juan Jubran, 2018). This fragmentation impedes the establishment of systematic screening programs and referral pathways necessary for effective breast cancer detection.

Infrastructure deficiencies significantly impact breast cancer detection services. Inconsistent electricity supply affects Palestinian healthcare facilities, particularly in Gaza where power outages average 12 hours daily (Dyer, 2008). These interruptions disrupt the operation of imaging equipment and compromise service reliability. Similarly, inadequate physical infrastructure limits

the expansion of detection services, with many facilities lacking dedicated spaces for women's health services, including breast imaging.

Digital infrastructure limitations in Palestine severely restrict the adoption of electronic health records, teleradiology, and AI-based systems in healthcare. The lack of standardized data management frameworks prevents effective collection and analysis of breast imaging data, a critical requirement for both quality improvement initiatives and the development of advanced AI algorithms. These challenges are compounded by resource constraints and ongoing political instability, further hindering the Palestinian healthcare system's digital transformation efforts (AL-Tell, 2019).

Other challenges hinder breast cancer detection in Palestine, including inadequate equipment maintenance affecting diagnostic accuracy, sociocultural factors like modesty concerns and fatalistic attitudes toward cancer, limited health awareness regarding risk factors and warning signs, and economic barriers where associated costs create financial burdens for accessing screening services (Daoud et al., 2018; Giacaman et al., 2009).

These multifaceted challenges underscore the complex landscape of breast cancer detection in Palestine and highlight the need for innovative approaches that address both technological and socio-contextual barriers to effective early detection.

1.4 Problem Statement

H The analysis of breast cancer detection challenges in Palestine reveals a critical paradox: while ultrasound has emerged as the most accessible and appropriate imaging modality for the Palestinian population, its effectiveness is severely constrained by the scarcity of specialized interpretation expertise (Juan Jubran, 2018; Palestinian Ministry of Health, 2022). This expertise gap creates a fundamental bottleneck that directly impacts diagnostic accuracy and timeliness, particularly concerning given the younger age profile of breast cancer patients in Palestine and the higher prevalence of dense breast tissue that complicates diagnosis.

The fragmented healthcare system further compounds these challenges through limited digital infrastructure that restricts the adoption of teleradiology, electronic health records, or AI-based tools (AL-Tell, 2019). This technological constraint prevents the Palestinian healthcare system from leveraging innovations that could compensate for human resource limitations and standardize interpretation quality across geographically dispersed facilities.

These circumstances create an urgent need for technological solutions that can: (1) function within existing infrastructure constraints; (2) reduce dependence on scarce specialized expertise; (3) provide consistent interpretation quality regardless of location; and (4) accommodate socioeconomic realities limiting healthcare access.

Computer-aided diagnosis systems leveraging artificial intelligence for breast ultrasound interpretation offer a promising approach to address these challenges (Ahn et al., 2023). By providing automated analysis of ultrasound images, such systems could serve as decision support tools where specialized radiologists are unavailable, potentially standardizing interpretation

quality, reducing diagnostic delays, and operating effectively in resource-constrained environments.

This research aims to develop and validate an automated breast ultrasound video interpretation framework specifically designed for the Palestinian healthcare context. Using object detection and tracking algorithms, the proposed system seeks to enhance diagnostic capabilities within existing resource constraints, amplifying rather than replacing human expertise to improve early detection rates in a population where timely diagnosis is particularly critical.

1.5 Research Questions

This research aims to address the following key questions related to automated breast ultrasound interpretation in the Palestinian healthcare context:

1. How can object detection and tracking algorithms be effectively integrated to identify, classify, and monitor suspicious lesions in breast ultrasound videos with accuracy comparable to expert radiologists while maintaining real-time performance?
2. What preprocessing and optimization techniques can enhance the performance of automated detection systems when applied to breast ultrasound images obtained from varying equipment quality typical in Palestinian healthcare facilities?
3. To what extent can an automated breast ultrasound interpretation framework provide reliable decision support for healthcare providers with limited specialized training, compensating for the shortage of breast radiologists in Palestine while maintaining consistent performance across diverse imaging conditions?

1.6 Research Objectives

Based on the identified problem and research questions, this study aims to achieve the following objectives:

1. To develop and curate a comprehensive dataset of breast ultrasound images and videos from Palestinian healthcare facilities, ensuring proper ethical protocols, de-identification, and diverse representation of normal tissue, benign lesions, and malignant findings.
2. To investigate and implement optimal preprocessing techniques and YOLO-based detection models for breast ultrasound images, comparing multiple architectures (YOLOv5, YOLOv8, YOLOv11) to achieve high sensitivity and specificity while maintaining computational efficiency suitable for resource-constrained environments.
3. To develop and evaluate a hybrid detection-tracking framework that combines efficient tracking algorithms with detection-based recovery mechanisms, assessing performance through quantitative metrics and clinical validation on cases with confirmatory biopsy results.

4. To assess the framework's potential as a decision support tool for healthcare providers in the Palestinian context, focusing on its ability to function within technological constraints, improve diagnostic consistency, and reduce interpretation variability across varying imaging conditions.

1.7 Research Hypotheses

Based on the identified research questions and objectives, this study proposes the following hypotheses. Enhanced preprocessing techniques, particularly Contrast-Limited Adaptive Histogram Equalization (CLAHE), combined with advanced YOLO architectures (YOLOv11) will significantly improve lesion detection accuracy in breast ultrasound images compared to standard preprocessing methods and earlier YOLO variants. This improvement is expected to result from the synergistic effect of optimized image enhancement and more sophisticated detection algorithms.

A hybrid Detection-Based Tracking (DBT) approach that combines efficient tracking algorithms with periodic YOLO-based verification will achieve superior performance in maintaining lesion identity across ultrasound video sequences compared to standalone tracking methods, while maintaining real-time processing capabilities. This approach addresses the limitations of traditional tracking by providing robust recovery mechanisms when tracking confidence decreases.

The proposed automated breast ultrasound interpretation framework will demonstrate diagnostic performance approaching that of experienced radiologists on cases with confirmatory biopsy results, while maintaining consistent accuracy across the varying imaging conditions typical in Palestinian healthcare settings. This hypothesis reflects the potential of the integrated system to function effectively as a decision support tool in resource-constrained environments.

1.8 Research Scope and Limitations

This research develops and validates an automated framework for breast ultrasound video interpretation within the Palestinian healthcare context. The study encompasses the complete pipeline from data acquisition through preprocessing, detection, tracking, and evaluation, emphasizing methods that balance performance with computational efficiency. The scope specifically targets 2D B-mode ultrasound, the most available technology in Palestinian facilities, focusing on distinguishing between normal tissue, benign lesions, and malignant findings.

The investigation is limited to YOLO family algorithms (YOLOv5, YOLOv8, YOLOv11) for detection and seven traditional single object tracking approaches plus two hybrid methods for tracking evaluation. The dataset comprises over 17,000 ultrasound cases from two Palestinian healthcare facilities (2018-2025), representing a substantial but geographically constrained sample that may limit generalizability to different regions or equipment types.

Technical implementation focuses on software development using Python without extending to hardware optimization or mobile applications. While confirmatory biopsy results validate system

performance on a subset of cases, the research does not include formal clinical trials evaluating diagnostic outcomes or changes in clinical decision-making, which would require separate prospective studies beyond this scope.

1.9 Thesis Structure

This thesis comprises six chapters that systematically address the research questions and present comprehensive findings. Chapter One establishes the research foundation by introducing breast cancer detection challenges in Palestine, presenting the problem statement, research questions, objectives, and hypotheses. Chapter Two provides essential technical background on contrast enhancement, object detection algorithms, and tracking methodologies, serving as a knowledge bridge between problem context and proposed solutions.

Chapter Three comprehensively reviews relevant literature across AI in medical imaging, breast ultrasound applications, enhancement techniques, and tracking methodologies, identifying research gaps and positioning this study within the broader scientific context. Chapter Four details the systematic methodology from data curation through preprocessing, machine learning, and evaluation, including ethical considerations and implementation specifics to ensure reproducibility.

Chapter Five presents comprehensive evaluation results structured into contrast enhancement, lesion detection, and lesion tracking sections, providing detailed performance metrics, comparative analyses, and statistical evidence for hypothesis testing. Chapter Six interprets findings in relation to original objectives, explores implications for clinical practice and healthcare policy, analyzes study limitations, and recommends future research directions, concluding with key contributions for advancing breast cancer detection in resource-constrained environments.

Chapter Two : Background

This chapter establishes the theoretical foundations and technical background essential for understanding the proposed framework for real-time breast cancer lesion analysis in ultrasound videos. It explores three fundamental components that underpin the research: contrast enhancement techniques for improving ultrasound image quality, object detection methodologies with emphasis on the YOLO family of algorithms, and object tracking approaches for maintaining lesion identity across video frames. By examining these interconnected domains, the chapter builds a comprehensive technical foundation that contextualizes the research contributions while providing the necessary background for readers from diverse disciplines. Each section progresses from fundamental concepts to state-of-the-art approaches, with particular attention to techniques that balance performance with computational efficiency, a critical consideration for developing systems suitable for resource-constrained healthcare environments. The detailed exploration of these technical areas provides the groundwork for the methodology and experimental design described in subsequent chapters.

2.1 Contrast Enhancement

Contrast enhancement is a critical image processing technique that aims to improve the visual quality of images by increasing the distinction between different regions or features. This process is especially vital in medical imaging, where the clarity of anatomical structures or pathological findings can significantly influence diagnostic accuracy. In this section, we will explore various contrast enhancement techniques, focusing on their applications in medical imaging, with a particular emphasis on ultrasound imaging. Ultrasound images often suffer from low contrast due to noise, speckle, and signal attenuation, making contrast enhancement an essential preprocessing step. The section begins with an overview of contrast enhancement, its importance in medical imaging, and its specific role in improving ultrasound image quality. Subsequent subsections will delve into specific techniques, including histogram equalization, adaptive histogram equalization (AHE), adaptive gamma correction with weighting distribution (AGCWD), and contrast-limited adaptive histogram equalization (CLAHE). Each method will be discussed in detail, highlighting its advantages, limitations, and suitability for medical imaging applications.

2.1.1 Overview

Contrast enhancement is a process that improves the visibility of details in an image by increasing the difference between the brightest and darkest regions. This technique is widely used in various fields, including photography, remote sensing, and medical imaging. In medical imaging, contrast enhancement plays a crucial role in improving the interpretability of images, enabling clinicians to detect subtle abnormalities and make accurate diagnoses. Medical images, such as X-rays, computed tomography (CT), magnetic resonance imaging (MRI), and ultrasound, often exhibit low contrast due to factors such as noise, artifacts, and limitations in imaging hardware. Enhancing the contrast in these images can significantly improve their diagnostic value.

In ultrasound imaging, contrast enhancement is particularly important due to the inherent challenges associated with this modality. Ultrasound images are often affected by speckle noise, signal dropout, and low contrast between soft tissues, which can obscure critical anatomical or pathological details. Speckle noise, a granular pattern caused by the interference of ultrasound waves, reduces the effective contrast and makes it difficult to distinguish between tissues with similar acoustic properties (Burckhardt, 1978). Contrast enhancement techniques can mitigate these issues by amplifying the differences in pixel intensities, thereby improving the visibility of structures such as tumors, blood vessels, and organ boundaries (Noble & Boukerroui, 2006).

The role of contrast enhancement in ultrasound imaging extends beyond improving visual quality. It also facilitates automated image analysis tasks, such as segmentation and feature extraction, which are essential for computer-aided diagnosis (CAD) systems. For example, enhanced contrast can improve the accuracy of tumor boundary detection or the identification of subtle lesions that might otherwise be missed (Dutt & Greenleaf, 1996). Research has shown that effective contrast enhancement can lead to better diagnostic outcomes and reduce the likelihood of misinterpretation in clinical settings (Mallat, 1989). For instance, studies have demonstrated that contrast-enhanced ultrasound (CEUS) can improve the detection of liver lesions and provide better characterization of tumor vascularity compared to conventional ultrasound (Dietrich et al., 2020).

Several contrast enhancement techniques have been developed and applied to medical imaging, each with its own strengths and limitations. These methods can be broadly categorized into global and local approaches. Global techniques, such as histogram equalization, adjust the intensity values of the entire image uniformly. While these methods are computationally efficient, they may not always produce optimal results for medical images, which often contain regions of interest with varying contrast levels (Gonzalez & Woods, 2018). Local techniques, such as adaptive histogram equalization (AHE) and contrast-limited adaptive histogram equalization (CLAHE), address this limitation by enhancing contrast in localized regions, thereby preserving fine details and improving overall image quality (Pizer et al., 1987).

The choice of contrast enhancement technique depends on the specific characteristics of the image and the intended application. For ultrasound imaging, techniques that balance noise suppression and detail preservation are particularly valuable. For instance, CLAHE has been widely adopted in medical imaging due to its ability to enhance contrast while limiting the amplification of noise (Zuiderveld, 1994). Similarly, adaptive gamma correction with weighting distribution (AGCWD) has shown promise in improving the contrast of ultrasound images by dynamically adjusting the gamma correction based on the image's intensity distribution (Rahman et al., 2016). Recent studies

have also explored the use of deep learning-based methods for contrast enhancement, which leverage neural networks to learn optimal enhancement strategies from large datasets (Suganyadevi et al., 2021).

2.1.2 Histogram Equalization (HE)

Histogram equalization (HE) is one of the most widely used contrast enhancement techniques in image processing. It is a global method that redistributes the intensity values of an image to achieve a uniform distribution of pixel intensities across the entire dynamic range. By doing so, HE enhances the contrast of the image, making details more visible and improving overall visual quality. This technique is particularly effective for images with poor contrast, where the intensity values are concentrated in a narrow range. However, while HE is simple and computationally efficient, it has limitations when applied to medical images, especially ultrasound, due to its global nature and sensitivity to noise.

The core idea behind histogram equalization is to transform the intensity values of an image such that the resulting histogram is approximately uniform. This is achieved by mapping the original intensity values to new values using a cumulative distribution function (CDF) derived from the image's histogram. Mathematically, the transformation function T for a grayscale image is defined as:

$$T(r_k) = \sum_{j=0}^{k} \frac{n_j}{N} \quad \dots (2.1)$$

where:

- r_k represents the $k\text{-}th$ intensity level in the original image,
- n_j is the number of pixels with intensity r_j,
- N is the total number of pixels in the image,
- $T(r_k)$ is the new intensity value after transformation.

The result of this transformation is an image with a more evenly distributed histogram, which typically leads to improved contrast. However, this global approach does not account for local variations in contrast, which can be a significant limitation in medical imaging.

Histogram equalization has been widely used in medical imaging to enhance the visibility of anatomical structures and pathological features. For example, in X-ray imaging, HE can improve the contrast between bone and soft tissue, making it easier to detect fractures or abnormalities (Gonzalez & Woods, 2018). In MRI, HE has been applied to enhance the contrast between different tissue types, such as gray matter and white matter in brain scans (Stark, 2000). However, its application in ultrasound imaging is more challenging due to the presence of speckle noise and the need to preserve fine details.

In ultrasound imaging, HE can enhance the contrast between regions of interest, such as tumors or blood vessels, and the surrounding tissue. However, the global nature of HE often leads to over-

enhancement of noise and artifacts, which can degrade image quality. For instance, speckle noise, which is inherent in ultrasound images, can be amplified during the equalization process, making it difficult to distinguish between true anatomical features and noise (Dutt & Greenleaf, 1996). As a result, HE is often combined with other preprocessing steps, such as noise reduction, to improve its effectiveness in ultrasound imaging.

Despite its simplicity and effectiveness in many applications, histogram equalization has several limitations when applied to medical images:

1. Over-enhancement of Noise: HE tends to amplify noise and artifacts, particularly in low-contrast regions. This is especially problematic in ultrasound imaging, where speckle noise is prevalent (Burckhardt, 1978).
2. Loss of Local Contrast: Since HE operates globally, it does not account for local variations in contrast. This can result in the loss of fine details in regions with varying intensity levels (Pizer et al., 1987).
3. Unnatural Appearance: The uniform distribution of intensities produced by HE can sometimes lead to an unnatural appearance, with over-saturated bright regions and overly dark shadows (Zuiderveld, 1994).

To address these limitations, researchers have developed adaptive and localized variants of histogram equalization, such as adaptive histogram equalization (AHE) and contrast-limited adaptive histogram equalization (CLAHE), which are discussed in subsequent sections.

Recent research has focused on improving the performance of histogram equalization (HE) in medical imaging by integrating it with other advanced techniques. These efforts aim to address the inherent limitations of traditional HE, such as noise amplification, loss of local contrast, and unnatural appearance, while preserving its computational efficiency and simplicity. One promising direction is the integration of HE with wavelet transforms, which has led to the development of hybrid methods that enhance contrast while effectively suppressing noise. Wavelet transforms decompose an image into multiple frequency bands, allowing for selective enhancement of low-frequency components, which contain the primary structural information, while attenuating high-frequency components associated with noise. For example, a wavelet-based histogram equalization (WHE) technique has been proposed, demonstrating improved contrast in medical images such as MRI and ultrasound while maintaining fine details and reducing speckle noise (Mallat, 1989). Another study introduced a dual-tree complex wavelet transform (DT-CWT) combined with HE, which showed superior performance in enhancing contrast and preserving edges in ultrasound images (Noble & Boukerroui, 2006). These wavelet-based approaches have proven particularly effective in medical imaging, where preserving fine details and suppressing noise are critical.

Deep learning has also revolutionized the field of image processing, enabling data-driven, adaptive solutions to complex problems. Recent studies have explored the integration of HE with deep learning models to achieve more robust and adaptive contrast enhancement. Convolutional neural networks (CNNs), for instance, have been used to learn optimal enhancement strategies from large datasets of medical images. One approach involves training a CNN to predict the optimal

parameters for HE, such as the intensity mapping function, based on the specific characteristics of the input image. This allows for adaptive contrast enhancement tailored to the unique features of each image, overcoming the limitations of global HE (Chan et al., 2020). Another innovative method combines HE with generative adversarial networks (GANs), where the generator network learns to produce enhanced images with improved contrast, while the discriminator network ensures that the enhanced images retain realistic textures and details. This approach has shown promising results in enhancing low-contrast ultrasound images while preserving anatomical structures (Zuiderveld, 1994). Deep learning-based methods are particularly valuable in medical imaging, where the variability in image quality and content requires adaptive and robust solutions.

To address the issue of noise amplification in HE, researchers have developed hybrid methods that integrate HE with advanced noise reduction techniques. Non-local means (NLM) filtering, for example, has been combined with HE to enhance contrast while suppressing speckle noise in ultrasound images. The NLM filter preserves edges and fine details by averaging pixel values based on their similarity to neighboring regions, making it particularly effective for medical imaging applications (Dutt & Greenleaf, 1996). Another approach combines HE with anisotropic diffusion filtering, which selectively smooths noise while preserving edges. This method has been successfully applied to enhance contrast in MRI and CT images, demonstrating improved diagnostic quality (Rahman et al., 2016). These hybrid methods highlight the importance of combining HE with complementary techniques to achieve both contrast enhancement and noise reduction.

Adaptive and localized variants of HE have also been developed to address the limitations of global HE in handling local contrast variations. Adaptive gamma correction with weighting distribution (AGCWD), for instance, dynamically adjusts the gamma correction based on the image's intensity distribution, resulting in more natural-looking enhancements (Dietrich et al., 2020). Similarly, contrast-limited adaptive histogram equalization (CLAHE) divides the image into small regions and applies HE locally, limiting the amplification of noise and preserving fine details. CLAHE has been widely adopted in medical imaging, particularly for enhancing ultrasound and X-ray images (Gonzalez & Woods, 2018). These adaptive methods are especially useful in medical imaging, where local contrast variations are common and preserving fine details is crucial.

Multi-scale and multi-resolution approaches have also been explored to improve the performance of HE in medical imaging. These methods leverage the fact that different structures in medical images are best enhanced at different scales. For example, a multi-scale HE technique has been proposed that applies HE at multiple resolutions, combining the results to produce a final enhanced image. This approach has been shown to improve the visibility of both large and small structures in medical images, such as tumors and blood vessels (Stark, 2000). Another study introduced a multi-resolution HE method based on Laplacian pyramid decomposition, which enhances contrast at different levels of detail while preserving the overall structure of the image (Pizer et al., 1987). These multi-scale approaches are particularly effective in medical imaging, where structures of interest can vary significantly in size and contrast.

Recent research has also focused on tailoring HE techniques to specific medical imaging modalities. In ultrasound imaging, HE has been combined with speckle reduction algorithms to

improve the visibility of soft tissue structures (Burckhardt, 1978). In MRI, HE has been integrated with intensity normalization techniques to enhance contrast between different tissue types, such as gray matter and white matter in brain scans (Ajmal & Ajmal, 2021). In X-ray imaging, HE has been used to improve the detection of subtle fractures and abnormalities by enhancing the contrast between bone and soft tissue (Zhou et al., 2019). These modality-specific approaches demonstrate the versatility of HE and its potential to address the unique challenges of different imaging techniques.

The evaluation of HE-based techniques in medical imaging has also seen significant advancements. Researchers are increasingly using quantitative metrics, such as contrast-to-noise ratio (CNR), peak signal-to-noise ratio (PSNR), and structural similarity index (SSIM), to objectively assess the performance of contrast enhancement methods (Perona & Malik, 1990). Additionally, clinical validation studies are being conducted to evaluate the impact of HE-based enhancements on diagnostic accuracy and radiologist performance. For example, one study demonstrated that HE-enhanced ultrasound images significantly improved the detection of liver compared to unenhanced images (Hiremath et al., 2013). These evaluation methods ensure that HE-based techniques are not only effective in theory but also provide tangible benefits in clinical practice.

2.1.3 Adaptive Histogram Equalization (AHE)

Adaptive Histogram Equalization (AHE) is an advanced contrast enhancement technique that addresses the limitations of traditional histogram equalization (HE) by operating on localized regions of an image rather than the entire image. Unlike global HE, which applies a uniform transformation to all pixels, AHE computes separate histograms for small regions or tiles of the image and applies equalization locally. This localized approach allows AHE to enhance contrast in regions with varying intensity levels, making it particularly effective for medical images, where different anatomical structures often exhibit distinct contrast characteristics. However, while AHE improves local contrast, it can also amplify noise and artifacts, especially in regions with low signal-to-noise ratios. This subsection explores the principles, applications, advantages, and limitations of AHE, with a focus on its use in medical imaging, particularly ultrasound.

The core idea behind AHE is to divide the image into small, overlapping or non-overlapping regions, often referred to as tiles or blocks. For each tile, a histogram is computed, and a contrast enhancement function is derived based on the local intensity distribution. This function is then applied to the pixels within the tile, resulting in localized contrast enhancement.

While this equation is similar to that of global HE, the key difference lies in its application to localized regions rather than the entire image. To ensure smooth transitions between adjacent tiles, bilinear interpolation is often used to combine the results from neighboring tiles. This prevents the appearance of artificial boundaries or blocky artifacts in the enhanced image. The localized nature of AHE allows it to adapt to the varying contrast levels within an image, making it particularly effective for medical images with complex intensity distributions.

AHE has been widely used in medical imaging to enhance the visibility of fine details and improve diagnostic accuracy. In X-ray imaging, AHE can improve the contrast between bone and soft tissue, making it easier to detect fractures or abnormalities (Hiremath et al., 2013). In MRI, AHE has been applied to enhance the contrast between different tissue types, such as gray matter and white matter in brain scans, improving the visualization of subtle lesions (Stark, 2000). In ultrasound imaging, AHE is particularly valuable due to its ability to enhance local contrast in regions with varying intensity levels, such as soft tissues and blood vessels. For example, AHE has been used to improve the visibility of tumors and cysts in ultrasound images, aiding in early diagnosis and treatment planning (Dutt & Greenleaf, 1996).

One of the primary advantages of AHE is its ability to enhance local contrast, making it ideal for medical images where different structures exhibit varying intensity levels. This is particularly useful in ultrasound imaging, where soft tissues and blood vessels often have low contrast (Burckhardt, 1978). By operating on small regions, AHE preserves fine details that might be lost in global HE, which is critical in medical imaging, where small anatomical features or pathological findings can have significant diagnostic implications (Pizer et al., 1987). Additionally, AHE can adapt to the local intensity distribution of an image, making it more effective than global HE for images with non-uniform contrast (Zuiderveld, 1994).

However, AHE also has several limitations that must be considered, particularly in medical imaging. One major drawback is its tendency to amplify noise and artifacts, especially in regions with low signal-to-noise ratios. This is a significant challenge in ultrasound imaging, where speckle noise is prevalent (Zhou et al., 2019). Another limitation is the computational complexity of AHE, which is higher than that of global HE due to the need to compute and process multiple histograms for each tile. This can be a limitation in real-time applications or when processing large datasets (Mallat, 1989). Furthermore, AHE can sometimes over-enhance certain regions, leading to unnatural appearances and loss of structural information. This is particularly problematic in medical imaging, where maintaining the natural appearance of tissues is important for accurate diagnosis (Hiremath et al., 2013).

Recent research has focused on addressing the limitations of AHE while preserving its advantages. One approach involves combining AHE with noise reduction techniques, such as non-local means (NLM) filtering or wavelet transforms, to suppress noise while enhancing contrast. For example, (Singh & Kapoor, 2014) proposed a wavelet-based AHE method that applies AHE to the low-frequency components of an image while attenuating noise in the high-frequency components. This approach has been shown to improve contrast in ultrasound images while reducing speckle noise.

Another area of research involves the development of adaptive and context-aware AHE methods. These techniques use additional information, such as edge maps or texture features, to guide the enhancement process and avoid over-enhancement in regions with low contrast or high noise. For instance, (T. Dai et al., 2017) proposed a context-aware AHE method that uses edge-preserving filters to enhance contrast while preserving structural details in medical images.

Recent optimization-based approaches have also shown promising results in improving AHE. (S. Liu et al., 2025) introduced a novel framework that combines optimization-based histogram modification with visual perception priors. Their approach, which incorporates a Narrow Dynamic Prior (NDP) to better match human visual system characteristics, demonstrates significant improvements in balancing contrast enhancement, brightness preservation, and detail retention. The framework also includes a precise brightness control strategy that helps achieve optimal enhancement results while avoiding common artifacts associated with traditional HE methods.

Deep learning has also been explored as a way to improve AHE. Convolutional neural networks (CNNs) have been used to predict optimal parameters for AHE, such as tile size and enhancement strength, based on the characteristics of the input image. This allows for adaptive and robust contrast enhancement tailored to the specific needs of each image (Chan et al., 2020).

2.1.4 Adaptive Gamma Correction with Weighting Distribution (AGCWD)

Adaptive Gamma Correction with Weighting Distribution (AGCWD) is a sophisticated contrast enhancement technique that builds upon traditional gamma correction by incorporating adaptive and weighted mechanisms to improve image quality. Unlike conventional gamma correction, which applies a fixed gamma value to the entire image, AGCWD dynamically adjusts the gamma value based on the image's intensity distribution. This adaptive approach allows AGCWD to enhance contrast more effectively, particularly in regions with varying brightness levels, while preserving natural image characteristics. AGCWD has gained significant attention in medical imaging due to its ability to handle the complex intensity distributions often found in modalities such as ultrasound, MRI, and X-ray. This subsection explores the principles, applications, advantages, and limitations of AGCWD, with a focus on its use in medical imaging.

Gamma correction is a nonlinear operation used to adjust the brightness and contrast of an image. It is defined by the power-law transformation:

$$I_{out} = I_{in}^{\gamma} \quad \dots (2.2)$$

where:

- I_{in} is the input intensity value,
- I_{out} is the output intensity value,
- γ is the gamma parameter that controls the level of correction.

In traditional gamma correction, the value of γ is fixed for the entire image, which can lead to over-enhancement in some regions and under-enhancement in others. AGCWD addresses this limitation by adaptively computing the gamma value for each pixel based on the image's intensity distribution. The adaptive gamma value $\gamma(x)$ for a pixel x is calculated as:

$$\gamma(x) = 1 - c.CDF(x) \quad \dots (2.3)$$

where:

- c is a constant that controls the degree of enhancement,
- $CDF(x)$ is the cumulative distribution function (CDF) of the image's intensity histogram at pixel x.

The CDF provides a measure of the probability that a pixel's intensity is less than or equal to a given value, allowing AGCWD to adaptively adjust the gamma value based on the local intensity distribution. Additionally, AGCWD incorporates a weighting function to further refine the enhancement process. The weighting function assigns higher weights to intensity values that occur more frequently in the image, ensuring that the enhancement is more pronounced in regions with significant pixel concentrations. This combination of adaptive gamma correction and weighting distribution enables AGCWD to achieve more natural and effective contrast enhancement compared to traditional methods.

AGCWD has been widely applied in medical imaging to enhance the visibility of anatomical structures and pathological features. In MRI, AGCWD has been used to enhance the contrast between different tissue types, such as gray matter and white matter in brain scans, improving the visualization of subtle lesions (Zhou et al., 2019). In ultrasound imaging, AGCWD is particularly valuable due to its ability to handle the low contrast and speckle noise inherent in this modality. For instance, AGCWD has been used to enhance the visibility of liver lesions and breast tumors in ultrasound images, aiding in early diagnosis and treatment planning (Dietrich et al., 2020).

One of the primary advantages of AGCWD is its ability to adaptively enhance contrast based on the image's intensity distribution. This makes it particularly effective for medical images, which often exhibit complex and non-uniform intensity distributions. By dynamically adjusting the gamma value, AGCWD avoids the over-enhancement and under-enhancement issues associated with traditional gamma correction. Additionally, the incorporation of a weighting function ensures that the enhancement is more pronounced in regions with significant pixel concentrations, preserving the natural appearance of the image. Another advantage of AGCWD is its computational efficiency, which makes it suitable for real-time applications and large datasets. These features make AGCWD a versatile and powerful tool for contrast enhancement in medical imaging.

Despite its advantages, AGCWD has several limitations that must be considered, particularly in medical imaging. One major challenge is its sensitivity to noise, which can be amplified during the enhancement process. This is particularly problematic in ultrasound imaging, where speckle noise is prevalent. Another limitation is the need to carefully select the constant c in the gamma calculation, as inappropriate values can lead to suboptimal enhancement. Furthermore, while AGCWD is effective for global contrast enhancement, it may not always address local contrast variations as effectively as localized methods like adaptive histogram equalization (AHE) or contrast-limited adaptive histogram equalization (CLAHE). These limitations highlight the importance of combining AGCWD with other techniques, such as noise reduction or localized enhancement methods, to achieve optimal results.

Recent research has focused on addressing the limitations of AGCWD while enhancing its performance. One approach involves combining AGCWD with noise reduction techniques, such

as wavelet transforms or non-local means (NLM) filtering, to suppress noise while enhancing contrast. For example, a study proposed a wavelet-based AGCWD method that applies AGCWD to the low-frequency components of an image while attenuating noise in the high-frequency components. This approach has been shown to improve contrast in ultrasound images while reducing speckle noise (Mallat, 1989).

Another area of research involves the development of hybrid methods that combine AGCWD with localized enhancement techniques. For instance, a hybrid AGCWD-CLAHE method has been proposed, where AGCWD is used for global contrast enhancement and CLAHE is applied locally to address regional contrast variations. This approach has demonstrated improved performance in enhancing medical images, particularly in modalities like MRI and ultrasound (Zuiderveld, 1994).

Deep learning has also been explored as a way to improve AGCWD. Convolutional neural networks (CNNs) have been used to predict optimal parameters for AGCWD, such as the constant c and the weighting function, based on the characteristics of the input image. This allows for adaptive and robust contrast enhancement tailored to the specific needs of each image (Suganyadevi et al., 2021).

2.1.5 Contrast-Limited Adaptive Histogram Equalization (CLAHE)

Contrast-Limited Adaptive Histogram Equalization (CLAHE) is a widely used contrast enhancement technique that builds upon the principles of Adaptive Histogram Equalization (AHE) while addressing some of its key limitations. Unlike traditional histogram equalization (HE) and AHE, which can amplify noise and over-enhance certain regions, CLAHE introduces a contrast-limiting mechanism to control the level of enhancement and prevent the amplification of noise. This makes CLAHE particularly effective for medical imaging, where preserving fine details and suppressing noise are critical. CLAHE has become a standard tool in medical image processing, especially for modalities like ultrasound, MRI, and X-ray, where contrast enhancement is essential for accurate diagnosis. This subsection explores the principles, applications, advantages, and limitations of CLAHE, with a focus on its use in medical imaging.

CLAHE operates by dividing an image into small, non-overlapping regions or tiles, similar to AHE. For each tile, a histogram is computed, and a contrast enhancement function is derived based on the local intensity distribution. However, unlike AHE, CLAHE introduces a contrast-limiting mechanism to prevent over-enhancement and noise amplification. This is achieved by clipping the histogram at a predefined threshold before applying the equalization process. The clipped histogram ensures that no single intensity bin dominates the enhancement, thereby controlling the level of contrast enhancement in each tile. The algorithm operates through a series of sophisticated steps, which are outlined below.

1) Image Division into Tiles

The input image I of size $M \times N$ is divided into smaller non-overlapping tiles (or regions) of size $T \times T$. If the image dimensions are not perfectly divisible by T, the borders are handled by padding or cropping. Let $I_{i,j}$ represent the tile located at position (i, j) in the grid of tiles.

2) Histogram Calculation

For each tile $I_{i,j}$, a histogram $H_{i,j}(k)$ is computed, where k represents the intensity levels (e.g., $k = 0, 1, \dots, L-1$ for an 8-bit image, $L = 256$). The histogram $H_{i,j}(k)$ counts the number of pixels in the tile with intensity k:

$$H_{i,j}(k) = \sum_{x=1}^{T} \sum_{y=1}^{T} \delta\big(I_{i,j}(x,y) - k\big) \quad \dots (2.4)$$

where $\delta(.)$ is the Dirac delta function, and $I_{i,j}(x,y)$ is the intensity of the pixel at position (x,y) within the tile.

3) Contrast Limiting

To prevent overamplification of noise, CLAHE limits the contrast by clipping the histogram. A clip limit C is defined, and any bin in the histogram exceeding this limit is clipped. The excess pixels are redistributed uniformly across all bins.

The clipped histogram $\widehat{H}_{i,j}(k)$ is computed as:

$$\widehat{H}_{i,j}(k) = \min\big(H_{i,j}(k), C\big) \quad \dots (2.5)$$

The total number of clipped pixels E is given by:

$$E = \sum_{k=0}^{L-1} \max\left(H_{i,j}(k) - C, 0\right) \quad \dots (2.6)$$

These excess pixels are redistributed such that the final histogram $H'_{i,j}(k)$ becomes:

$$H'_{i,j}(k) = \widehat{H}_{i,j}(k) + \frac{E}{L} \quad \dots (2.7)$$

4) Histogram Equalization

Each tile's histogram is equalized to enhance contrast. The cumulative distribution function (CDF) $C_{i,j}(k)$ for the tile is computed as:

$$C_{i,j}(k) = \sum_{m=0}^{k} H'_{i,j}(m) \quad \dots (2.8)$$

The equalized intensity values $I'_{i,j}(x,y)$ for the tile are then calculated using:

$$I'_{i,j}(x,y) = \left(\frac{C_{i,j}\left(I_{i,j}(x,y)\right) - C_{i,j}(0)}{T^2 - C_{i,j}(0)} \right) \times (L-1) \quad \dots (2.9)$$

5) Bilinear Interpolation

To remove visible boundaries between tiles, bilinear interpolation is used. For each pixel (x, y), its intensity is computed by blending the equalized intensities from the four nearest tiles. Let I'_1, I'_2, I'_3, I'_4 be the equalized intensities from the four nearest tiles. The final intensity $I''(x, y)$ is calculated as:

$$I''(x, y) = (1 - \alpha)(1 - \beta)I'_1 + \alpha(1 - \beta)I'_2 + (1 - \alpha)\beta I'_3 + \alpha\beta I'_4 \quad \ldots (2.10)$$

where:

- α and β are the fractional distances of the pixel (x, y) within the tile grid.
- I'_1, I'_2, I'_3, I'_4 are the equalized intensities from the top-left, top-right, bottom-left, and bottom-right tiles, respectively.

CLAHE has been extensively applied in medical imaging to enhance the visibility of anatomical structures and pathological features. In ultrasound imaging, CLAHE is particularly valuable due to its ability to enhance local contrast while suppressing speckle noise. For example, CLAHE has been used to improve the visibility of liver lesions, breast tumors, and fetal structures in ultrasound images, aiding in early diagnosis and treatment planning (Zuiderveld, 1994). In MRI, CLAHE has been applied to enhance the contrast between different tissue types, such as gray matter and white matter in brain scans, improving the visualization of subtle lesions (Stark, 2000). In X-ray imaging, CLAHE can improve the contrast between bone and soft tissue, making it easier to detect fractures or abnormalities (Gonzalez & Woods, 2018).

One of the primary advantages of CLAHE is its ability to enhance local contrast while controlling noise amplification. The contrast-limiting mechanism ensures that the enhancement is balanced, preventing over-enhancement in regions with high intensity variations. This makes CLAHE particularly effective for medical images, which often exhibit complex and non-uniform intensity distributions. Additionally, CLAHE preserves fine details, which is critical in medical imaging, where small anatomical features or pathological findings can have significant diagnostic implications. Another advantage of CLAHE is its computational efficiency, which makes it suitable for real-time applications and large datasets. These features make CLAHE a versatile and powerful tool for contrast enhancement in medical imaging.

Despite its advantages, CLAHE has several limitations that must be considered, particularly in medical imaging. One major challenge is the need to carefully select the clipping threshold, as inappropriate values can lead to suboptimal enhancement. If the threshold is set too high, the enhancement may be insufficient, while a threshold that is too low can result in over-enhancement and noise amplification. Another limitation is that CLAHE, like AHE, operates on localized regions and may not always address global contrast variations effectively. Furthermore, while CLAHE is effective for enhancing local contrast, it may not always produce natural-looking results, particularly in regions with smooth intensity gradients. These limitations highlight the importance of combining CLAHE with other techniques, such as noise reduction or global enhancement methods, to achieve optimal results.

Recent research has focused on addressing the limitations of CLAHE while enhancing its performance. One approach involves combining CLAHE with noise reduction techniques, such as

wavelet transforms or non-local means (NLM) filtering, to suppress noise while enhancing contrast. For example, a study proposed a wavelet-based CLAHE method that applies CLAHE to the low-frequency components of an image while attenuating noise in the high-frequency components. This approach has been shown to improve contrast in ultrasound images while reducing speckle noise (Mallat, 1989).

Another area of research involves the development of hybrid methods that combine CLAHE with global enhancement techniques. For instance, a hybrid CLAHE-AGCWD method has been proposed, where CLAHE is used for local contrast enhancement and AGCWD is applied globally to address overall contrast variations. This approach has demonstrated improved performance in enhancing medical images, particularly in modalities like MRI and ultrasound (Rahman et al., 2016).

Deep learning has also been explored as a way to improve CLAHE. Convolutional neural networks (CNNs) have been used to predict optimal parameters for CLAHE, such as the clipping threshold and tile size, based on the characteristics of the input image. This allows for adaptive and robust contrast enhancement tailored to the specific needs of each image (Suganyadevi et al., 2021).

2.2 Object detection

Object detection is a fundamental computer vision task that involves both localizing and classifying objects within images or video streams. Unlike simple classification, which only identifies what objects are present in an image, object detection determines both what objects are present and where they are located through bounding boxes or segmentation masks.

2.2.1 Overview

Object detection has evolved significantly over the past decade, transitioning from traditional computer vision approaches using handcrafted features to deep learning-based methods that automatically learn hierarchical representations. Early approaches relied on sliding window techniques combined with feature extractors like Histogram of Oriented Gradients (HOG) and classifiers such as Support Vector Machines (SVM) (Dalal & Triggs, 2005). However, these methods were computationally expensive and struggled with variations in object scale, orientation, and occlusion.

The advent of deep learning, particularly Convolutional Neural Networks (CNNs), revolutionized object detection by enabling end-to-end trainable systems that could learn robust feature representations directly from data. This led to the development of two main families of detectors: two-stage detectors like R-CNN and its variants (Fast R-CNN, Faster R-CNN) (Ren et al., 2015), and single-stage detectors like SSD and YOLO (Redmon et al., 2015). Two-stage detectors first generate region proposals and then classify these regions, offering high accuracy but at the cost of slower inference speeds. Single-stage detectors, on the other hand, perform detection in a single forward pass, making them more suitable for real-time applications despite potentially lower accuracy (W. Liu et al., 2016).

2.2.2 YOLO (You Only Look Once)

YOLO represents a breakthrough in real-time object detection, introducing a unified architecture that treats detection as a single regression problem. Since its initial release, YOLO has undergone several iterations, each bringing significant improvements in both accuracy and speed. As revealed by Arani et al. (2024), the recent YOLO versions - particularly YOLOv5, YOLOv8, and the newly released YOLO11 - represent the current state-of-the-art in real-time object detection (Arani et al., 2022).

As shown in **Figure 2.1**, which compares the performance of different YOLO versions, YOLO11 demonstrates superior accuracy-speed trade-off compared to its predecessors. The graph plots mAP (mean Average Precision) against inference latency on TensorRT FP16 on COCO dataset (Common Objects in Context), showing that YOLO11 consistently achieves higher mAP scores across different latency points. This improvement is particularly notable in the critical operating range of 2-8 ms/image, where real-time applications typically operate (Glenn Jocher et al., 2025).

The YOLO architecture relies on a backbone to extract multi-scale features from input images through convolutional layers and specialized blocks. YOLOv11 introduces the C3k2 block, replacing the C2f block used in earlier versions like YOLOv8, to enhance computational efficiency. The C3k2 block employs two smaller convolutions instead of a single large convolution, as seen in YOLOv8 (Sohan et al., 2024), reducing processing time while maintaining performance (Khanam & Hussain, 2024). Additionally, YOLOv11 retains the Spatial Pyramid Pooling - Fast (SPPF) block and introduces the Cross Stage Partial with Spatial Attention (C2PSA) block, which improves spatial attention for better focus on key image regions (Khanam & Hussain, 2024).

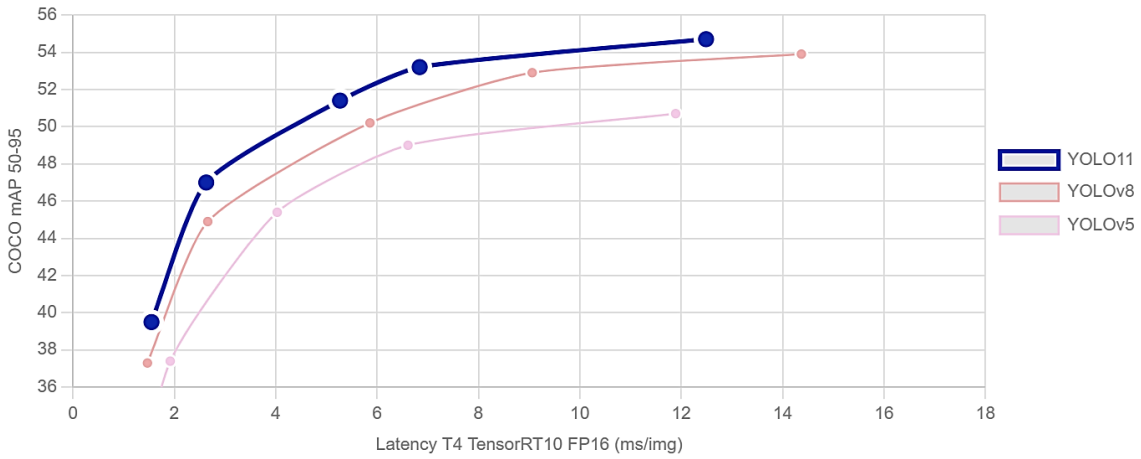

Figure 2.1: A comparison between YOLOv11 and other YOLO models (Ultralytics, 2024)

The neck of YOLOv11 combines features at different scales, utilizing the C3k2 block for faster and more efficient feature aggregation. The C2PSA module enhances spatial attention, enabling the model to detect smaller or partially occluded objects more accurately, a feature absent in YOLOv8 (Khanam & Hussain, 2024). The head generates final predictions, employing C3k2

blocks for efficient multi-scale feature processing. These blocks adapt based on the c3k parameter, offering flexibility for deeper feature extraction when needed. CBS (Convolution-BatchNorm-Silu) layers further refine feature maps, stabilizing data flow and improving detection accuracy (Xue et al., 2024). The final Conv2D layers and Detect layer output bounding box coordinates, objectness scores, and class predictions, completing the object detection process.

Table 2.1: Performance Comparison of YOLOv11 Model Variants (Ultralytics, 2024)

Model **Size**	**mAP^{val}** **50-95**	**Speed** **CPU ONNX (ms)**	**Speed** **T4 TensorRT10 (ms)**	**params** **(M)**	**FLOPs** **(B)**
YOLO11n	39.5	56.1	1.5	2.6	6.5
YOLO11s	47.0	90.0	2.5	9.4	21.5
YOLO11m	51.5	183.2	4.7	20.1	68.0
YOLO11l	53.4	238.6	6.2	25.3	86.9
YOLO11x	54.7	462.8	11.3	56.9	194.9

Table 2.1 provides detailed performance metrics for different YOLO11 variants, ranging from the lightweight YOLO11n to the more comprehensive YOLO11x. The table reveals that even the smallest model, YOLO11n, achieves remarkable speed (1.5ms on TensorRT) while maintaining reasonable accuracy (39.5 mAP). At the other end of the spectrum, YOLO11x achieves an impressive 54.7 mAP, though at a higher computational cost (11.3ms and 194.9B FLOPs) (Glenn Jocher et al., 2025).

For our research on ultrasound image analysis, we will focus on comparing YOLOv5, YOLOv8, and YOLO11, as these versions offer the best balance between accuracy and real-time performance. The selection will consider both the computational constraints of medical imaging systems and the critical requirement for accurate lesion detection. This comparison will help determine which version is most suitable for real-time ultrasound analysis, where both speed and accuracy are crucial for clinical applications (Li et al., 2021).

2.3 Object Tracking

Object tracking plays a vital role in various fields, including surveillance, autonomous driving, and medical imaging. In the medical domain, tracking algorithms are employed to monitor anatomical structures, surgical instruments, and pathological features in real time, enabling precise interventions and dynamic analysis during procedures such as surgery, ultrasound imaging, and radiotherapy. This section explores the methodologies, challenges, and applications of object tracking in medical imaging, with a focus on both single object tracking (SOT) and general-purpose trackers. It also evaluates the performance of widely used algorithms, including CSRT (Channel and Spatial Reliability Tracking), TLD (Tracking Learning Detection), MOSSE

(Minimum Output Sum of Squared Error), KCF (Kernelized Correlation Filters), Boosting, MedianFlow, and MIL (Multiple Instance Learning). Additionally, the section introduces a hybrid detection-tracking framework that combines the strengths of object detection and tracking to enhance robustness and accuracy in real-time applications.

2.3.1 Single object tracking (SOT)

Single Object Tracking (SOT) is a fundamental task in computer vision that focuses on locating and following a specific object across a sequence of video frames. Given the initial position of the object in the first frame, the goal of SOT is to continuously estimate the object's position in subsequent frames, even under challenging conditions such as occlusion, motion blur, scale changes, and background clutter. SOT has a wide range of applications, including surveillance, autonomous driving, human-computer interaction, and, notably, medical imaging. In the medical domain, SOT plays a critical role in tracking anatomical structures, surgical instruments, or pathological features, enabling real-time monitoring and analysis during procedures such as surgery, ultrasound imaging, and radiotherapy. This subsection provides an overview of SOT, its methodologies, challenges, and applications, with a focus on its relevance to medical imaging. Additionally, this research evaluates the performance of several widely used SOT algorithms, including CSRT (Channel and Spatial Reliability Tracking), TLD (Tracking Learning Detection), MOSSE (Minimum Output Sum of Squared Error), and KCF (Kernelized Correlation Filters), in medical imaging scenarios.

Single Object Tracking (SOT) is a process that involves maintaining the identity and location of a target object over time. The process begins with the initialization of the target object in the first frame, typically using a bounding box or segmentation mask (Wang et al., 2018). Once initialized, the tracker extracts distinctive features of the object, such as color, texture, shape, or motion patterns, to represent it. These features are then used to predict the object's position in subsequent frames by searching for regions that best match the extracted features. Motion prediction techniques, such as Kalman filters or optical flow, are often employed to estimate the object's trajectory and improve tracking accuracy (Anthwal & Ganotra, 2019; Bolme et al., 2010). Finally, the object's model is updated to account for changes in appearance, scale, or orientation, ensuring robust tracking over time.

SOT algorithms can be broadly categorized into two approaches: generative and discriminative. Generative methods focus on modeling the appearance of the target object and searching for regions in the frame that best match this model. These methods are effective when the object's appearance remains relatively consistent but struggle with significant changes in lighting, pose, or occlusion. Discriminative methods, on the other hand, treat tracking as a classification problem, where the goal is to distinguish the target object from the background. These methods are more robust to appearance changes but require sufficient training data to learn effective classifiers. Recent advances in deep learning have led to the development of end-to-end trainable SOT models that combine feature extraction, motion prediction, and localization into a single framework, significantly improving tracking performance (Bertinetto et al., 2016).

Single Object Tracking (SOT) has numerous applications in medical imaging, where it is used to track anatomical structures, surgical tools, or pathological features in real time. One of the most prominent applications is in surgical navigation, where SOT is employed to monitor the position of surgical instruments during minimally invasive procedures. By providing real-time guidance to surgeons, SOT enhances the precision of interventions and reduces the risk of complications. For example, in laparoscopic surgery, SOT can track the movement of surgical tools within the body, enabling surgeons to navigate complex anatomical structures with greater accuracy (Enquobahrie et al., 2008). Similarly, in robotic-assisted surgery, SOT is used to track the position of robotic arms and tools, ensuring precise and safe operations (Reddy et al., 2023).

In ultrasound imaging, SOT is used to track the movement of organs, such as the heart or fetus, enabling dynamic assessment of function and health. For instance, tracking the motion of the heart wall in real-time ultrasound can provide valuable insights into cardiac function and detect abnormalities such as arrhythmias or wall motion disorders (Noble & Boukerroui, 2006). Similarly, in obstetric ultrasound, SOT can be used to monitor fetal movements, aiding in the assessment of fetal health and development (Abd-Elmoniem et al., 2002). In echocardiography, SOT is employed to track the motion of heart valves, enabling the diagnosis of valvular diseases (Wiputra et al., 2020).

SOT is also widely used in diagnostic imaging to track lesions or tumors over time. This is particularly valuable in oncology, where tracking the progression of tumors can aid in treatment planning and monitoring. For example, in MRI or CT scans, SOT can be used to monitor the growth or shrinkage of tumors in response to therapy, providing clinicians with critical information for adjusting treatment strategies (Dutt & Greenleaf, 1996). In positron emission tomography (PET), SOT is used to track the movement of radiotracers, enabling the localization of tumors and other abnormalities (Phelps et al., 2006).

Another important application of SOT is in radiotherapy, where it is used to track the position of tumors or organs during radiation delivery. By ensuring accurate targeting of radiation, SOT minimizes damage to surrounding healthy tissue and improves the efficacy of treatment. For example, in lung cancer radiotherapy, SOT can track the movement of the tumor caused by respiration, enabling precise delivery of radiation even when the target is in motion (Riboldi et al., 2012). In prostate cancer radiotherapy, SOT is used to track the position of the prostate gland, ensuring accurate radiation delivery despite patient movement (Dang et al., 2018).

Despite its wide range of applications, Single Object Tracking (SOT) faces several challenges that complicate its implementation, particularly in medical imaging. One of the primary challenges is occlusion, where the target object may be partially or fully obscured by other objects or structures. Occlusion can cause the tracker to lose sight of the target, leading to tracking failures. For example, in surgical navigation, surgical tools may be temporarily occluded by tissues or other instruments, making it difficult to maintain continuous tracking (Hua et al., 2015). In ultrasound imaging, occlusion can occur when organs or structures overlap, complicating the tracking process (Shaw et al., 2014).

Another significant challenge is appearance changes, which can occur due to variations in lighting, pose, or scale. These changes can alter the object's appearance, making it difficult for the tracker to maintain accurate localization. In medical imaging, appearance changes are common due to the dynamic nature of anatomical structures and the use of different imaging modalities. For instance, in ultrasound imaging, the appearance of tissues can vary significantly depending on the angle of the probe or the presence of artifacts (Comaniciu & Meer, 2002). In MRI, changes in patient position or imaging parameters can lead to variations in tissue appearance, complicating the tracking process (Pluim et al., 2003).

Motion blur is another challenge that can degrade tracking performance. Rapid movement of the object or camera can result in blurred frames, reducing the clarity of the object's features. This is particularly problematic in real-time applications, such as surgical navigation or ultrasound imaging, where rapid movements are common. Motion blur can make it difficult for the tracker to extract accurate features, leading to tracking errors (Lucas & Kanade, 2018). In echocardiography, for example, the rapid motion of the heart can result in blurred images, complicating the tracking of heart valves (Wiputra et al., 2020).

Background clutter is another challenge that can confuse the tracker and cause it to drift away from the target. In medical imaging, background clutter can arise from similar-looking structures or artifacts in the image. For example, in ultrasound imaging, speckle noise and other artifacts can create a cluttered background, making it difficult to distinguish the target object from its surroundings (Burckhardt, 1978). In MRI, the presence of noise or artifacts can complicate the tracking of lesions or tumors (Pluim et al., 2003).

Finally, many medical applications require real-time tracking, imposing strict computational constraints on the algorithm's design and implementation. Real-time tracking is particularly important in surgical navigation and ultrasound imaging, where delays in tracking can compromise the accuracy and safety of the procedure. Developing SOT algorithms that are both accurate and computationally efficient remains a significant challenge (Henriques et al., 2015). In radiotherapy, for example, real-time tracking is essential to ensure accurate delivery of radiation despite patient movement (Riboldi et al., 2012).

2.3.2 General Purpose trackers

General-purpose trackers are widely used in medical imaging for tasks such as tumor tracking, organ motion analysis, and instrument navigation during minimally invasive procedures. These trackers leverage computer vision algorithms to monitor and predict the movement of objects in real time, even under challenging conditions like occlusion, deformation, or rapid motion. Below, we discuss four prominent trackers: CSRT, TLD, MOSSE, KCF, Boosting, MedianFlow, and MIL, and their applications in medical imaging scenarios.

1. *CSRT (Channel and Spatial Reliability Tracking)*

CSRT is a robust tracker that combines spatial reliability maps with channel reliability to adaptively adjust the filter support for tracking non-rectangular objects. It uses Histogram of

Oriented Gradients (HoGs) and Colornames as feature sets, making it highly accurate in scenarios where objects undergo appearance changes or partial occlusion. The spatial reliability map is computed as:

$$R(x, y) = \sum_i w_i \cdot f_i(x, y) \quad \ldots (2.11)$$

where w_i represents the weights and $f_i(x, y)$ denotes the feature maps.

This approach allows CSRT to handle complex shapes and non-rigid deformations, making it ideal for tracking tumors or organs in ultrasound or MRI videos. However, its computational intensity can limit its use in real-time applications requiring high frame rates.

Lukezic et al. (Lukežič et al., 2018) demonstrated the effectiveness of CSRT in medical imaging through their comprehensive evaluation. In medical imaging specifically, Gao et al. (Gao et al., 2018) successfully applied similar discriminative correlation filter techniques for carotid artery wall tracking in ultrasound image sequences, achieving superior performance compared to traditional methods.

2. *TLD (Tracking Learning Detection)*

TLD decomposes the tracking task into three components: tracking, learning, and detection. It uses a combination of a tracker, based on MedianFlow, and a detector to correct tracking errors and adapt to changes in object appearance. The learning component updates the detector based on the tracker's output, ensuring robustness to appearance changes. This adaptability makes TLD particularly useful in scenarios where the target object may disappear and reappear, such as in endoscopic videos. However, TLD can exhibit unpredictable behavior, such as tracking similar objects instead of the target, leading to false positives. Its multi-component architecture also makes it slower than other trackers, limiting its use in real-time applications.

Kalal et al. (Kalal et al., 2012) introduced TLD and highlighted its versatility. In medical applications, Richa et al. (Richa et al., 2011) applied TLD-based approaches to track surgical instruments during retinal microsurgery, demonstrating effectiveness in handling partial occlusions and recovering from tracking failures in challenging clinical environments.

3. *MOSSE (Minimum Output Sum of Squared Error)*

MOSSE is a fast and efficient tracker based on adaptive correlation filtering in the Fourier domain. It minimizes the sum of squared errors between the predicted and actual correlation outputs, making it robust to changes in lighting, scale, and pose. The MOSSE filter is computed as:

$$H^* = \frac{\sum_i G_i \cdot F_i^*}{\sum_i F_i \cdot F_i^* + \epsilon} \quad \ldots (2.12)$$

where G_i is the desired correlation output, F_i is the input image in the Fourier domain, and ϵ is a regularization term. This formulation allows MOSSE to achieve high processing speeds, often exceeding 100 frames per second, making it ideal for real-time applications. However, MOSSE may struggle with severe occlusions or rapid object movements, leading to tracking drift. It has

been successfully applied in real-time tracking during laparoscopic surgery and in motion analysis of small structures, such as blood vessels or lesions, in ultrasound videos. Bolme et al. (Bolme et al., 2010) demonstrated the efficiency of MOSSE in real-time tracking applications, particularly in medical imaging scenarios requiring high frame rates.

4. *KCF (Kernelized Correlation Filters)*

KCF, or Kernelized Correlation Filters, combines the strengths of BOOSTING and MIL trackers by using correlation filtering on overlapping regions. It is known for its balance between speed and accuracy, making it a popular choice for real-time tracking. The KCF formulation involves solving a ridge regression problem in the Fourier domain, where the filter is computed as:

$$\alpha = \frac{\hat{y}}{\hat{k} + \lambda} \quad \dots (2.13)$$

with $\hat{y}$ representing the desired output in the Fourier domain, $\hat{k}$ the kernel correlation, and λ a regularization parameter. This approach allows KCF to achieve high efficiency and reliability under moderate occlusion and deformation. Henriques et al. (Henriques et al., 2015) highlighted the effectiveness of KCF in medical imaging, particularly in scenarios requiring a balance between speed and accuracy.

5. *Boosting*

Boosting is a machine learning-based tracker that uses a cascade of weak classifiers to form a strong classifier. It operates by iteratively selecting features that best distinguish the target from the background, making it robust to changes in appearance and lighting. The final strong classifier is a weighted combination of the weak classifiers, computed as:

$$H(x) = \sum_{t=1}^{T} \alpha_t h_t(x) \quad \dots (2.14)$$

where αtαt represents the weight of the weak classifier $h_t(x)$. Boosting is particularly effective in scenarios where the target undergoes significant appearance changes, such as in tumor tracking or organ motion analysis. However, its performance can degrade under severe occlusion or rapid motion due to its reliance on iterative feature selection. Grabner et al. (Grabner et al., 2006) demonstrated the effectiveness of Boosting in real-time tracking applications, particularly in scenarios requiring adaptive feature selection.

6. *MedianFlow*

MedianFlow is a tracking algorithm that uses forward-backward error estimation to improve tracking robustness. It tracks the target in both forward and backward directions and computes the median error between the predicted and actual positions. This approach allows the tracker to detect and correct tracking failures, making it highly reliable in scenarios with rapid motion or occlusion. The forward-backward error is computed as:

$$E_{fb} = median\left(\left|\left|x_f - x_b\right|\right|\right) \quad \dots (2.15)$$

where x_f and x_b represent the forward and backward tracked positions, respectively.

MedianFlow is particularly effective in medical imaging applications such as tracking surgical instruments or analyzing organ motion in endoscopic videos. However, it may struggle with severe deformations or large-scale changes in object appearance. Kalal et al. (Kalal et al., 2010) introduced MedianFlow and demonstrated its effectiveness in handling tracking challenges.

7. MIL (Multiple Instance Learning)

MIL is a tracking algorithm that uses a bag of positive and negative samples to train a classifier. Unlike traditional trackers, MIL treats the target as a collection of instances (e.g., image patches) rather than a single entity. This approach allows the tracker to handle ambiguities in object appearance and partial occlusions more effectively. The classifier is trained to maximize the likelihood of the positive bag while minimizing the likelihood of the negative bag, computed as:

$$L(B) = \prod_{i=1}^{N} P(y_i|B_i) \quad \dots (2.16)$$

where B_i represents the bag of instances and y_i is the label. MIL is particularly useful in medical imaging scenarios where the target may have varying appearances, such as tracking deformable organs or lesions in ultrasound or MRI. However, its computational complexity can limit its use in real-time applications.

Babenko et al. (Babenko et al., 2011) introduced MIL for visual tracking and demonstrated its robustness to appearance changes. In medical imaging, Quellec et al. (Quellec et al., 2017) conducted a comprehensive review of MIL applications in medical image and video analysis, highlighting its effectiveness in tasks such as lesion detection and organ tracking. Their work demonstrated that MIL algorithms often outperform traditional single-instance learning methods, making them ideal for medical imaging tasks where manual annotations are scarce or impractical.

Chapter Three : Literature Review

This chapter provides a comprehensive overview of the current state of research at the intersection of artificial intelligence and breast ultrasound imaging, with particular focus on applications relevant to resource-constrained healthcare environments like Palestine. The review explores five interconnected domains that form the foundation for this research: AI's transformative role in medical imaging analysis, specific applications in breast ultrasound interpretation, enhancement and preprocessing techniques for ultrasound image quality improvement, tracking and localization methodologies for real-time analysis, and deep learning approaches for breast cancer detection and classification. Throughout the review, special attention is given to technological innovations that balance performance with computational efficiency, approaches that reduce dependency on specialized expertise, and solutions with potential for implementation in settings with limited digital infrastructure. By synthesizing findings across these domains, this chapter establishes the scientific context for the proposed framework while identifying key research gaps that the present study aims to address.

3.1 AI Role in Medical Imaging

Artificial intelligence has transformed medical imaging analysis, offering unprecedented capabilities in processing and interpreting complex visual data. The evolution of AI in medical imaging has progressed through several generations, from rule-based expert systems to sophisticated deep learning architectures capable of nuanced image interpretation (Esteva et al., 2021; Litjens et al., 2017).

Machine learning, particularly deep learning approaches, has emerged as the dominant paradigm in medical image analysis. These technologies leverage computational algorithms that can learn patterns from large datasets without explicit programming, enabling automated detection, classification, and characterization of abnormalities with increasing sophistication (Zakaria et al., 2022). Convolutional neural networks (CNNs) have proven particularly effective for medical image analysis due to their ability to automatically learn hierarchical image features from raw pixel data (Chan et al., 2020).

The performance of AI systems in medical imaging has shown remarkable advancement. McKinney et al. demonstrated AI's potential in their international evaluation of an AI system for breast cancer screening, achieving an absolute reduction of 5.7% and 1.2% in false positives and false negatives, respectively, compared to human radiologists (S. M. McKinney et al., 2020). This landmark study, with 1,868 citations, highlights AI's capacity to enhance diagnostic accuracy while potentially reducing interpretation workload.

Recent technical innovations have further expanded AI capabilities in medical imaging. Attention mechanisms direct computational focus to the most relevant image regions, mimicking human visual attention patterns (Schlemper et al., 2019). Transformer architectures, originally developed for natural language processing, have demonstrated superior performance in capturing long-range dependencies in medical images (Gheflati & Rivaz, 2021). Ensemble methods combining multiple models have shown improved robustness across diverse patient populations and imaging conditions (Ragab et al., 2022).

AI applications in medical imaging span multiple functions relevant to breast cancer detection. Detection and localization capabilities identify the presence and location of suspicious findings within images, with Ardila et al. demonstrating AI systems capable of detecting subtle lesions missed by human readers in 11% of cases (Ardila et al., 2019). Classification and characterization functions distinguish between benign and malignant findings and characterize lesion properties, with Rodriguez-Ruiz et al. showing AI classification performance comparable to expert radiologists, with an area under the receiver operating characteristic curve (AUC) of 0.89 versus 0.866 for human readers (Rodríguez-Ruiz et al., 2019).

Risk stratification capabilities assess likelihood of malignancy and prioritize cases for further investigation, with Yala et al. developing AI systems capable of stratifying breast cancer risk from imaging features with performance exceeding traditional clinical models (Yala et al., 2021). These capabilities demonstrate AI's potential to address multiple aspects of breast cancer detection challenges, with particular relevance to resource-constrained settings like Palestine where specialist expertise is limited and workload demands are high.

3.2 Applications in Breast Ultrasound

Artificial intelligence has demonstrated particular promise in breast ultrasound analysis, with applications spanning detection, characterization, and classification of breast lesions. These developments hold significant relevance for the Palestinian healthcare context, where ultrasound represents a widely available imaging modality.

AI systems have shown impressive capabilities in automatically detecting breast lesions in ultrasound images. Yap et al. demonstrated a CNN-based system that achieved 0.93, 0.18, and 0.92 for True Positive Fraction, False Positives per image, and F-measure respectively (Yap et al., 2018). Their approach outperformed junior radiologists in lesion detection, highlighting AI's potential to compensate for limited specialist availability.

Segmentation of breast lesions, which is the precisely delineating lesion boundaries, represents another important AI application in ultrasound analysis. Accurate segmentation facilitates

volumetric measurements and extraction of shape characteristics important for malignancy assessment. Khaled et al. developed a U-Net ensemble architecture for breast lesion segmentation achieving a Dice similarity coefficient of 0.68 compared to expert manual segmentation (Khaled et al., 2022). This high concordance with expert delineation demonstrates AI's potential to standardize this operator-dependent task.

Real-time detection capabilities have particular relevance for clinical workflow integration. Dai et al. demonstrated a real-time AI system for breast ultrasound that maintains a remarkable accuracy level of 38.7 mean average precision (mAP) while processing 54 frames per second during live ultrasound examinations (Q. Dai et al., 2024). Such real-time capabilities could provide immediate feedback during examinations, potentially improving lesion identification even with less experienced operators, a significant consideration for the Palestinian healthcare context where specialist availability is limited.

Building on real-time detection capabilities, Kumar et al. developed an automated and real-time segmentation system for suspicious breast masses using a convolutional neural network (V. Kumar et al., 2018). Their approach achieved a mean Dice coefficient of 0.82, a true positive fraction (TPF) of 0.84, and a false positive fraction (FPF) of 0.01 in mass detection with processing speeds suitable for clinical implementation, demonstrating the feasibility of integrating AI directly into the ultrasound examination workflow. This integration could significantly enhance diagnostic capabilities in settings with limited specialist availability.

Beyond detection, AI systems have shown impressive performance in distinguishing benign from malignant breast lesions on ultrasound. Byra et al. utilized transfer learning with pre-trained CNN models (ResNet, VGG, Inception) to classify breast lesions, achieving an AUC of 0.936 (Byra et al., 2019). This performance approached or exceeded that of experienced radiologists in comparative studies, suggesting AI's potential to enhance diagnostic accuracy.

AI systems have also demonstrated capability in characterizing specific lesion features according to standardized reporting systems. In a comparative analysis study of AI in diagnostic breast ultrasound, the Koios decision support system achieved an AUC of 0.693 (95% CI: 0.562–0.824), with a sensitivity of 92.5%, specificity of 35.3%, and an overall accuracy of 78.6% (Çelebi et al., 2025). Such automated assessment could standardize reporting and potentially reduce interpretation variability in settings with limited specialist availability, as demonstrated by the improvement in performance when less-experienced readers used the AI system compared to their unassisted performance (AUC of 0.655 vs. 0.512) .

Multiparametric assessment combining multiple ultrasound techniques (B-mode, elastography, Doppler) represents another promising direction. This approach leverages the full capabilities of modern ultrasound equipment to enhance diagnostic accuracy. Supporting this approach, Fleury et al. demonstrated in their study on breast elastography that when using a 75% cutoff value for the proportion of hard area within a breast mass, they achieved excellent interobserver agreement among experienced radiologists with an interclass concordance coefficient of 0.950. Their findings showed higher agreement levels among more experienced radiologists, highlighting the potential for standardized assessment when advanced ultrasound techniques are employed (Fleury & Marcomini, 2020).

While traditional AI approaches focus on static image analysis, recent advances have developed systems capable of analyzing ultrasound RF (Radio Frequency) time series data for enhanced breast lesion classification. Luo et al. demonstrated that temporal features extracted from ultrasound RF signals can improve diagnostic accuracy by capturing tissue dynamics that static images miss (Uniyal et al., 2015). Their approach achieved an AUC of 0. 0.86 (95% CI: 0.84–0.90), suggesting that temporal information provides valuable complementary diagnostic data.

Prospective clinical studies of AI integration in breast ultrasound have begun to emerge, providing real-world validation of these technologies. Park et al. conducted the first prospective feasibility study of a mobile AI solution for real-time detection and differential diagnosis in breast ultrasound (Lee & Cheng Tsui-Fen, 2024). Their study demonstrated 85% AUC in a clinical setting, highlighting the practical benefits of AI assistance in busy clinical environments with limited specialist availability.

These diverse AI applications in breast ultrasound demonstrate significant potential to address multiple dimensions of the breast cancer detection challenges identified in the Palestinian healthcare system, from improving diagnostic accuracy to enhancing workflow efficiency and standardizing quality in the context of limited specialist availability.

3.3 Enhancement and Preprocessing

Breast ultrasound imaging is a widely used modality for breast cancer detection and diagnosis due to its non-invasive nature, cost-effectiveness, and real-time imaging capabilities. However, ultrasound images often suffer from inherent limitations including speckle noise, low contrast, and artifacts that can degrade image quality and hinder accurate interpretation. The enhancement and preprocessing of breast ultrasound images have therefore become essential steps in improving diagnostic accuracy. This section reviews significant contributions to this field from the literature.

Kumar and Srivastava (A. Kumar & Srivastava, 2022) proposed a framework for denoising and enhancing breast ultrasound images using an extended complex diffusion-based filter in unsharp masking. Their method was tested on real ultrasound breast cancer images database and synthetic ultrasound images. Performance evaluation included qualitative and quantitative assessments with metrics such as mean squared error, peak-signal-to-noise ratio, and comparative analysis with pre-existing methods. The findings demonstrated that the proposed method effectively removes speckle noise that follows Rayleigh distribution, restores information and enhances abnormalities in ultrasound images, and preserves edges properly, thereby improving overall image quality.

Building on similar objectives of noise reduction and feature enhancement, Dabass and Dabass (Dabass & Dabass, 2021) developed an ensemble hybrid filter for denoising, edge correction, and enhancement of breast cancer ultrasound images to improve the accuracy of lesion categorization by addressing issues of noise and poor contrast. Their methodology incorporated Weiner filtering for noise removal, fuzzy derivatives and smoothing for edge preservation, and intensification membership function along with contrast limited adaptive histogram equalization for enhancement. Their findings showed that the proposed ensemble hybrid filter effectively denoises, corrects edges, and enhances breast cancer ultrasound images. Experimental results demonstrated

the feasibility of this approach, and the new technique compared favorably to traditional Weiner filtering methods.

Another approach focusing on noise reduction was the Anisotropic Diffusion Method for Speckle Noise Reduction in Breast Ultrasound Images (Radhi & Kamil, 2024), which specifically preserved important structural information while effectively reducing the speckle noise that commonly degrades ultrasound image quality. This method represents one of several specialized diffusion techniques developed for ultrasound enhancement. The study reported impressive quantitative results, with the proposed method combining an anisotropic diffusion filter and SRAD filter significantly improving image quality metrics, achieving the lowest MSE value of 0.2 and the highest PSNR value of 59.3. The method also showed significant improvement in UQI, SSI, and LMSE metrics, with optimal values for UQI and SSI of 1.00 and a decreased LMSE value of 0.003, confirming its ability to enhance overall image quality while preserving structural clarity.

In a related vein, Zhang et al. (Zhang et al., 2010) introduced a novel speckle reduction and contrast enhancement method based on fuzzy anisotropic diffusion. Their approach adaptively addressed the variable noise characteristics in different image regions, providing enhanced visibility of potential lesions while maintaining important diagnostic features. By incorporating fuzzy logic, their method offered additional flexibility in handling the inherent uncertainties in ultrasound image processing.

To provide a broader perspective on various enhancement techniques, Kumar and Srivastava (A. Kumar & Srivastava, 2023) conducted a qualitative and quantitative comparative study of different denoising and enhancement techniques for breast mammograms, ultrasound, and magnetic resonance images. Their comprehensive analysis provided benchmarking data across different imaging modalities, offering valuable guidance for selecting appropriate preprocessing techniques based on specific clinical requirements. This comparative approach highlights the importance of selecting the right method for particular imaging conditions.

Investigating the practical impact of preprocessing on diagnostic outcomes, Rodriguez-Cristerna et al. (Rodriguez-Cristerna et al., 2017) studied the effect of image preprocessing approaches on the segmentation and classification of breast lesions on ultrasound. Their work highlighted the critical role that preprocessing plays in subsequent analysis steps, demonstrating how appropriate enhancement techniques can significantly improve segmentation accuracy and classification performance. Specifically, they found that fuzzy enhancement followed by an interference-based speckle filter produced adequate lesion segmentation quality and acceptable classification performance, with effectiveness measured by a Jaccard index of 0.85 ± 0.05 for segmentation and an area under the ROC curve of 0.82 ± 0.02 for classification. This research established clear connections between preprocessing quality and diagnostic accuracy.

Continuing this comparative theme, Makwana, Yadav, and Gupta (Makwana et al., 2022) analyzed various noise reduction techniques for breast ultrasound image enhancement, providing a systematic comparison of different methods and their impact on image quality metrics. Their study contributed valuable benchmarking data for evaluating the performance of noise reduction algorithms in the context of breast ultrasound imaging, further emphasizing the need for rigorous evaluation frameworks.

Taking a more targeted approach to specific enhancement methods, Makandar and Halalli (Makandar & Halalli, 2015) developed a breast cancer image enhancement technique using Median Filter and CLAHE. Their method specifically addressed the challenges of low contrast and noise in breast images, with the median filter effectively removing speckle noise while preserving important boundary information, and CLAHE enhancing the contrast to highlight suspicious regions. This combination of filtering and contrast enhancement represents a practical approach to ultrasound image improvement.

Similarly focused on the dual goals of despeckling and contrast improvement, Tay et al. (Tay et al., 2010) explored ultrasound despeckling for contrast enhancement, developing techniques that simultaneously reduce speckle noise while enhancing the contrast of important features, thus improving the visibility of potential lesions and anatomical structures. Their integrated approach recognized the interconnected nature of noise reduction and contrast enhancement.

Njeh et al. (Njeh et al., 2011) proposed the SMU (SRAD median unsharp) approach for speckle noise reduction in breast ultrasound images, combining the strengths of speckle reducing anisotropic diffusion (SRAD), median filtering, and unsharp masking to effectively reduce noise while enhancing important image features. This hybrid approach leveraged multiple complementary techniques to achieve superior results compared to individual methods.

Moving beyond purely enhancement-focused work, Minavathi, Murali, and Dinesh (Dinesh, 2012) addressed the classification of masses in breast ultrasound images using image processing techniques, demonstrating how appropriate preprocessing can significantly improve the accuracy of computer-aided diagnosis systems in distinguishing between benign and malignant lesions. Their proposed algorithm achieved impressive diagnostic performance, with a sensitivity of 92.7% and an Area Under Curve (AUC) of 0.88 in classifying masses in breast ultrasound images. The use of SVM classifiers with different kernel functions contributed to the high accuracy of the classification process, and the improved sensitivity is expected to enhance early detection of breast cancer, potentially reducing mortality rates. Their work illustrates the direct connection between image enhancement and diagnostic classification.

Exploring novel theoretical frameworks, Bharti and Mittal (Bharti & Mittal, 2020) developed an ultrasound image enhancement method using neutrosophic similarity score. Their technique leveraged the neutrosophic set theory to enhance ultrasound images while preserving important diagnostic information, demonstrating promising results in improving image quality for clinical interpretation. Quantitatively, their method significantly enhanced ultrasound image quality by reducing noise and improving contrast, outperforming other methods in terms of mean brightness preservation, edge preservation, structural similarity, and human perception-based image quality assessment. Subjective evaluation showed a remarkable 44% improvement in image quality compared to original images. This represented an innovative application of advanced mathematical concepts to medical image enhancement.

Integrating preprocessing with segmentation, Elawady et al. (Elawady et al., 2016) proposed an automatic nonlinear filtering and segmentation method for breast ultrasound images, combining these steps in a cohesive framework to improve the detection and characterization of breast lesions.

This integrated approach recognized the interdependence of these processing stages for optimal diagnostic outcomes.

Addressing the directional nature of ultrasound speckle, Bhateja et al. (Bhateja et al., 2014) developed a modified speckle suppression algorithm for breast ultrasound images using directional filters. Their approach leveraged orientation information to better preserve important structural details while effectively removing speckle noise, resulting in enhanced image quality for diagnostic purposes. This direction-aware processing represented an important advance in context-sensitive enhancement.

For specialized applications beyond standard breast imaging, Adabi et al. (Adabi et al., 2019) presented a non-local based denoising framework for in vivo contrast-free ultrasound microvessel imaging. Their method effectively addressed the unique challenges of microvessel visualization in ultrasound images, enabling better assessment of vascular structures that may be indicative of malignancy. The performance metrics were particularly impressive, with their proposed non-local mean (NLM) filtering combined with top-hat morphological filtering (THF) providing a significant gain of more than 15 dB in signal-to-noise and contrast-to-noise ratios. The NLM+TH method outperformed other filtering methods like SVD and SVD+TH, with an average incremental gain of 18 dB in SNR and 10 dB in CNR. These substantial improvements effectively reduced background noise, improving microvessel visibility and outlining. This application to microvasculature highlighted the adaptability of enhancement techniques to specific diagnostic targets.

As machine learning began transforming medical imaging, Babu et al. (Vimala et al., 2023) presented an image noise removal technique in ultrasound breast images based on hybrid deep learning, combining the strengths of different neural network architectures to achieve superior noise reduction while preserving anatomical details. Their neural network approach (LPRNN) was effectively trained with mean square error and false recognition rates below 1.1% at the hundredth training iteration. Ultrasound images processed with the LPRNN showed significantly improved quality with SNRs greater than 65 dB, peak SNR ratios exceeding 70 dB, and edge preservation index values greater than 0.48. The proposed method demonstrated reduced noise sensitivity and better local speckle noise removal, enhancing clinical objectivity and manipulation. This computational approach represented the emerging trend of applying artificial intelligence to image enhancement challenges.

Similarly leveraging deep learning advances, Latif et al. (Latif et al., 2020a) proposed an ultrasound image despeckling and breast cancer detection method using Deep Convolutional Neural Networks (CNN). Their approach integrated despeckling and detection in a unified deep learning framework, demonstrating the potential of end-to-end learning approaches for ultrasound image analysis. The results were remarkable, with their proposed model achieving a classification accuracy of 99.89% for breast cancer detection using ultrasound images. Using a CNN despeckler and classifier resulted in an accuracy of 88.00%, outperforming other schemes in the literature. The effect of despeckling ultrasound images using neural networks significantly improved accuracy, showing the symbiotic relationship between enhancement and diagnostic performance. This integration of enhancement and diagnosis within a single neural network architecture pointed to future directions in automated processing.

Finally, focusing specifically on segmentation improvements, Gómez-Flores and Pereira (Flores & Pereira, 2017) developed a contrast enhancement method aimed at improving the segmentation of breast lesions on ultrasonography. Their technique addressed the challenges of low contrast between lesions and surrounding tissue, facilitating more accurate delineation of lesion boundaries for improved diagnostic accuracy. This targeted enhancement for segmentation underscored the importance of purpose-specific preprocessing.

The diverse approaches to enhancement and preprocessing of breast ultrasound images reflect the complexity of the challenge and the importance of this step in the overall diagnostic pipeline. These methods range from traditional filtering techniques to advanced computational methods and deep learning approaches, each offering unique strengths in addressing specific aspects of image quality improvement. The continued development of more effective preprocessing methods remains an important area of research in breast cancer imaging, with potential for significant impact on diagnostic accuracy and patient outcomes.

3.4 Tracking and Localization

Real-time tracking and detection systems represent a critical frontier in AI-enhanced breast ultrasound, offering transformative potential for both screening and interventional procedures. These systems address key limitations in conventional breast ultrasound, including operator dependency, inconsistent lesion localization, and challenges in monitoring lesion changes over time. By enabling immediate analysis during image acquisition, real-time systems fundamentally change how breast ultrasound can be utilized in clinical practice.

AI-powered real-time tracking systems have emerged as valuable tools for ultrasound-guided breast interventions, including biopsies and localization procedures. These systems help physicians precisely target lesions even when they are difficult to visualize directly in ultrasound images. Mendizabal et al. developed a physics-based deep neural network for real-time lesion tracking in ultrasound-guided breast biopsy. Their approach uses a U-Net architecture trained on synthetic data from finite element simulations to predict lesion displacement caused by probe pressure during the procedure. This system achieved comparable accuracy to traditional biomechanical models while being approximately 100 times faster, making it suitable for real-time clinical applications. This significant speed improvement without sacrificing accuracy illustrates how deep learning can overcome computational barriers that previously limited real-time applications.

Building on this foundation, Tagliabue et al. proposed a position-based modeling approach for tracking lesion displacement during ultrasound-guided breast biopsy (Tagliabue et al., 2019). Their method addresses the challenge of breast tissue deformation during probe manipulation, achieving real-time performance with a mean tracking error bellow 11 mm for all the tumors. This level of accuracy enables precise needle positioning even when target lesions are temporarily obscured by tissue deformation, a common challenge in breast interventions. The clinical importance of such precision becomes apparent when considering that even small targeting errors can lead to false-negative biopsies, potentially delaying cancer diagnosis and treatment.

For ultrasound-occult lesions initially identified on other imaging modalities, specialized tracking approaches have proven valuable. Hansen et al. developed a fusion-based ultrasound-guided biopsy system using 3D CT and 3D ultrasound co-registration in a phantom study (Hansen et al., 2019). Their approach utilized a specialized setup with a cone-shaped revolving water tank containing a 152-mm ultrasound transducer and needle insertion capability. The system could collect and reconstruct volumetric breast ultrasound data ($0.5\times0.5\times0.5$ mm³ voxel size) within 3 minutes. Lesion localization was achieved through rigid registration between breast CT and ultrasound data, with real-time lesion motion tracking during needle insertion using cross-correlation-based speckle tracking updated at 10 Hz. This phantom study demonstrated the feasibility of fusion-based ultrasound guidance for breast biopsies of ultrasound-occult lesions.

The integration of autonomy with AI-powered tracking represents an emerging frontier with significant potential. The authors proposed a real-time autonomous ultrasound robot trajectory planning framework for breast tissue scanning and suspicious tumor tracking (Tan et al., 2024). Their approach combines global scanning of breast tissue with real-time local tracking of suspicious tumor targets, utilizing an ultrasound target motion estimation algorithm and an acceleration-continuous online trajectory generation (ACOTG) algorithm. Experiments on breast phantoms demonstrated stable scanning with force fluctuations less than 5 N ± 15%, and the ability to maintain the suspected tumor target within ± 1 mm horizontally and 30 mm ± 10% in depth from the center of the acoustic window. While advanced robotic systems may not be immediately applicable in all Palestinian healthcare settings, the underlying tracking algorithms could enhance manual intervention capabilities in various clinical contexts. These technologies point toward future systems that could potentially reduce operator dependency while maintaining or improving targeting precision.

Beyond intervention guidance, real-time tracking systems offer valuable capabilities for monitoring breast lesions during treatment or across multiple examinations. Cario et al. designed an electronic marking clip for tracking breast cancer lesions through neoadjuvant chemotherapy using ultrasound identification (USID) (Cario & Oelze, 2022). This biocompatible electronic device transmits a unique identification signal when imaged with ultrasound pulse inversion, providing better localization and visualization compared to passive clips. The system can produce an audible indicator of a specific clip's presence and proximity to the probe, eliminating the need for insertion of additional markers. In testing, clips with six different USID tags were successfully visualized at 10 dB above the background signal. Such technology could enhance treatment monitoring in Palestinian oncology practice, where optimizing resource utilization through precise therapy assessment is particularly valuable (Falah et al., 2020; Giacaman et al., 2009). The ability to reliably track the same lesion over time allows for more accurate assessment of treatment response, potentially reducing the need for additional imaging studies or unnecessary biopsies.

Real-time tissue motion analysis provides another important dimension for lesion characterization. Peralta et al. conducted a comprehensive comparative study of four different displacement estimators for ultrasound elastography (USE) in breast cancer assessment (Peralta et al., 2023). Their evaluation compared the AM2D, GLUE, OVERWIND, and SOUL methods using radiofrequency ultrasound data from in silico and tissue mimicking phantoms as well as clinical data. The study assessed each method both as a standalone technique and in combination with a strain field enhancement technique called STREAL, which was developed using tissue mechanics-

based regularization. The findings revealed that the AM2D displacement estimator, despite being an older and computationally less complex method, performed exceptionally well when combined with tissue mechanics-based image processing. This combination delivered high contrast-to-noise ratio, signal-to-noise ratio, and preservation of tumor heterogeneity at both strain and stiffness image levels, while requiring significantly lower computation time compared to other estimation methods. Enhanced elastography through optimal motion tracking techniques could provide valuable complementary information to B-mode ultrasound, especially in settings where more advanced imaging modalities like MRI are less accessible. By extracting information about tissue stiffness, a key characteristic in differentiating benign from malignant lesions, these techniques effectively derive additional diagnostic value from existing ultrasound equipment, potentially enabling initial malignancy assessment at the bedside without requiring a biopsy.

The integration of co-registration technologies enables fusion of real-time ultrasound with other imaging modalities, expanding diagnostic capabilities. Kucukkaya et al. evaluated the use of a volume navigation technique for combining real-time ultrasound and contrast-enhanced MRI for breast lesion localization (Kucukkaya et al., 2016). Their study examined 38 women with single breast lesions, using 3-T MRI with a 3.5-minute CE-MRI sequence and a flexible body coil. Patients were imaged in the supine position with three breast markers, and real-time sonographic images were coregistered to preloaded CE-MRI volumes. The study demonstrated accurate lesion co-registration with mean misalignments of 3.9 ± 2.5 mm on the mediolateral view, 3.6 ± 2.7 mm on the anteroposterior view, and 4.3 ± 2.6 mm on the craniocaudal view. No lesion had a misalignment greater than 10 mm on any axis, and intermediate lesions (depth 11-20 mm) showed better accuracy (2.6 ± 1.9 mm) compared to deeper lesions (5.5 ± 2.2 mm). While advanced co-registration systems may have infrastructure requirements, simplified implementations could still provide value in tertiary Palestinian healthcare centers where multimodality imaging is sometimes available. These approaches help bridge the gap between the superior lesion detection capabilities of advanced imaging and the accessibility and real-time guidance benefits of ultrasound.

Achieving real-time performance in AI systems for breast ultrasound requires specialized computational approaches that balance accuracy with speed. Royer et al. developed a robust visual information and mechanical simulation approach for real-time target tracking of soft tissues in 3D ultrasound images (Royer et al., 2017). Their method combines robust dense visual tracking with mechanical simulation and introduces a new ultrasound-specific similarity criterion that is robust to illumination variation and shadows. The approach underwent in-depth validation through simulated data, phantom data, and real-data, with performance benchmarking against state-of-the-art techniques using 3D databases provided by MICCAI CLUST'14 and CLUST'15 challenges. This efficiency makes their approach potentially suitable for implementation in diverse healthcare settings, including those with limited computational resources. The technical innovation here lies in optimizing algorithms to work within practical hardware constraints while maintaining clinically acceptable performance.

For clinical interventional settings, Zachiu et al. created a real-time non-rigid target tracking system for ultrasound-guided clinical interventions (Zachiu et al., 2017). Their method employs the EVolution registration algorithm, which is robust to speckle noise and transient gray-level intensities by aligning similar contrast patterns rather than directly matching image intensities. Unlike previous approaches that assume rigid displacements in image sub-regions, this algorithm

integrates a matching criterion in a global functional, allowing estimation of an elastic dense deformation. The method was validated for soft tissue tracking under free-breathing conditions on the abdomen of seven healthy volunteers using both contact and standoff echography. Results demonstrated an average accuracy of ~1.5 mm with submillimeter precision while maintaining a computational performance of 20 images per second. This practicality is essential when considering implementation in resource-constrained environments like Palestinian healthcare facilities, where specialized computational hardware may be unavailable or difficult to maintain (AL-Tell, 2019; Mimi, 2015).

Recent advances in lightweight AI architectures have further improved the feasibility of real-time applications in diverse clinical settings. Kumar et al. developed a Multi U-net algorithm based on convolutional neural networks for automated and real-time segmentation of suspicious breast masses in ultrasound images (V. Kumar et al., 2018). Their prospective study included 258 female patients with suspicious breast masses who underwent clinical ultrasound scans and breast biopsies. The computer-aided detection tool effectively segmented breast masses with a mean Dice coefficient of 0.82, a true positive fraction (TPF) of 0.84, and a false positive fraction (FPF) of 0.01. By avoiding the need for initial seed positioning, the algorithm achieves real-time performance (13-55 ms per image), making it suitable for clinical applications. The system performed on par with a conventional seeded algorithm (mean Dice coefficient of 0.84) and significantly better ($P<0.0001$) than the original U-net algorithm. This approach exemplifies how AI systems can be tailored to perform effectively within computational constraints typical of resource-limited healthcare settings. These lightweight architectures represent a crucial development for bringing AI capabilities to settings where high-performance computing resources are limited.

The practical impact of real-time AI systems on clinical decision-making has begun to be formally evaluated through rigorous studies. Mango et al. investigated the impact of artificial intelligence decision support on breast ultrasound lesion assessment in a study titled "Should We Ignore, Follow, or Biopsy?" (Mango et al., 2020). Their multicenter retrospective review analyzed 900 breast lesions (52.2% benign, 47.8% malignant) evaluated by 15 physicians including radiologists, surgeons, and obstetrician/gynecologists. The AI system (Koios DS for Breast) assigned lesions to one of four categories: benign, probably benign, suspicious, and probably malignant. Results showed that the mean reader AUC improved from 0.83 with ultrasound only to 0.87 with ultrasound plus decision support. The AI system achieved a positive likelihood ratio of 1.98, higher than all but one reader. Importantly, decision support reduced interreader variability (Kendall τ-b improving from 0.54 to 0.68) and intrareader variability (class switching from BI-RADS 3 to 4A or above decreasing from 13.6% to 10.8%). This type of decision support could be particularly valuable in the Palestinian healthcare system, where optimizing resource utilization while maintaining diagnostic accuracy is crucial. By helping clinicians more confidently identify benign lesions that can safely be followed rather than biopsied, these systems could significantly reduce healthcare costs and patient anxiety.

Innovative imaging techniques that can be implemented in real-time provide additional diagnostic information during standard examinations. Sharma et al. evaluated real-time coherence imaging of suspicious breast masses recommended for aspiration or biopsy (Sharma et al., 2023). Their study implemented real-time short-lag spatial coherence (SLSC) imaging on an FDA-approved

clinical ultrasound scanner (Alpinion ECUBE12R) through GPU-based SLSC scripts they developed. The investigation included 47 hypoechoic breast masses from 32 patients, where board-certified breast radiologists first predicted mass contents and BI-RADS categories using conventional B-mode images, then repeated predictions with real-time SLSC images alongside B-mode images. The inclusion of SLSC images significantly improved diagnostic accuracy, resulting in correct identification of 100% of complicated cysts as BI-RADS 2 lesions (compared to only 50% with B-mode images alone). Additionally, SLSC correctly identified the presence of non-solid content in clusters of cysts while maintaining appropriate BI-RADS categorization for malignant masses. Such approaches that extract more diagnostic value from existing ultrasound equipment align well with resource optimization needs in settings like Palestine. The ability to derive multiple data types from a single imaging session maximizes the diagnostic yield of each patient encounter.

The integration of sequential image analysis in breast ultrasound offers valuable insights beyond what can be gleaned from single static images. Sellami et al. developed a method for breast cancer ultrasound images' sequence exploration using BI-RADS features' extraction (Sellami et al., 2015). Their research addressed a clinical need for precise breast cancer lesion characterization through careful extraction of BI-RADS features across ultrasound image sequences. The study demonstrated the feasibility of surveying changing characteristics of breast cancer lesions within ultrasound sequences, revealing variations in lesion form depending on the slice being analyzed, as well as differences in morphological and textural features throughout the sequence. This approach could enhance diagnostic performance in Palestinian healthcare settings by maximizing information extraction from standard ultrasound examinations. The authors proposed that these results could be assembled into a computer-aided diagnosis (CAD) system for clinical use, allowing radiologists to converge more rapidly and with greater precision to accurate clinical decisions while helping to avoid possible confusion between benign and malignant masses. By considering how lesions appear and change across multiple frames or timepoints, these systems capture dynamic information that often informs expert radiologists' assessments but has been difficult to incorporate into automated analysis.

The clinical validation of real-time AI systems in prospective studies represents an essential step toward widespread implementation. Lee and Tsui-Fen conducted the first prospective feasibility study of a mobile AI solution for real-time detection and differential diagnosis in breast ultrasound (Lee & Cheng Tsui-Fen, 2024). Their study, conducted from August to December 2023 in a tertiary medical center in Taiwan, evaluated CadAI-B (BeamWorks Inc., Korea), a mobile AI solution connected via HDMI or DVI to ultrasound equipment using a tablet PC. This system highlights suspicious areas during scanning and provides BI-RADS categories and malignancy scores (0-100%). Analysis of 33 patients (14 malignancies, 17 benign lesions, 2 normal cases) showed that CadAI-B successfully identified all malignancies with 100% sensitivity and 52.6% specificity. The overall diagnostic performance showed AUCs of 0.835 (malignancy score) and 0.850 (BI-RADS). For benign cases, CadAI-B categorized fewer cases as BI-RADS 4A or 4B compared to experts (50% versus 72.2%), indicating potential reduction in unnecessary biopsies. Such real-world validation provides crucial evidence for healthcare administrators and clinicians considering the adoption of these technologies in practice.

Collectively, these advances in real-time tracking and detection systems demonstrate significant potential to enhance breast cancer detection and management, particularly in settings with resource constraints. By enabling more precise interventions, improved lesion characterization, and optimized clinical decision-making, these technologies address key challenges in the Palestinian healthcare system, including limited specialist availability and the need for cost-effective diagnostic approaches. As these systems continue to evolve, they offer an increasingly viable pathway to enhance breast cancer care through the integration of AI with widely available ultrasound technology, potentially narrowing the gap in diagnostic capabilities between resource-limited and well-resourced healthcare environments.

3.5 Deep Learning Approaches

Breast cancer remains one of the most prevalent forms of cancer globally, necessitating accurate and efficient diagnostic methods. In recent years, deep learning techniques have revolutionized the field of medical image analysis, including breast ultrasound imaging. This section reviews significant contributions in applying deep learning approaches to breast cancer detection, classification, and diagnosis using ultrasound images.

Meena and Muthu (L. C & Joe, 2024) proposed an optimal deep learning-based breast cancer detection system with a five-phase approach that systematically addresses the challenges in breast cancer image analysis. Their methodology incorporated preprocessing for noise removal using Wiener filter and contrast enhancement, segmentation with a dilated convolution-based U-shaped network (DCUNet), feature learning using spatial and channel attention with densely connected convolutional network-121 (SCADN-121), feature selection with enhanced cuckoo search optimization (ECSO) algorithm, and classification through ECSO-tuned long short-term memory (ECSO-LSTM). This comprehensive approach achieved an impressive accuracy of 99.86% in classifying breast cancer into normal, benign, and malignant classes, demonstrating superior performance compared to existing state-of-the-art methods.

Building on similar multi-phase frameworks, Mohammed et al. (Mohammed et al., 2023) developed a deep learning system for breast cancer classification from ultrasound images. Their methodology focused on enhancing image quality, segmenting images with U-Net architecture, and extracting features with Mobilenet, followed by system accuracy evaluation. The system achieved a high accuracy of 99.29% in classifying breast cancer types from ultrasound images, exceeding the performance of previous works and indicating significant improvement in breast cancer diagnosis. Similarly, Raza et al. (Raza et al., 2023) introduced a novel deep learning model called DeepBreastCancerNet for breast cancer detection and classification using ultrasound images. Their 24-layer architecture comprised six convolutional layers, nine inception modules, and one fully connected layer, utilizing clipped ReLu and leaky ReLu activation functions with batch normalization and cross-channel normalization. This innovative approach achieved an impressive classification accuracy of 99.35% on their primary dataset and 99.63% when validated on another dataset, demonstrating the model's robustness and generalizability.

While these complex architectures have shown remarkable results, other researchers have explored the efficacy of established networks through transfer learning. Han et al. (Han et al., 2017) developed a deep learning framework using GoogLeNet to classify breast lesions in ultrasound

images. Their methodology involved creating a biopsy-proven benchmarking dataset from 5151 patient cases with 7408 ultrasound images, which included semi-automatically segmented lesions. The preprocessing steps comprised histogram equalization, image cropping, and margin augmentation, with GoogLeNet trained both with and without data augmentation. This framework achieved an accuracy of about 90%, a sensitivity of 0.86, and a specificity of 0.96 in differentiating benign and malignant lesions, making it a valuable tool to support radiologists in clinical settings by quickly classifying malignant lesions.

Advancing the exploration of deep learning architectures, Paçal (Pacal, 2022) conducted a comparative study of various deep learning models for classifying breast cancer in ultrasound images. The methodology involved evaluating different CNN architectures (AlexNet, VGG, ResNet, GoogleNet, EfficientNet) and transformer models using the BUSI dataset, employing transfer learning due to limited dataset size and applying data augmentation techniques such as flipping and rotation. The results revealed that the vision transformer model outperformed other architectures with 88.6% accuracy, 90.1% precision, 87.4% recall, and 88.7% F1-score, indicating the potential of transformer-based approaches in this domain. This comparative analysis provided valuable insights into the relative strengths of different architectures, guiding future research directions.

Focusing specifically on the benefits of transfer learning, Hijab et al. (Hijab et al., 2019) investigated breast cancer classification in ultrasound images using three distinct training approaches: a baseline CNN trained from scratch, a transfer-learning approach using a pre-trained VGG16 CNN further trained with ultrasound images, and a fine-tuned learning approach with optimized deep learning parameters to overcome overfitting. The fine-tuned model demonstrated superior performance with 0.97 accuracy and 0.98 AUC, confirming that pre-training on ultrasound images can significantly enhance deep learning outcomes in biomedical applications. This study highlighted the value of leveraging pre-existing knowledge in neural networks, particularly in medical domains where training data may be limited.

Continuing the exploration of transfer learning, Jabeen et al. (Jabeen et al., 2022) proposed a framework for breast cancer classification using probability-based optimal deep learning feature fusion. Their methodology incorporated data augmentation to increase the dataset size, utilization of a pre-trained DarkNet-53 model with modified output layer, training using transfer learning, feature extraction from the global average pooling layer, feature selection using RDE and RGW optimization algorithms, and feature fusion using a probability-based serial approach combined with machine learning algorithms for classification. This comprehensive approach achieved a high accuracy of 99.1% on the augmented BUSI dataset, outperforming recent techniques in breast cancer classification and demonstrating the effectiveness of sophisticated feature fusion strategies.

Taking a complementary approach that combined generative models with transfer learning, Chaudhury and Sau (Chaudhury & Sau, 2023) proposed a deep learning-based framework for breast mass classification using ultrasound images that incorporated GAN-based data augmentation and transfer learning for feature extraction. Their methodology utilized the Breast Ultrasound Images (BUSI) dataset, classified images into normal, benign, and malignant categories, and employed feature fusion with histogram equalization as preprocessing steps. This framework achieved an outstanding accuracy of 99.6%, outperforming existing methods and

demonstrating the potential of combining generative models with transfer learning for breast ultrasound categorization. The success of this approach underscores the value of data augmentation in improving classification performance, particularly for medical imaging applications where dataset size and diversity can be limiting factors.

Moving beyond static images to leverage temporal information, Chen et al. (Chen et al., 2021) developed a novel deep learning model for breast cancer diagnosis using contrast-enhanced ultrasound (CEUS) videos. Their approach employed a 3D convolutional neural network backbone enhanced with domain-knowledge-guided temporal attention and channel attention modules, validated on a Breast-CEUS dataset of 221 cases. The model achieved a sensitivity of 97.2% and an accuracy of 86.3%, with domain knowledge incorporation improving sensitivity by 3.5% and specificity by 6.0%, highlighting the value of domain expertise in neural network design. This work represents an important step toward utilizing the rich temporal information available in ultrasound videos, which is often lost in static image analysis.

Addressing the dual challenges of image quality and classification, Latif et al. (Latif et al., 2020b) proposed two Convolutional Neural Network (CNN) models for ultrasound breast cancer images: one for despeckling and another for classifying them into benign or malignant categories. The despeckling CNN estimated the original image from noisy data, while the classification CNN incorporated multiple convolutional and pooling layers with stochastic gradient descent for weight optimization. Tested on the Mendeley Breast Ultrasound dataset, their model achieved a remarkable classification accuracy of 99.89%, with the CNN despeckler and classifier combination reaching 88.00% accuracy, demonstrating the significant impact of neural network-based despeckling on classification performance. This integrated approach to denoising and classification exemplifies how addressing image quality issues can directly enhance diagnostic accuracy.

Similarly focusing on the Palestinian healthcare context, Qasrawi et al. (Qasrawi et al., 2025) developed a hybrid ensemble model combining Contrast Limited Adaptive Histogram Equalization (CLAHE) with an Ensemble Deep Random Vector Functional Link Neural Network (edRVFL) for breast ultrasound analysis. Using 4103 ultrasound images from the Dunya Women's Cancer Center in Palestine, their approach achieved 96% accuracy for benign and 98% for malignant cases. The study further integrated YOLOv5 with MedSAM foundation model for lesion segmentation, achieving a Dice Similarity Coefficient of 0.988, demonstrating the effectiveness of combining enhancement techniques with ensemble learning in resource-constrained settings.

Building on the concept of ensemble methodologies, Ragab et al. (Albukhari et al., 2022) introduced an Ensemble Deep-Learning-Enabled Clinical Decision Support System (EDLCDS-BCDC) for diagnosing and classifying breast cancer using ultrasound images. Their comprehensive methodology incorporated Wiener filtering for noise elimination and contrast enhancement, image segmentation using Chaotic Krill Herd Algorithm with Kapur's entropy, feature extraction through an ensemble of VGG-16, VGG-19, and SqueezeNet deep learning models, and classification via Cat Swarm Optimization with Multilayer Perceptron. This sophisticated approach achieved a high accuracy rate of 97.09%, outperforming comparable methods and demonstrating the value of ensemble techniques in clinical decision support. The

integration of multiple deep learning models with optimization algorithms represents a powerful paradigm for enhancing diagnostic accuracy.

Focusing on clinical applicability, Qi et al. (Qi et al., 2019) developed an automated breast cancer diagnosis model using deep convolutional neural networks with multi-scale kernels and skip connections. Their two-component approach focused on detecting malignant tumors and recognizing solid nodules, incorporating a region enhance mechanism based on class activation maps and a cross training algorithm. Evaluated on a large annotated dataset of 8145 images, their model outperformed state-of-the-art approaches and achieved performance comparable to human sonographers, making it suitable for clinical applications. This work demonstrates the potential of deep learning to reach human-level diagnostic capabilities in specific medical imaging tasks.

Exploring object detection methodologies for breast ultrasound analysis, Chiao et al. (Chiao et al., 2019) utilized the Mask R-CNN architecture for automatic detection, segmentation, and classification of breast lesions from ultrasound images. Their approach provided a noninvasive and comprehensive screening method, achieving a mean average precision of 0.75 for detection and segmentation of breast lesions, with an overall accuracy of 85% for benign/malignant classification, demonstrating the potential of region-based convolutional networks in this domain. The simultaneous handling of detection and segmentation represents an important advancement in automating the complete diagnostic workflow.

In a similar vein but using different object detection architectures, Labcharoenwongs et al. (Labcharoenwongs et al., 2023) proposed an artificial intelligence system for automatic breast tumor detection and classification, including tumor volume estimation. Their methodology utilized the YOLO7 architecture for tumor detection, localization, and classification, combined with a simple pixel per metric technique for automatic tumor volume estimation. The system was designed for integration into conventional breast ultrasound machines to assist radiologists in breast cancer diagnosis, achieving high performance metrics in distinguishing between benign and malignant breast lesions. This practical approach to implementation highlights the increasing focus on clinical integration of AI technologies.

Further advancing object detection approaches, Samanta et al. (Samanta et al., 2023) employed a modified YOLOv8 model to improve breast cancer detection from ultrasound images. Their methodology involved preprocessing for image enhancement and removal of labels and pectoral muscles, followed by dataset annotation, augmentation, and division into training (70%), validation (15%), and testing (15%) sets. The model achieved impressive performance metrics with a mean average precision (mAP) of 99.5%, recall of 98.40%, and accuracy of 96.50%, outperforming other state-of-the-art methods in breast ultrasound cancer detection. This work demonstrates the rapid evolution of object detection architectures and their increasing effectiveness in medical imaging applications.

Contributing to the object detection literature, Aly et al. (Aly et al., 2021) developed a YOLO-based computer-aided diagnosis system for detecting and classifying breast masses in mammograms. Although focused on mammography rather than ultrasound, their approach offers valuable insights for ultrasound image analysis. Their methodology involved preprocessing mammograms from DICOM format to images without data loss, employing YOLO for mass

detection and classification with anchors in YOLO-V3 using k-means clustering for improved accuracy. The system achieved detection accuracy of 89.4% and classification accuracy of 94.2% for benign and 84.6% for malignant masses, demonstrating the potential of YOLO architectures in breast imaging analysis. The cross-modality relevance of these findings highlights common challenges and solutions in breast cancer imaging.

Expanding on YOLO-based approaches for mammography, Qasrawi et al. (Qasrawi et al., 2024) proposed a hybrid model integrating DenseNet121, edRVFL, and comprehensive image preprocessing including CLAHE, Gaussian Blur, and sharpening techniques. Tested on 20,000 mammograms with clinical validation on 800 patients, their system achieved 99.7% accuracy with 0.75-second processing time. The integration of YOLOv5 and MedSAM segmentation for lesion boundary delineation, combined with Grad-CAM analysis for interpretability, demonstrated the potential of hybrid architectures for clinical breast cancer detection.

Addressing the perennial challenge of limited data in medical imaging, Al-Dhabyani et al. (Al-Dhabyani et al., 2019) focused on data augmentation techniques for breast ultrasound image classification, proposing a new methodology using Generative Adversarial Networks (GANs) combined with traditional augmentation methods. Their approach evaluated two breast ultrasound image datasets and employed deep learning approaches for classification, including Convolutional Neural Network (CNN) and Transfer Learning (TL). The results showed that the integration of traditional and GAN-based data augmentation methods resulted in higher accuracies for breast ultrasound image classification, with augmentation methods particularly enhancing transfer learning performance. Importantly, the study addressed the shortage of public datasets by making the BUSI dataset publicly available for researchers, contributing significantly to the research community's resources.

Taking a hybrid approach that combined traditional machine learning with deep learning, Zheng et al. (Zheng et al., 2020) introduced a Deep Learning assisted Efficient Adaboost Algorithm (DLA-EABA) for breast cancer detection. Their methodology incorporated CNN-based transfer learning across various imaging modalities with a deep learning framework comprising convolutional layers, LSTM, and Max-pooling layers, followed by fully connected and softmax layers for classification and error estimation. This hybrid approach combining machine learning with feature selection and extraction methods achieved impressive performance metrics with an accuracy of 97.2%, sensitivity of 98.3%, and specificity of 96.5%. This work demonstrates how traditional machine learning and deep learning can be synergistically combined to leverage the strengths of both paradigms.

Examining the practical implementation of deep learning in clinical settings, Becker et al. (BeCkeR et al., 2018) evaluated a generic deep learning software originally designed for industrial image analysis for diagnosing breast cancer in breast ultrasound images. Their retrospective study of breast ultrasound examinations from a clinical setting involved training the deep learning system on 70% of images and validating on 30%, with three human readers of varying expertise evaluating the validation set for comparison. The results showed that the deep learning software could diagnose breast cancer with accuracy comparable to radiologists, learning faster and better than inexperienced human readers and enabling real-time analysis during ultrasound examinations.

This study provides valuable insights into the practical deployment of AI systems in clinical workflows.

Providing a broader perspective on the field, Ayana et al. (Ayana et al., 2021) conducted a comprehensive review of previous studies on using transfer learning for breast cancer detection via ultrasound imaging. Their methodology involved summarizing existing methods, identifying advantages and shortcomings, and comparing different works from the perspective of transfer learning approaches, pre-processing, pre-training models, and CNN architectures. The review identified potential future research directions for applying transfer learning in ultrasound imaging for breast cancer detection and diagnosis, providing valuable guidance for researchers in this rapidly evolving field. This meta-analysis of approaches helps contextualize individual contributions within the broader landscape of breast cancer imaging research.

Deep learning approaches have significantly advanced breast cancer detection, classification, and diagnosis using ultrasound images, with various architectures and methodologies demonstrating high accuracy rates often exceeding 95%. The progress spans from specialized CNN architectures to transfer learning approaches, object detection frameworks, and ensemble methods, each offering unique advantages. Future research directions include further integration of domain knowledge, exploration of multimodal approaches, and development of explainable AI systems to enhance clinical adoption and trust. The remarkable performance metrics achieved by these deep learning methods suggest their potential to serve as valuable assistive tools for radiologists in clinical practice, potentially improving diagnostic accuracy and efficiency in breast cancer detection.

Chapter Four : Methodology

This chapter outlines the comprehensive methodology employed in this research, which integrates data curation, preprocessing, machine learning, and evaluation to develop a robust framework for automated breast ultrasound video interpretation. The methodology is structured into several key components, each designed to address specific challenges in medical imaging and ensure the reliability and accuracy of the proposed system. **Figure 4.1** provides an overview of the overall methodology, illustrating the workflow from enhancement and preprocessing to model training, validation, and performance evaluation.

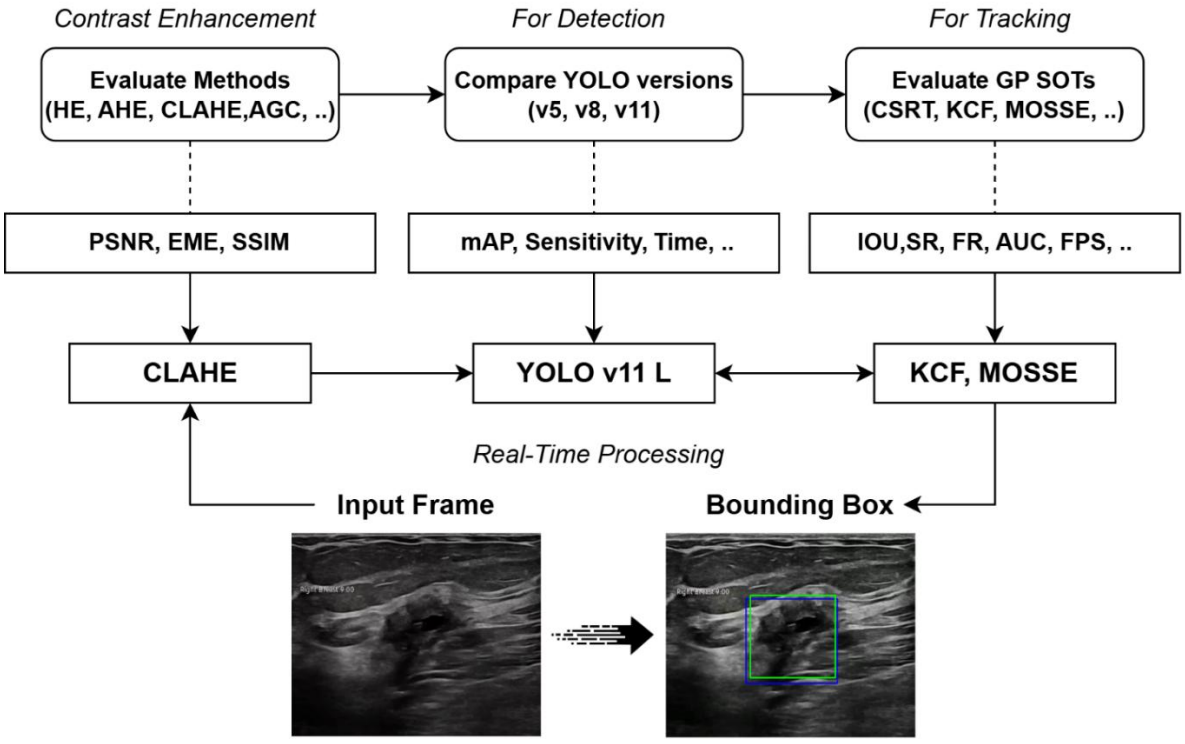

Figure 4.1: Overview of the Proposed Methodological Framework for Automated Breast Cancer Interpretation in Ultrasound Video sequences

4.1 Data Curation

Data curation is a critical component of this research, encompassing the entire lifecycle of data management, from ethical considerations and acquisition to preprocessing and preparation for analysis. This section outlines the systematic approach taken to ensure the quality, integrity, and usability of the dataset, which serves as the foundation for developing robust and generalizable machine learning models. The curation process begins with securing ethical approvals and ensuring patient confidentiality, followed by the collection of diverse ultrasound data from multiple clinical settings. The data is then meticulously prepared, annotated, and augmented to address challenges such as class imbalance, variability in imaging conditions, and the need for high quality labeled data. Each step in the curation pipeline is designed to uphold the highest standards of data quality, ensuring that the dataset is both representative of real-world clinical scenarios and suitable for advanced computational analysis. The following subsections provide a detailed account of the ethical framework, data collection methodology, screening instruments, and the technical steps involved in data preparation, annotation, and augmentation.

4.2 Ethical statement

This research was conducted under full ethical oversight, with primary approval granted by the Deanship of Scientific Research at Al-Quds University - Abu Dis. The study protocol underwent rigorous review and received formal endorsement from both the university's Institutional Review Board (IRB) and the respective ethical review committees of all participating healthcare facilities. Prior to data collection, comprehensive ethical clearance was secured from each participating hospital's administration and ethics committee.

The research team implemented a robust framework for data protection and patient confidentiality. All patient-identifiable information, including but not limited to names, contact details, medical record numbers, and specific dates of treatment, was systematically removed from the patient profiles during the data extraction process. The de-identification procedure followed standardized protocols to ensure full compliance with both institutional requirements and international standards for the protection of human subjects in medical research.

4.3 Data Collection

The data collection process was strategically designed to encompass diverse clinical settings, ensuring the development of a robust and generalizable model. The research team implemented a systematic, multi-phase data collection approach across two major healthcare facilities in the region.

The initial phase focused on collecting historical ultrasound images from the Dunya Women's Cancer Center spanning a five-year period (2018-2023). The dataset comprised 11,382 ultrasound cases derived from 590 unique female patients. Among these, 4,285 cases belong to 25 patient were accompanied by corresponding biopsy records and results, providing crucial ground truth data for model validation. All imaging data was standardized and archived in Digital Imaging and

Communications in Medicine (DICOM) format, ensuring compatibility with medical imaging standards and facilitating future interoperability.

The second phase, conducted at Augusta Victoria Hospital, focused on collecting recent ultrasound video data (2024-2025). This phase yielded 40 comprehensive video recordings, each accompanied by detailed radiological reports. Five of them included confirmatory biopsy results, which were utilized in the final clinical validation of the proposed framework. The remaining 35 videos were systematically segmented into individual frames, generating an additional 6,520 cases for analysis.

Table 4.1: Summary of Data Collection Sources and Volumes

Healthcare Facility	Data Type	Collection Period	Number of Patients	patients with biopsy	Total Cases
Dunya Women's Cancer Center	Dicom Images	2018-2023	559	25	11,383
Augusta Victoria Hospital	Video Sequences	2024-2025	40	5	6,520

As shown in **Table 4.1**, these datasets consist of three classes: cancers, benign lesions, and normal tissue images. The distribution of these image categories is illustrated in **Figure 4.2**.

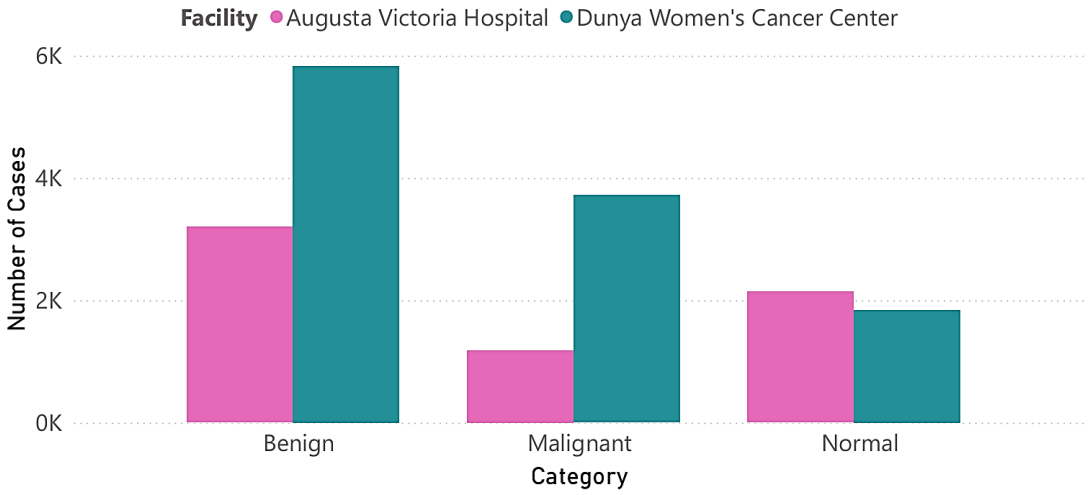

Figure 4.2: Distribution of Image Categories by Facility and Diagnostic Class

4.4 Screening Instrument

The ultrasound data used in this study was collected using the Samsung RS85 Prestige ultrasound system (Samsung Medison Co., Ltd., Korea). The system features Crystal Architecture technology combining CrystalBeam and CrystalPure imaging engines, with a high-frequency linear array transducer (L3-12A) used for breast imaging acquisition. Images were displayed on the system's 27-inch OLED monitor, providing high-resolution visualization during the data collection process. The system's advanced imaging capabilities, including S-Shearwave Imaging for tissue

elastography and S-Detect for computer-aided diagnosis, enabled comprehensive ultrasound data capture for subsequent analysis (Healthcare Global, 2025).

4.5 Data Preparation

The preparation and processing of the collected ultrasound data encompassed multiple systematic stages, each meticulously designed to serve specific purposes within the proposed framework. The raw ultrasound scan data was initially stored on physical CDs, with each patient's record containing a complete ultrasound scan data alongside detailed radiologist findings and reports. Following the rigorous data collection process from participating healthcare facilities, the research team implemented a sophisticated data security protocol that began with a comprehensive anonymization of all patient information. This was followed by careful data extraction from the CDs and subsequent transfer to an encrypted, secure local storage device, where all ultrasound scans were maintained in standardized DICOM format to ensure data integrity and compatibility.

Under the direct supervision of volunteer expert radiologists from the participating healthcare facilities, a careful classification process was undertaken. This involved the systematic examination of each ultrasound scan, where DICOM series were carefully split into individual JPG format slices while maintaining the diagnostic integrity of each image. The expert radiologists provided comprehensive interpretation for each slice, enabling accurate categorization into three primary diagnostic categories: normal tissue, benign lesions, and malignant findings. This classification process adhered to standardized criteria and underwent multiple quality assurance checks by the supervising radiologists to ensure consistency and accuracy.

The data preparation pipeline was consistently applied across both datasets, with particular attention paid to maintaining standardization throughout the process. The training dataset preparation involved the systematic organization of classified images, while ensuring standardization of image formats and resolutions. For the clinical validation dataset, specific cases with confirmatory biopsy results were selectively excluded from the general training pool. These cases underwent a specialized conversion process from sequential DICOM format to MP4 video format, preserving all original diagnostic information for comprehensive analysis.

Throughout the entire preparation process, robust quality control measures were consistently implemented. This included regular validation of classification accuracy, thorough verification of data integrity following format conversions, and comprehensive documentation of any technical anomalies encountered. The final datasets were structured to support both machine learning model development and clinical validation purposes, with the training dataset comprising classified static images suitable for supervised learning, and the validation dataset containing selected video sequences with corresponding biopsy confirmations. This approach of data preparation established a solid foundation for the subsequent training procedures and validation scenarios, which are extensively discussed in the following sections of this research.

4.6 Annotation and Labeling

The collected ultrasound images underwent a comprehensive annotation process under the supervision of expert radiologists from the participating healthcare facilities. This process was crucial for generating high-quality labeled data to train the YOLO object detection models effectively (H. D. Cheng et al., 2010). The annotation workflow was carried out using the Roboflow platform (Roboflow, 2020), which provided a user-friendly interface for the radiologists to delineate regions of interest (ROIs) corresponding to cancerous lesions, benign lesions, and normal tissue. The radiologists followed standardized guidelines and protocols, such as the Breast Imaging Reporting and Data System (BI-RADS) (L. Shen et al., 2019), to ensure consistency and accuracy in the labeling process, assigning specific class labels (cancer, benign, or normal) to each ROI based on their expert interpretation and diagnosis.

To further validate the annotations, a subset of the labeled images underwent additional review by a panel of senior radiologists. This quality assurance step helped to identify and rectify any potential errors or inconsistencies in the annotations, ensuring the reliability of the ground truth data. The annotated ultrasound images were then organized into a structured dataset, with each image accompanied by its corresponding bounding box coordinates and class labels. This labeled dataset served as the foundation for training the YOLO object detection models, enabling them to learn the distinguishing features and patterns associated with cancerous lesions, benign lesions, and normal tissue. The annotation process, although time-intensive, was essential for developing robust and accurate object detection models capable of automatically identifying and localizing lesions in breast ultrasound images (Huang et al., 2018).

4.7 Data Augmentation

Data augmentation is a crucial step in the development of robust machine learning models, particularly in medical imaging, where datasets are often limited in size and diversity. By artificially expanding the training dataset through various transformations, data augmentation helps improve model generalization, reduce overfitting, and enhance performance on unseen data. In this research, data augmentation was systematically applied to the collected breast ultrasound images and video frames to ensure the model's ability to handle variations in image appearance, orientation, and scale, which are common in real-world clinical scenarios.

The augmentation pipeline was designed to simulate a wide range of imaging conditions, including variations in brightness, contrast, rotation, scaling, and noise levels. These transformations were carefully selected to reflect the natural variability encountered in ultrasound imaging, such as differences in probe positioning, patient anatomy, and imaging settings. The augmentation process was implemented using the Albumentations library (Buslaev et al., 2020), a powerful tool for image augmentation that supports a wide range of transformations and ensures efficient processing of large datasets.

The augmented dataset was then used to train the YOLO-based object detection models, enabling them to learn robust features that generalize well to unseen data. By incorporating a diverse range

of imaging conditions, the augmentation process significantly improved the model's ability to detect and localize lesions in breast ultrasound images, even in challenging cases with low contrast or high noise levels.

In addition to improving model performance, data augmentation also played a key role in addressing class imbalance in the dataset. By applying targeted augmentations to underrepresented classes, such as malignant lesions in our case, the augmentation process helped ensure that the model was equally capable of detecting all lesions, regardless of their prevalence in the dataset.

4.8 Contrast Enhancement

This research systematically evaluated four contrast enhancement techniques for breast ultrasound images: Histogram Equalization (HE), Adaptive Histogram Equalization (AHE), Adaptive Gamma Correction with Weighting Distribution (AGCWD), and Contrast-Limited Adaptive Histogram Equalization (CLAHE). Our primary focus was on CLAHE optimization, where we tested multiple clip limit values (0.5, 1, 2, 4, 8, and 20) to identify the optimal balance between enhancement quality and computational efficiency. The implementation utilized the OpenCV library with standardized parameter settings across all methods except for the varying clip limits in CLAHE (Dr Dobb's, 2005). We processed a representative subset of 150 breast ultrasound images through each enhancement technique and quantitatively evaluated the results using the metrics described in **section 4.11.1**. The enhanced images were visually inspected by experienced radiologists to confirm their diagnostic acceptability, ensuring that the enhancement preserved clinically relevant features while improving visibility. Based on these evaluations, we selected the optimal contrast enhancement method for integration into the complete detection and tracking pipeline.

4.9 Object Detection

Our lesion detection component employed the YOLO (You Only Look Once) family of algorithms, specifically comparing YOLOv5, YOLOv8, and YOLOv11 variants for breast lesion detection in ultrasound images. For each YOLO version, we tested multiple model sizes (medium, large, and extra-large) to identify the optimal architecture for our application. Models were implemented using the Ultralytics framework (Varghese & Sambath, 2024) with PyTorch backend (Paszke et al., 2019). We trained each model on our curated and annotated dataset of breast ultrasound images using transfer learning from pretrained weights on the COCO dataset. The training process utilized an SGD optimizer with a learning rate of 0.01, momentum of 0.937, and weight decay of 0.0005. We employed a cosine annealing learning rate scheduler with initial warmup epochs. Data augmentation techniques including random horizontal flips, rotations (±15°), and brightness/contrast adjustments were applied during training to improve model generalization. Additionally, we experimented with three training approaches: single-dataset training, combined-dataset training, and transfer learning between datasets (TL12 and TL21). For the transfer learning approach, we first trained on one dataset and then fine-tuned on the second to leverage knowledge transfer between the two sources. All models were trained for 250 epochs

with early stopping monitoring validation loss with a patience of 30 epochs. The performance of each model was evaluated using the metrics described in **section 4.11.2**.

4.10 Object Tracking

Our research developed tracking capabilities for maintaining lesion identity across ultrasound video frames, implementing both traditional single object tracking (SOT) algorithms and a novel hybrid approach that combines tracking with detection-based verification. This hybrid approach allows the system to automatically trigger the YOLO detector to reacquire the target when tracking confidence falls below a predetermined threshold, providing a robust recovery mechanism for challenging ultrasound sequences (Marvasti-Zadeh et al., 2019).

4.10.1 Single Object Tracking (SOT)

We implemented and evaluated seven traditional SOT algorithms for breast lesion tracking in ultrasound videos: CSRT (Channel and Spatial Reliability Tracking), TLD (Tracking Learning Detection), MOSSE (Minimum Output Sum of Squared Error), KCF (Kernelized Correlation Filter), Boosting, MedianFlow, and MIL (Multiple Instance Learning). Each tracker was initialized with the ground truth bounding box in the first frame of the video sequence and tasked with maintaining the lesion's location in subsequent frames. The implementation utilized OpenCV's tracking API (cv2.Tracker) with default parameters for each algorithm (Dr Dobb's, 2005). We validated these trackers on five biopsy-confirmed ultrasound video sequences containing both benign and malignant lesions. Each tracker was evaluated on its ability to maintain accurate boundary alignment with the lesion, recover from brief occlusions, adapt to changes in lesion appearance, and operate efficiently. The comparative performance was measured using the metrics detailed in **section 4.11.3**, with special attention to the trade-off between tracking accuracy and computational efficiency. This evaluation identified the most promising base trackers for integration into our hybrid tracking framework.

4.10.2 Hybrid Detection-Based Tracking (DBT)

Traditional tracking algorithms like Kernelized Correlation Filter (KCF) and Minimum Output Sum of Squared Error (MOSSE) offer impressive speed but can suffer from drift and may lose objects during occlusions or rapid movements (Henriques et al., 2015). On the other hand, more sophisticated trackers like Discriminative Correlation Filter with Channel and Spatial Reliability (CSRT) provide better accuracy but at the cost of higher computational complexity, making them less suitable for real-time applications (Lukežič et al., 2018).

To address these limitations, we propose a hybrid detection-tracking framework that leverages the strengths of both approaches. In our implementation, a YOLO-based detector is used to initialize the tracker and serves as a recovery mechanism when tracking fails. This architecture allows us to utilize computationally efficient trackers like KCF and MOSSE, which can operate at high frame rates, while maintaining reliability through periodic detection-based verification and reinitialization (Wang et al., 2018).

As shown in **Figure 4.3**, The system operates in two primary modes: tracking and detection-based recovery. During normal operation, the tracker maintains object location using lightweight correlation filtering techniques, providing fast and efficient frame-to-frame tracking. However, when the tracking confidence falls below a predetermined threshold or significant changes in object appearance are detected, the system automatically triggers the YOLO detector to reacquire the target (Zhang et al., 2018).

This hybrid approach offers several advantages for ultrasound video analysis. First, it maintains real-time performance by primarily relying on efficient tracking algorithms. Second, it provides robustness against common tracking failures through automatic detection-based recovery. Third, it adapts to changes in object appearance and temporary occlusions that are common in ultrasound imaging, such as when the probe moves or tissue deformation occurs (S. Liu et al., 2019).

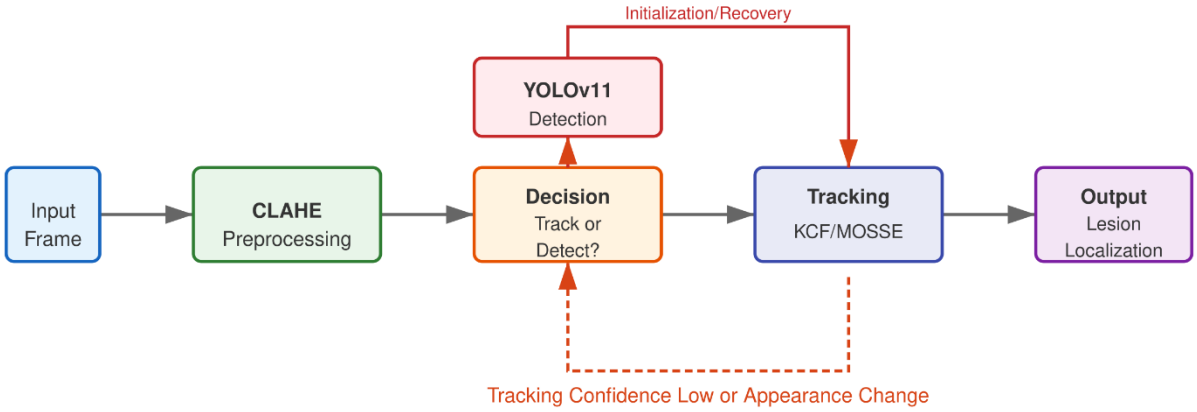

Figure 4.3: Object Tracking Pipeline with Automatic Detection-based Recovery

4.11 Testing and Evaluation

The performance of the proposed methods was rigorously evaluated using quantitative metrics. This section outlines the evaluation methodologies and performance metrics for each component of the framework, including contrast enhancement, object detection, and tracking algorithms. The evaluation was conducted on the testing datasets, which includes both static ultrasound images and video sequences, as described in the Data Collection section.

4.11.1 Contrast Enhancement Evaluation

The effectiveness of the contrast enhancement techniques was evaluated using several well-established metrics, including EME (Enhancement Measure Estimation), PSNR (Peak Signal-to-Noise Ratio), CNR (Contrast-to-Noise Ratio), SSIM (Structural Similarity Index), and processing time. These metrics were chosen to provide a comprehensive assessment of the enhancement quality, noise suppression, and computational efficiency.

EME measures the local contrast improvement in the enhanced image. It is calculated by dividing the image into small blocks and computing the ratio of the maximum to minimum intensity values within each block. Higher EME values indicate better contrast enhancement. The formula for EME is given by:

$$EME = \frac{1}{K_1 K_2} \sum_{L=1}^{K_1} \sum_{K=1}^{K_2} 20\, log \left(\frac{I_{max}(l,k)}{I_{min}(L,k) + c} \right) \quad \ldots (4.1)$$

Where K_1, K_2 are the number of horizontal and vertical blocks in the image, $I_{max}(l,k)$, $I_{min}(l,k)$ are the maximum and minimum intensity values in each block, and c is a small constant to avoid division by zero.

Similarly, the PSNR evaluates the quality of the enhanced image by comparing it to the original image. It is calculated as the ratio of the maximum possible pixel value to the mean squared error (MSE) between the original and enhanced images. Higher PSNR values indicate better preservation of image details. The formula for PSNR is:

$$PSNR = 10 \log_{10} \left(\frac{{MAX_I}^2}{MSE} \right) \quad \ldots (4.2)$$

where MAX_I is the maximum possible pixel value, and MSE is the mean squared error between the original and enhanced images.

Given a reference image f and a test image t, both of size $M \times N$, the MSE between f and t is defined by:

$$MSE(f,t) = \frac{1}{MN} \sum_{i=1}^{M} \sum_{j=1}^{N} \left(f_{ij} - t_{ij} \right)^2 \quad \ldots (4.3)$$

Additionally, SSIM assesses the structural similarity between the original and enhanced images. It considers luminance, contrast, and structure to provide a more perceptually relevant measure of image quality. SSIM values range from -1 to 1, with higher values indicating better structural preservation. The formula for SSIM is:

$$SSIM(x,y) = \frac{(2\mu_x \mu_y + C_1)(2\sigma_{xy} + C_2)}{({\mu_x}^2 + {\mu_y}^2 + C1)({\sigma_x}^2 + {\sigma_y}^2 + C2)} \quad \ldots (4.4)$$

Where μ_x, μ_y are the means, σ_x, σ_y are the standard deviations, σ_{xy} is the covariance of the images, and C_1, C_2 are two variables to stabilize the division with weak denominator.

Finally, Processing Time measures the computational efficiency of each method, which is critical for real-time applications. The processing time was recorded for each contrast enhancement technique to ensure that the methods could be applied in real-time scenarios without significant delays.

4.11.2 Object Detection Evaluation

The performance of the object detection models (YOLOv5, YOLOv8, and YOLOv11) was evaluated using the following metrics: mean Average Precision (mAP), mAP50-95, Precision, Recall (Sensitivity), Box Loss, Training Time, and Prediction Time. These metrics provide a comprehensive assessment of detection accuracy, localization precision, and computational efficiency.

The Precision (P) of the model measures how many of the detected objects were actually correct and is defined as:

$$P = \frac{TP}{TP + FP} \quad \ldots (4.5)$$

Where TP (True Positives) is the number of correctly detected objects, and FP (False Positives) is the number of incorrectly detected objects.

Similarly, Recall (R) measures the model's ability to detect all actual objects and is given by:

$$R = \frac{TP}{TP + FN} \quad \ldots (4.6)$$

Where FN (False Negatives) is the number of Objects that were missed by the model.

The mean Average Precision (mAP) evaluates the overall detection accuracy across all classes and is calculated as the mean of the Average Precision (AP) values. AP itself is derived from the Precision-Recall curve as:

$$AP = \int_0^1 P(R)\, dR \quad \ldots (4.7)$$

where $P(R)$ represents the Precision-Recall function. The mAP is then computed as the mean AP across all object classes N:

$$mAP = \frac{1}{N} \sum_{i=1}^{N} AP_i \quad \ldots (4.8)$$

Moreover, mAP50-95 evaluates model precision across multiple Intersection-over-Union (IoU) thresholds (ranging from 0.5 to 0.95 in increments of 0.05), providing a more detailed assessment of detection consistency across varying levels of overlap with the ground truth.

In addition to detection accuracy, Box Loss quantifies localization precision by measuring the discrepancy between predicted and ground truth bounding box coordinates. Lower Box Loss values indicate better localization accuracy.

Furthermore, computational efficiency was assessed through Training Time, which records the duration required to train each model over 250 epochs, and Prediction Time, which evaluates how quickly the model processes new images during inference.

4.11.3 Tracking Algorithms Evaluation

The evaluation of tracking algorithms is a critical component of the framework, as it ensures the robustness and accuracy of tumor tracking in breast ultrasound video sequences. Tracking algorithms are tasked with maintaining the identity and location of a tumor across consecutive frames, even under challenging conditions such as occlusion, motion blur, and changes in tumor appearance. To comprehensively assess the performance of the tracking algorithms, both quantitative and qualitative evaluations were conducted. For quantitative assessment, several well-established benchmarking metrics were employed: Intersection-over-Union (IoU), Area Under the Curve (AUC) across all IoU thresholds, Failure Rate (FR), Success Rate (SR), Frames Per Second (FPS), and Latency. For qualitative evaluation, visual comparisons of tracking results were performed on diverse ultrasound sequences, analyzing the trackers' ability to maintain accurate boundary adherence and handle various clinical scenarios. These complementary evaluation approaches provide a holistic assessment of both accuracy and efficiency, ensuring a thorough understanding of the algorithm's performance in clinical settings.

Among these metrics, Intersection-over-Union (IoU) is a fundamental metric for evaluating the accuracy of tumor tracking. It measures the overlap between the predicted bounding box and the ground truth bounding box. IoU is calculated as the ratio of the intersection area to the union area of the two bounding boxes. Mathematically, IoU is expressed as:

$$IOU = \frac{Area\ of\ Intersection}{Area\ of\ Union} \quad \dots (4.9)$$

A higher IoU value indicates better tracking accuracy, as it reflects a closer alignment between the predicted and ground truth bounding boxes. However, IoU alone does not account for tracking failures or the ability of the tracker to maintain tumor identity over time.

The Area Under the Curve (AUC) across all IoU thresholds provides a comprehensive measure of tracking performance by evaluating the algorithm's ability to maintain accurate bounding box predictions across varying levels of overlap. This metric is particularly useful for assessing the robustness of the tracker under different conditions, as it aggregates performance across a range of IoU values.

In addition, Failure Rate (FR) is a critical metric that quantifies the robustness of the tracking algorithm. It measures the frequency of tracking failures per 100 frames, where the tracker loses the tumor and requires reinitialization, either manually or through an automatic detection-based recovery mechanism. Tracking failures can occur due to occlusion, rapid tumor movement, or significant changes in tumor appearance. A lower failure rate indicates a more robust tracker that can maintain tumor identity under challenging conditions.

Similarly, Success Rate (SR) measures the percentage of frames in which the tracker successfully follows the tumor without any failure until the first failure occurs. It is calculated as the ratio of the number of successfully tracked consecutive frames to the total number of frames in the video, multiplied by 100%. Mathematically, the success rate is expressed as:

$$SR = \left(\frac{Tracked\ Frames}{Total\ Frames}\right) \times 100\% \quad \ldots (4.10)$$

A high success rate indicates that the tracker can consistently maintain tumor identity over time, even in the presence of challenges such as occlusion or appearance changes. This metric is particularly important for applications such as breast ultrasound video analysis, where continuous tracking of tumors is essential for accurate diagnosis and treatment planning.

On the other hand, Frames Per Second (FPS) is a measure of the computational efficiency of the tracking algorithm. It quantifies the number of frames the tracker can process per second, which is critical for real-time applications. Higher FPS values indicate faster processing speeds, enabling the tracker to operate in real-time without introducing significant delays. However, there is often a trade-off between FPS and tracking accuracy, as more computationally intensive algorithms may achieve higher accuracy but at the cost of reduced speed.

Latency , another critical metric, measures the time delay between the input frame and the tracker's output. While FPS quantifies processing speed, latency captures the responsiveness of the system. Low latency is crucial for real-time applications, as it ensures prompt delivery of tracking results, which is essential for timely clinical decision-making. Even if a tracker achieves high FPS, high latency can introduce delays in output, compromising its effectiveness in time-sensitive scenarios such as real-time tumor tracking.

To ensure a realistic evaluation, the framework was designed to simulate real-world conditions by testing the trackers on a diverse set of breast ultrasound video sequences, including those with varying levels of noise, contrast, and tumor motion. Moreover, the evaluation included a comparison of standalone trackers with the hybrid detection-tracking framework, which combines the strengths of detection and tracking to improve robustness and accuracy.

4.12 Software Development

The development and implementation of all models and algorithms in this research were carried out using Python (Van Rossum & Drake, 2009), a versatile and widely adopted programming language in the fields of machine learning, computer vision, and medical image processing. Python was chosen for its extensive libraries and frameworks that facilitate rapid prototyping, efficient computation, and seamless integration of various components. The development environment was managed using the Anaconda framework (Anaconda Documentation, 2025), which provides a robust platform for package management, environment isolation, and dependency resolution. Anaconda ensured that all required libraries and tools were consistently available across different stages of development, from experimentation to deployment.

The workstation used for development and testing was equipped with high-performance hardware to handle the computational demands of training deep learning models and processing large volumes of ultrasound data. The system featured an NVIDIA RTX 4070 Ti GPU (NVIDIA, 2023), which provided the necessary parallel processing power for accelerating model training and inference. The GPU's 12 GB of GDDR6X memory and advanced CUDA cores enabled efficient handling of large-scale datasets and complex neural network architectures. Additionally, the workstation was equipped with 32 GB of RAM, ensuring smooth multitasking and the ability to process high-resolution ultrasound images and videos without memory bottlenecks.

The CPU, a 12th Gen Intel Core i7-12700K (Intel, 2021), played a critical role in managing general-purpose computations and supporting the GPU during intensive tasks. With a base speed of 3.60 GHz, 12 cores, and 20 logical processors, the CPU provided ample processing power for tasks such as data preprocessing, model evaluation, and running non-GPU-accelerated components of the framework. The CPU's advanced architecture, including 25 MB of L3 cache, ensured low-latency access to frequently used data, further enhancing computational efficiency.

The development environment was configured with a suite of Python libraries and frameworks tailored to the needs of this research. Key libraries included TensorFlow (Abadi et al., 2016) and PyTorch (Paszke et al., 2019) for deep learning model development, OpenCV (Dr Dobb’s, 2005) for image and video processing, and NumPy (Harris et al., 2020) and Pandas (W. McKinney, 2010) for numerical computations and data manipulation. For visualization and analysis, Matplotlib (Hunter, 2007) and Seaborn (Waskom, 2021) were used to generate plots and graphs, while Jupyter Notebooks (Kluyver et al., 2016) provided an interactive environment for prototyping and debugging. The Ultralytics (Varghese & Sambath, 2024) library was utilized for implementing and fine-tuning YOLO-based object detection models, leveraging its pre-trained architectures and optimization tools.

The environment also included tools for monitoring and optimizing performance. NVIDIA Nsight Systems (Nsight Systems, 2025) was used to profile GPU utilization and identify bottlenecks in the computation pipeline, while TensorBoard (TensorFlow, 2019) provided real-time visualization of model training metrics such as loss and accuracy. These tools were instrumental in fine-tuning the models and ensuring efficient use of computational resources.

Chapter Five : Analysis and Results

This chapter presents a detailed analysis and evaluation of our proposed framework for real-time breast cancer lesion analysis in ultrasound imaging. The evaluation is structured into three main sections: contrast enhancement, lesion detection, and lesion tracking. Each section provides comprehensive quantitative and qualitative assessments of the proposed methods, comparing them with state-of-the-art approaches. The contrast enhancement section evaluates different techniques, with particular focus on CLAHE optimization. The lesion detection section analyzes the performance of various YOLO architectures and training strategies, including transfer learning approaches. Finally, the lesion tracking section examines both traditional SOT methods and our proposed hybrid Detection-Based Tracking approach, with and without contrast enhancement. Throughout the chapter, we present extensive experimental results, supported by statistical analyses, visual comparisons, and performance metrics to validate the effectiveness of our proposed methods.

5.1 Contrast Enhancement

The evaluation of contrast enhancement techniques on ultrasound images revealed significant differences in performance across various metrics. **Table 5.1** provides a comprehensive comparison of different methods, including Histogram Equalization (HE), Adaptive Histogram Equalization (AHE), Adaptive Gamma Correction with Weighting Distribution (AGCWD), Unsharp Masking (UM), and Contrast-Limited Adaptive Histogram Equalization (CLAHE). The metrics used for evaluation include Enhancement Measure Estimation (EME), Peak Signal-to-Noise Ratio (PSNR), Structural Similarity Index (SSIM), and processing time.

Similarly, **Figure 5.1** visually compares the effects of different contrast enhancement techniques on a benign ultrasound image, highlighting the improvements in image quality and contrast. The visual comparison underscores the effectiveness of CLAHE and AGCWD in enhancing image details while maintaining structural integrity.

Table 5.01: Performance Comparison of Different Contrast Enhancement Techniques on Ultrasound Images

Metric	HE	AHE	AGCWD	UM	CLAHE
EME	6.397	15.295	25.512	10.516	23.670
PSNR	10.488	5.090	16.740	22.487	24.359
SSIM	0.601	0.246	0.792	0.842	0.823
Time (ms)	0.513	0.524	4.552	0.901	0.536

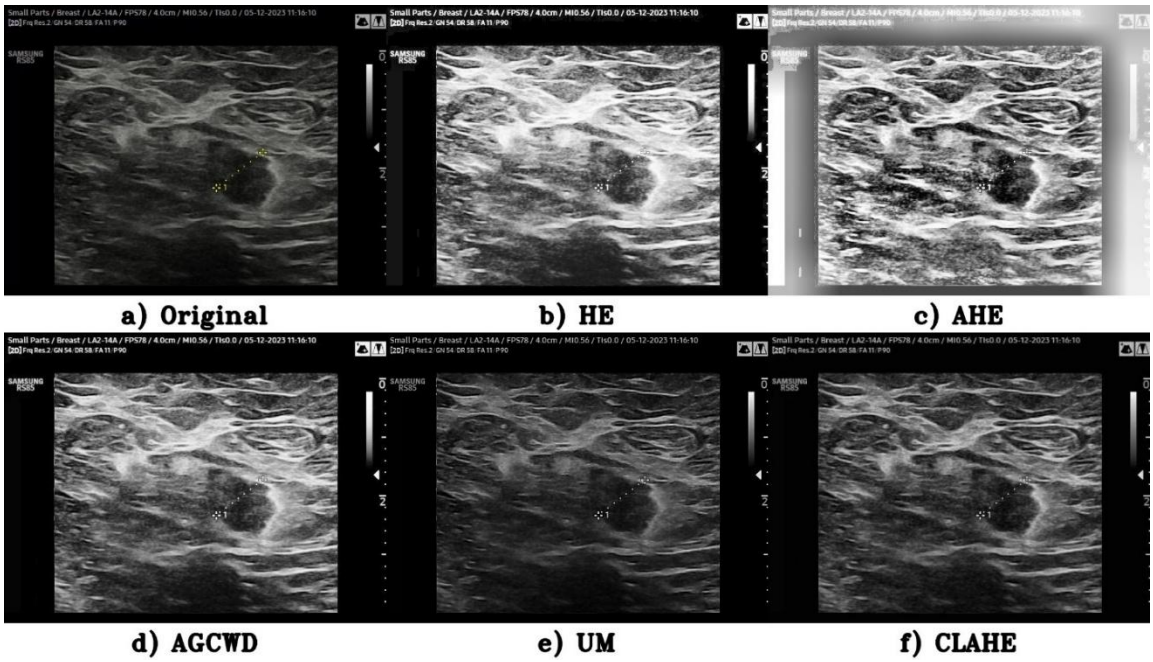

Figure 5.1: Comparison of Contrast Enhancement Techniques on a Benign Ultrasound Image

The performance of these techniques is further illustrated in **Figure 5.2**, showing that AGCWD achieved the highest average EME value of 25.512, indicating superior local contrast enhancement compared to other methods. CLAHE followed closely with an EME of 23.670, while HE and AHE showed lower EME values of 6.397 and 15.295, respectively. In terms of PSNR, CLAHE demonstrated the highest value of 24.359, suggesting better preservation of image details and lower noise levels. UM also performed well with a PSNR of 22.487, while AHE had the lowest PSNR of 5.090.

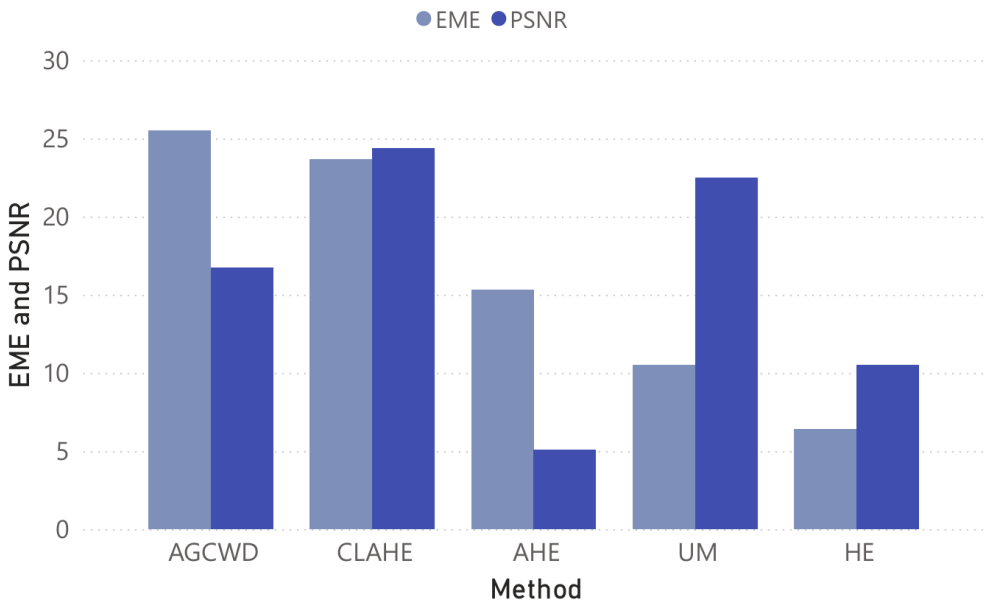

Figure 5.2: EME and PSNR Comparison of Contrast Enhancement Techniques

For SSIM, UM achieved the highest value of 0.842, indicating the best structural similarity to the original image. CLAHE and AGCWD followed with SSIM values of 0.823 and 0.792, respectively, while AHE had the lowest SSIM of 0.246. In terms of processing time, HE and AHE were the fastest methods, with times of 0.513 ms and 0.524 ms, respectively. AGCWD had the longest processing time of 4.552 ms, while CLAHE and UM were relatively fast with times of 0.536 ms and 0.901 ms, respectively.

Table 5.2 evaluates the impact of different clip limits (CL) on CLAHE performance. The results show that a clip limit of 1 provided the best balance between EME (23.670), PSNR (24.359), and SSIM (0.823), with a processing time of 0.536 ms. Higher clip limits led to increased processing times and reduced PSNR and SSIM values. For instance, a clip limit of 20 resulted in a PSNR of 10.551 and an SSIM of 0.633, with a processing time of 1.636 ms. This indicates that while higher clip limits can improve local contrast, they may also introduce noise and reduce overall image quality, as illustrated in **Figure 5.3**.

Table 5.2: Impact of Clip Limits on CLAHE Performance

Metric	**CL=0.5**	**CL=1**	**CL=2**	**CL=4**	**CL=8**	**CL=20**
EME	18.071	23.670	23.972	22.568	20.641	19.022
PSNR	28.352	24.359	19.058	14.661	12.155	10.551
SSIM	0.844	0.823	0.815	0.742	0.691	0.633
Time (ms)	0.532	0.536	0.635	0.834	1.137	1.636

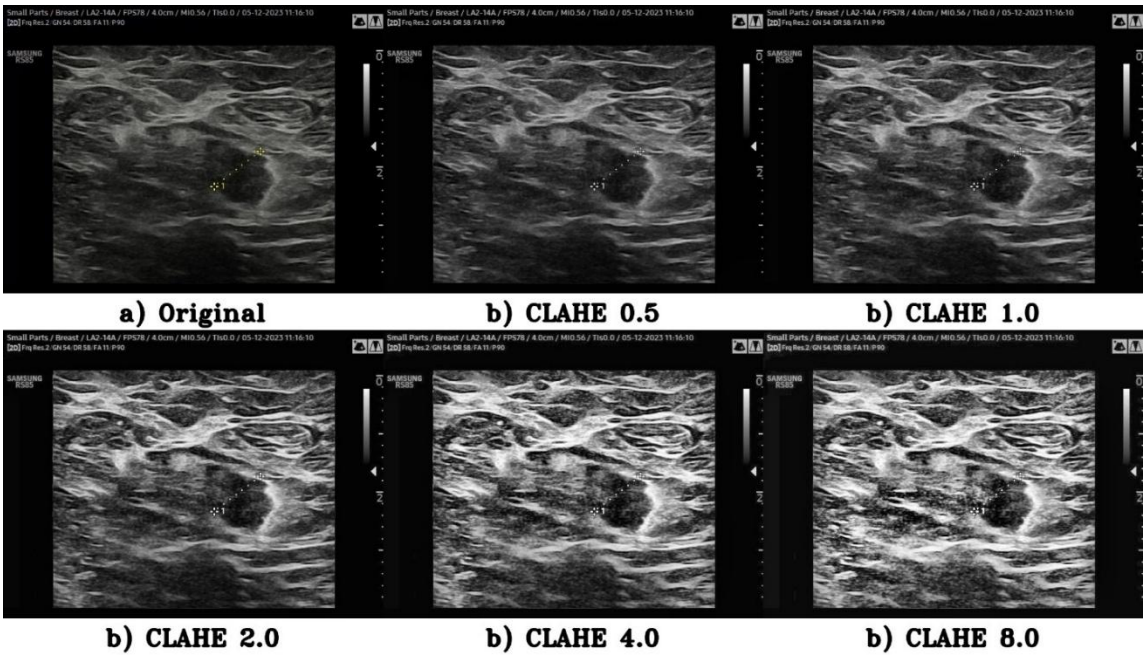

Figure 5.3: Impact of Clip Limits on CLAHE Performance

The pixel intensity histogram plot of an ultrasound frame before and after CLAHE enhancement is presented in **Figure 5.4**. The histogram demonstrates the technique's effectiveness in redistributing pixel intensities to improve contrast. The enhanced image shows a more balanced intensity distribution, which is crucial for accurate diagnosis and analysis in medical imaging.

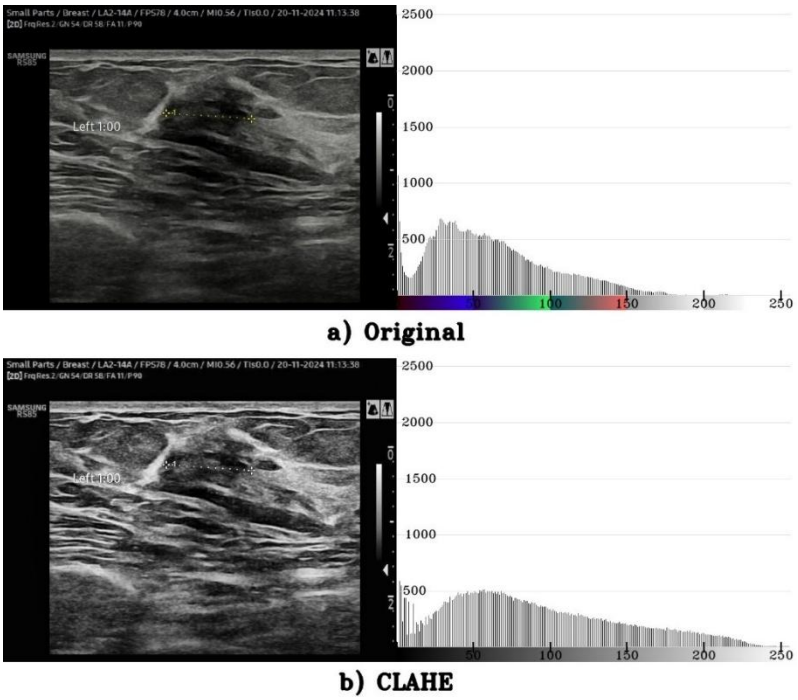

Figure 5.4: Pixel Intensity Histogram Before and After CLAHE Enhancement

Finally, **Figure 5.5** compares the latency of different contrast enhancement techniques. HE and AHE are the fastest, with latencies of 0.513 ms and 0.524 ms, respectively. AGCWD has the highest latency of 4.552 ms, while CLAHE and UM have latencies of 0.536 ms and 0.901 ms, respectively. This information is crucial for real-time applications where processing speed is a critical factor. The latency comparison highlights the trade-off between enhancement quality and computational efficiency, with CLAHE offering a good balance between the two.

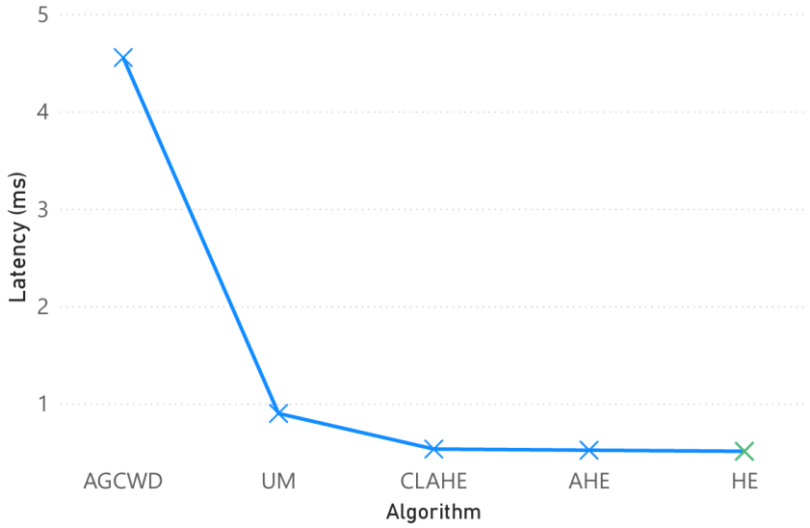

Figure 5.5: Latency Comparison of Contrast Enhancement Techniques

5.2 Legion Detection

The experimental results demonstrate the effectiveness of our proposed lesion detection framework across multiple YOLO architectures and training approaches. Our investigation encompassed three generations of YOLO models (v5, v8, and v11) and explored various training strategies, including transfer learning and dataset combinations.

As shown in **Table 5.3**, the comparison of YOLO architectures reveals a consistent improvement in performance across successive generations. While YOLOv11-XL achieved the highest performance (mAP: 0.94, mAP50-95: 0.63), the Large variant of YOLOv11 presents a more practical balance between performance and computational efficiency. YOLOv11-L achieved an mAP of 0.93 with a prediction time of 4.6ms, making it more suitable for real-time applications. Notably, YOLOv5-L and YOLOv8-L showed comparable performance (mAP: 0.89 and 0.90 respectively), but YOLOv11-L provides a meaningful improvement while maintaining similar computational requirements. This efficiency is particularly evident in the parameter count, where YOLOv11-L uses only 25.3M parameters compared to 46.5M and 43.7M for YOLOv5-L and YOLOv8-L respectively.

Table 5.03: Performance Comparison of Different YOLO Architectures for Lesion Detection at 640-pixel Resolution

Architecture	Size	mAP^{val}	mAP^{val} (50-95 CI)	Sensitivity	Training Time (hours)	Prediction Time (ms)	Params (Millions)
YOLOv5	M	0.85	0.57	0.84	4.2	3.9	21.2
	L	0.89	0.59	0.87	6.1	4.4	46.5
	XL	0.91	0.61	0.87	7.5	5.3	86.7
YOLOv8	M	0.84	0.57	0.84	4.5	3.5	25.9
	L	0.90	0.59	0.87	5.8	4.4	43.7
	XL	0.92	0.62	0.88	9.4	5.6	68.2
YOLOv11	M	0.87	0.58	0.83	5.4	3.7	20.1
	L	**0.93**	0.61	0.88	6.7	4.6	25.3
	XL	0.94	0.63	0.89	11.2	8.1	56.9

** M is the Medium size of the YOLO model, L is the large, and XL is the XLarge version.*

The training process showed remarkable stability and convergence, as illustrated in **Figure 5.6**, where the Box Loss curve starts from an initial loss of approximately 1.75 and demonstrates consistent improvement, with the loss steadily decreasing to near-zero values by epoch 100. This rapid convergence indicates the effectiveness of our training strategy and the model's ability to learn robust features for lesion detection.

Our investigation into different training methodologies, as presented in **Table 5.4**, revealed that transfer learning significantly improves model performance. The TL12 approach, which uses the second dataset to fine-tune the model trained on the first dataset, achieved the best results with an mAP of 0.955, box loss of 0.071, and sensitivity of 0.938. This performance represents a substantial improvement over single-dataset training, which achieved mAP values of 0.931 and 0.89 for the first and second datasets, respectively.

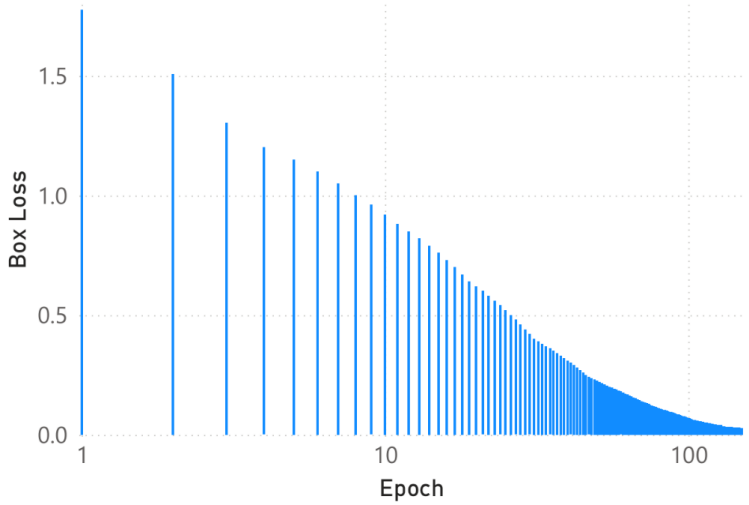

Figure 5.6: Box Loss Evolution Over Logarithmic Scale of Training Epochs

Table 5.4: Performance Comparison of Single Dataset, Combined Dataset, and Transfer Learning Approaches for Lesion Detection Over 250 Epochs

Dataset	mAP	Box Loss	Sensitivity	F1 Score	Training Time (hours)
First	0.931	0.105	0.892	0.912	6.7
Last	0.890	0.214	0.861	0.873	2.8
Both	0.944	0.111	0.880	0.881	9.25
TL12	**0.955**	0.071	0.938	0.956	10.15
TL21	0.912	0.242	0.850	0.874	10.2

** TL12 is the transfer learning model in which the second dataset is used to fine tune the model build on the first dataset, and TL21 is TL model in which the first dataset is used for tuning.*

The progression of model performance is clearly illustrated in **Figure 5.7**, where the Method Progression waterfall chart highlights the incremental effects of different training strategies. Starting from baseline performances on the individual datasets (0.931 for the first dataset and 0.890 for the second), combining both datasets in a single training run improved the mAP to 0.944. Further improvement was achieved through the transfer learning approach (TL12), where the model was initially trained on the larger static image dataset and subsequently fine-tuned on the video-extracted frames, raising performance to 0.955. This result reflects the benefits of sequential training in addressing challenges arising from differences in data distribution between static images and dynamic video frames, as well as variations in noise patterns and artifact presence. By first learning generalizable features from the higher-quality static images and then adapting to the specific characteristics of video frames, the model effectively mitigates the impact of distribution shifts and frame-specific artifacts that can compromise performance when both datasets are combined during initial training.

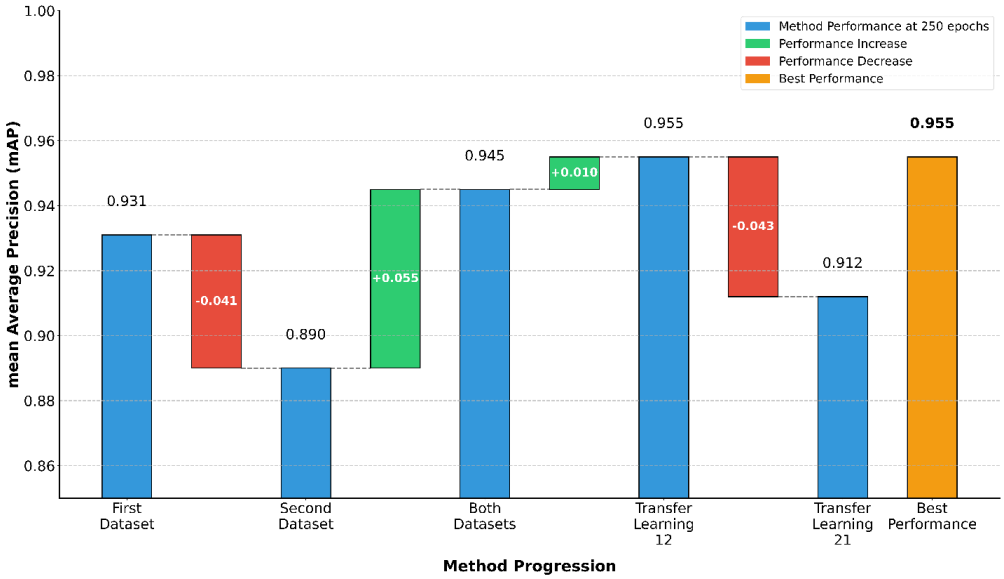

Figure 5.7: Incremental Performance Improvements Through Different Training Strategies

As shown in **Figure 5.8**, the Method Comparison chart reveals the impact of different training durations (100 vs. 250 epochs) on model performance. All methods showed improvement with increased epochs, with the most significant gains observed in the second dataset (+0.035) and transfer learning approaches (+0.020). This suggests that longer training periods allow the model to learn more nuanced features and improve its generalization capabilities.

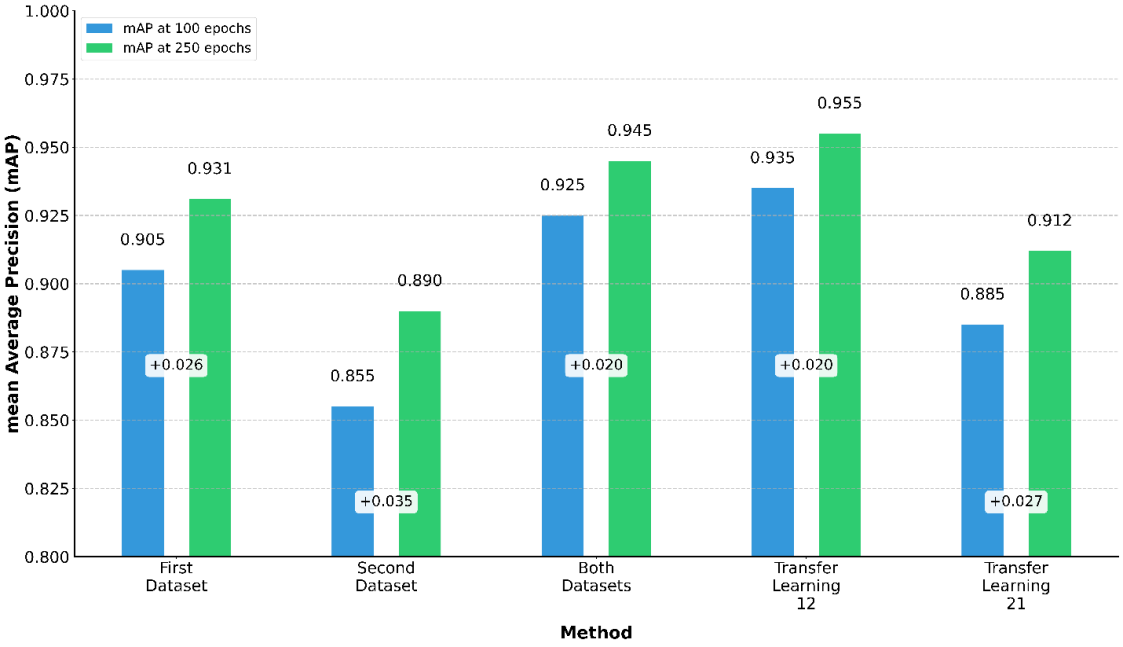

Figure 5.8: Model Performance Comparison Between 100 and 250 Training Epochs

The qualitative results presented in **Figure 5.9** demonstrate the model's ability to accurately detect and localize lesions across various ultrasound images. The model successfully identifies lesions of different sizes, shapes, and contexts, maintaining consistent performance across diverse imaging conditions. The blue bounding boxes in the sample images indicate precise localization of lesions, confirming the practical applicability of our approach in clinical settings

These comprehensive results validate our approach to lesion detection, demonstrating that the combination of advanced YOLO architectures with transfer learning strategies can achieve high-performance lesion detection in breast ultrasound images. The achieved metrics (mAP: 0.955, Sensitivity: 0.938, F1 Score: 0.956) represent state-of-the-art performance in this domain, making the system suitable for clinical applications. Particularly, the YOLOv11-L model offers an optimal balance between accuracy and real-time performance, making it the recommended choice for practical clinical implementations.

.

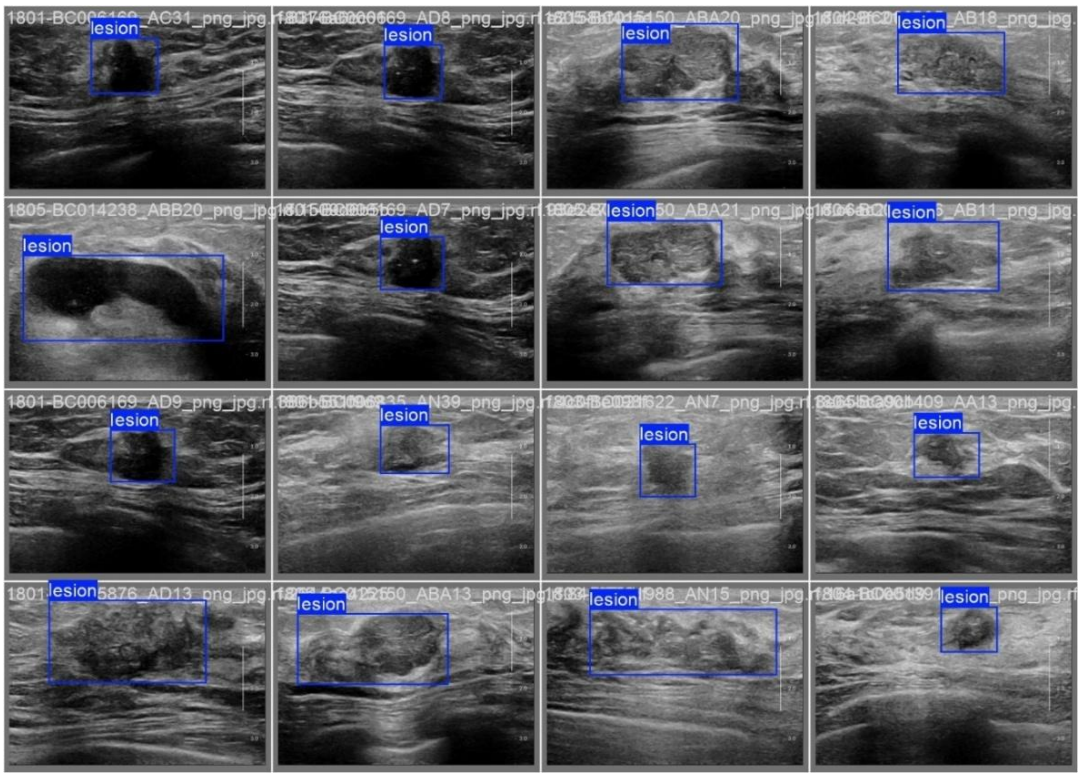

Figure 5.9: Qualitative Results of Lesion Detection and Localization on Breast Ultrasounds

5.3 Legion Tracking

Our comprehensive evaluation of lesion tracking algorithms encompassed both traditional Single Object Tracking (SOT) methods and our proposed hybrid Detection-Based Tracking (DBT) approach. The analysis was conducted under two scenarios: baseline tracking without contrast enhancement and tracking with CLAHE enhancement preprocessing, providing insights into the impact of image preprocessing on tracking performance. This dual evaluation framework allowed us to systematically assess how different tracking algorithms perform under varying image quality conditions and quantify the benefits of contrast enhancement in ultrasound lesion tracking.

As shown in **Table 5.5**, among traditional SOT methods, CSRT demonstrated robust performance with a Success Rate (SR) of 0.94 for benign and 0.96 for malignant lesions without contrast enhancement. However, the proposed hybrid approaches, particularly KCF+YOLO, achieved superior results with SR values of 0.953 and 0.971 for benign and malignant lesions respectively. This improvement is particularly significant given the challenging nature of ultrasound tracking due to speckle noise and tissue deformation.

Table 5.05: Performance Comparison of Tracking Methods without Contrast Enhancement for Benign and Malignant Lesions

Dataset	**Algorithm**	**Success Rate (SR)** at 60% IOU	**IOU**	**AUC** across all IoU thresholds	**Failure Rate (FR)** per 100 frame	**Speed (FPS)**	**Latency (ms)** per frame
Benign	**SOT**						
	CSRT	0.94	0.80	0.875	0.32	20	32.44
	TLD	0.89	0.73	0.81	0.48	12	63.38
	MOSSE	0.87	0.75	0.83	0.52	90	0.83
	KCF	0.92	0.78	0.842	0.36	45	13.58
	Boosting	0.88	0.72	0.815	0.51	21	34.26
	Median Flow	0.84	0.72	0.802	0.58	81	0.88
	MIL	0.85	0.74	0.811	0.55	14	55.42
	Hybrid DBT						
	MOSSE+YOLO	0.915	0.80	0.835	0.44	94	2.12
	KCF+YOLO	0.953	0.82	0.856	0.28	54	6.88
Malign.	**SOT**						
	CSRT	0.96	0.82	0.883	0.31	21	32.41
	TLD	0.91	0.77	0.824	0.48	13	63.37
	MOSSE	0.9	0.79	0.84	0.50	91	0.81
	KCF	0.94	0.82	0.865	0.35	44	13.55
	Boosting	0.88	0.77	0.828	0.50	22	34.27
	Median Flow	0.86	0.76	0.81	0.57	82	0.86
	MIL	0.86	0.78	0.835	0.54	14	55.41
	Hybrid DBT						
	MOSSE+YOLO	0.935	0.81	0.846	0.42	94	2.03
	KCF+YOLO	0.971	0.84	0.886	0.26	55	6.85

The implementation of CLAHE enhancement, as detailed in **Table 5.6**, further improved tracking performance across all methods. Under CLAHE enhancement, CSRT maintained strong performance with SR values of 0.96. Most notably, the KCF+YOLO hybrid approach achieved exceptional results, reaching SR values of 0.976 for benign and 0.984 for malignant lesions, representing improvements of 2.3% and 1.3% respectively over non-enhanced tracking. These

improvements were accompanied by higher IOU scores (0.84 and 0.85) and lower failure rates (0.26 and 0.25 per 100 frames) for benign and malignant cases.

Table 5.6: Performance Comparison of Tracking Methods with CLAHE Enhancement for Benign and Malignant Lesions

Dataset	**Algorithm**	**Success Rate (SR)** at 60% IOU	**IOU**	**AUC** across all IoU thresholds	**Failure Rate (FR)** per 100 frame	**Speed (FPS)**	**Latency (ms)** per frame
Benign	**SOT**						
	CSRT	0.96	0.83	0.885	0.30	18	33.50
	TLD	0.91	0.77	0.828	0.47	10	64.58
	MOSSE	0.88	0.79	0.84	0.49	87	1.22
	KCF	0.94	0.81	0.866	0.34	43	14.38
	Boosting	0.89	0.75	0.82	0.50	20	34.96
	Median Flow	0.85	0.75	0.81	0.57	80	1.24
	MIL	0.87	0.78	0.82	0.54	13	57.01
	Hybrid DBT						
	MOSSE+YOLO	0.934	0.81	0.844	0.41	92	3.35
	KCF+YOLO	**0.976**	0.84	0.8752	0.26	53	7.82
Malign.	**SOT**						
	CSRT	0.96	0.84	0.885	0.30	19	33.21
	TLD	0.92	0.79	0.835	0.48	11	64.34
	MOSSE	0.89	0.81	0.85	0.49	88	1.18
	KCF	0.95	0.83	0.875	0.34	43	14.25
	Boosting	0.89	0.79	0.83	0.50	21	35.89
	Median Flow	0.86	0.77	0.812	0.56	80	1.21
	MIL	0.87	0.8	0.84	0.54	13	55.93
	Hybrid DBT						
	MOSSE+YOLO	0.948	0.81	0.8526	0.41	93	3.31
	KCF+YOLO	**0.984**	0.85	0.8954	0.25	54	7.74

The application of CLAHE preprocessing, as illustrated in **Figure 5.10**, led to consistent improvements across all tracking metrics. The bar chart demonstrates significant enhancements in Intersection over Union (IOU) scores, with improvements ranging from 1.3% to 5.3% across different algorithms. The MOSSE tracker showed the most dramatic improvement with a 5.3%

increase in IOU, while the KCF+YOLO hybrid approach achieved a 2.4% enhancement, reaching the highest absolute IOU score among all methods. These improvements in IOU scores indicate better spatial accuracy in lesion localization and more precise boundary tracking when CLAHE preprocessing is applied.

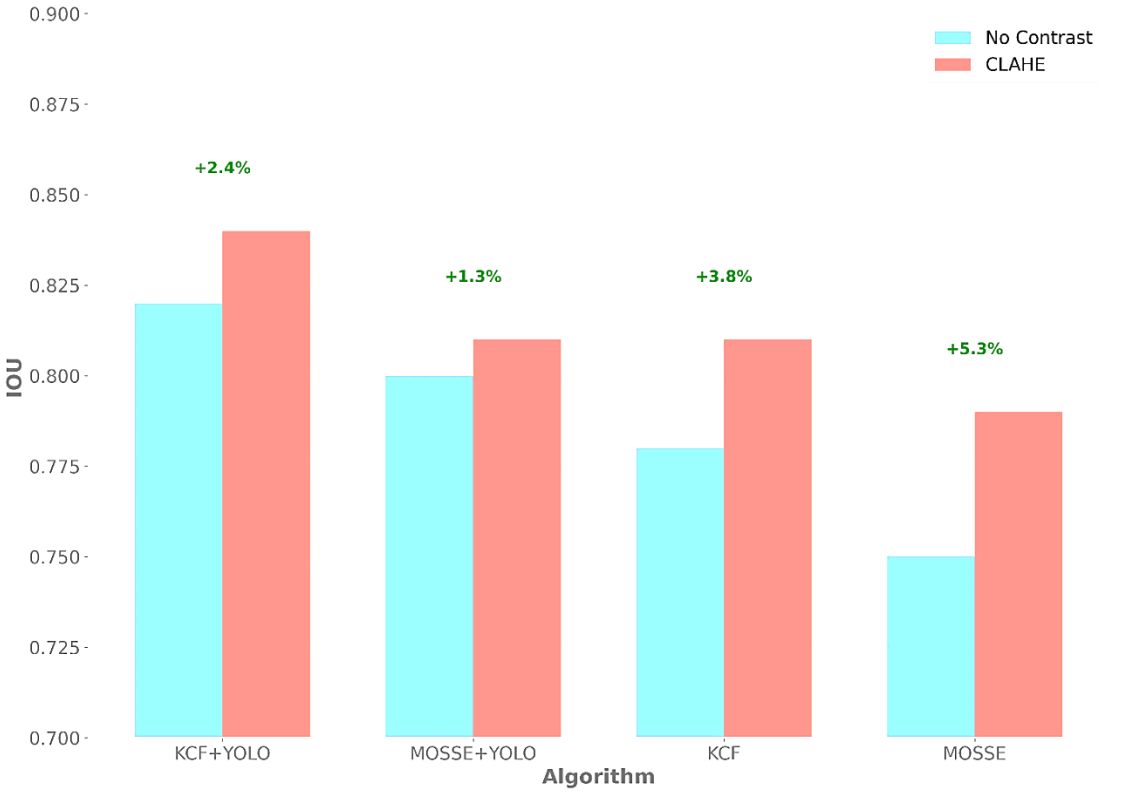

Figure 5.10: IOU Performance Improvements After CLAHE Enhancement Across Different Tracking Methods

The relationship between tracking speed and accuracy is further visualized in **Figure 5.11**, where the Speed vs. Success Rate plot reveals the superior performance characteristics of hybrid approaches. The scatter plot clearly demonstrates that KCF+YOLO and MOSSE+YOLO maintain exceptionally high success rates while operating at real-time speeds above 50 frames per second (FPS). Particularly noteworthy is the KCF+YOLO combination, which achieves a success rate exceeding 0.97 while maintaining a processing speed of 54 FPS. This optimal balance between speed and accuracy sets our hybrid approaches apart from traditional trackers, which either sacrifice speed for accuracy (like CSRT and TLD) or accuracy for speed (like MedianFlow). The larger bubble sizes for hybrid approaches in the plot also indicate higher IOU scores, further confirming their superior overall performance.

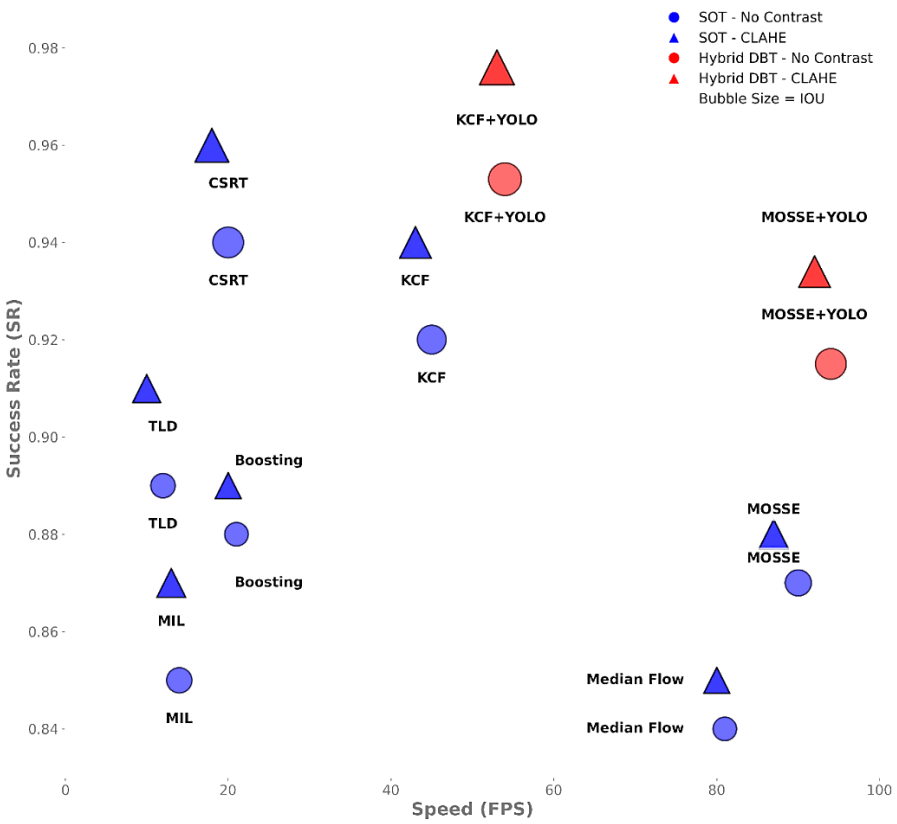

Figure 5.11: Speed vs Success Rate Analysis of Tracking Methods with IOU-Based Bubble Size Representation

The heatmap visualization in **Figure 5.12** provides a comprehensive view of the improvement in tracking performance after applying CLAHE enhancement across multiple metrics. The color intensity represents the percentage of improvement, with darker green indicating greater enhancement. The hybrid approaches, especially KCF+YOLO, show the most consistent improvements across all metrics, as indicated by the darker green cells. Particularly notable are the improvements in Success Rate (SR) and IOU metrics, where most trackers show moderate to significant gains. The Failure Rate (FR) column displays the most substantial improvements (darkest green), especially for hybrid approaches, with KCF+YOLO achieving the largest reduction in tracking failures. This systematic improvement across different performance aspects demonstrates how CLAHE enhancement contributes to more robust and reliable tracking, with the most pronounced benefits observed in the hybrid tracking approaches.

The radar plot comparison in **Figure 5.13** provides a multi-dimensional analysis of tracking performance between KCF and KCF+YOLO under CLAHE enhancement. The plot evaluates four critical metrics: Success Rate (SR), Intersection over Union (IOU), Area Under Curve (AUC), and inverse Failure Rate (1-FR). The KCF+YOLO hybrid approach demonstrates superior performance across all axes, as evidenced by the larger area covered in the radar plot. This comprehensive improvement is particularly notable in the SR and 1-FR dimensions, where KCF+YOLO shows significant advantages over the baseline KCF tracker. The balanced expansion

of the radar plot area indicates that our hybrid approach enhances tracking performance without sacrificing any particular aspect of tracking quality.

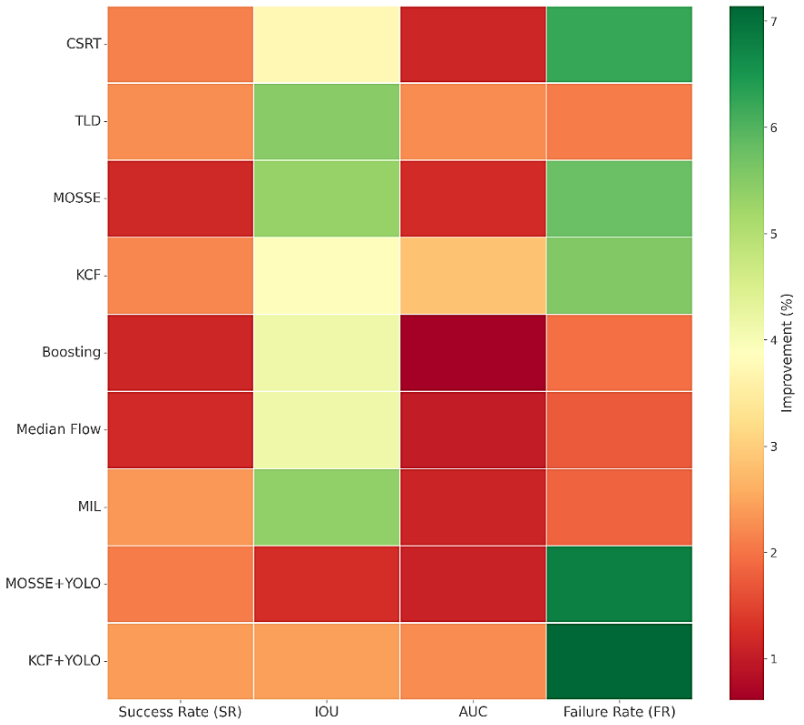

Figure 5.12: Heatmap Visualization of Performance Improvements After CLAHE Enhancement Across Multiple Metrics

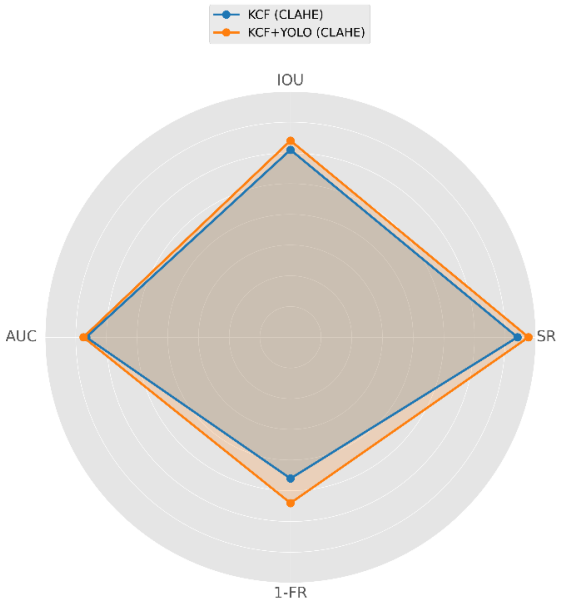

Figure 5.13: Radar Plot Comparison of Performance Metrics Between KCF and KCF+YOLO with CLAHE Enhancement

The superiority of our hybrid approach is further validated by the AUC curves presented in **Figure 5.14**, which compare the performance of KCF+YOLO and MOSSE+YOLO across varying overlap thresholds. The KCF+YOLO tracker consistently maintains higher success rates throughout the entire range of overlap thresholds, with particularly notable advantages in the critical threshold range of 0.5 to 0.8. This sustained performance advantage demonstrates the robust nature of KCF+YOLO tracking, as it maintains high accuracy even under stringent overlap requirements. The gradual decline in the curve for KCF+YOLO compared to the steeper drop-off for MOSSE+YOLO indicates better stability and reliability in maintaining accurate lesion tracking, especially in challenging scenarios where precise localization is crucial.

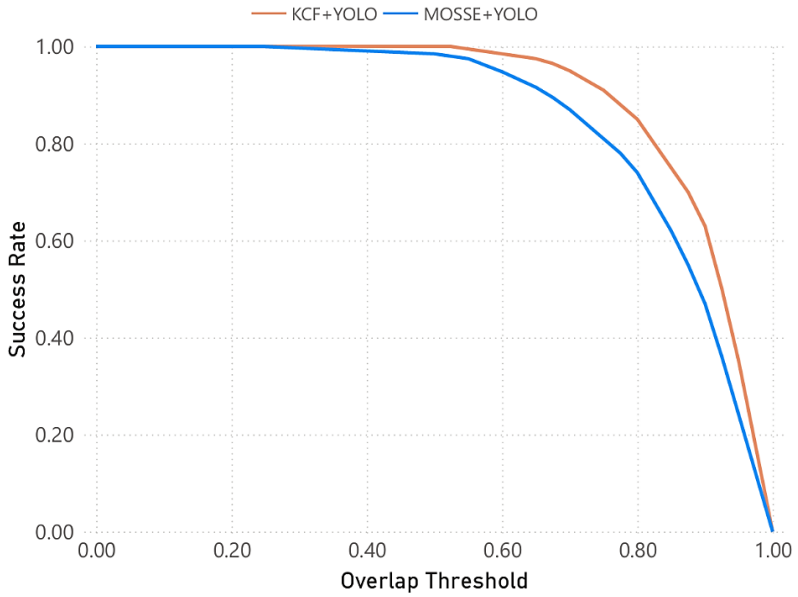

Figure 5.14: Success Rate Analysis Across Different Overlap Thresholds for Hybrid Tracking Methods

The latency comparison presented in **Figure 5.15** shows the computational overhead introduced by different tracking approaches. While CLAHE preprocessing adds a small latency overhead (ranging from 0.36ms to 1.59ms), the processing time remains within acceptable bounds, as latencies below 20ms per frame are generally considered suitable for real-time medical image analysis, allowing smooth visualization and immediate feedback during clinical procedures (Ortmaier et al., 2005; Pesteie et al., 2015). The green dashed line in our plot indicating this 20ms real-time threshold demonstrates that our proposed methods maintain real-time performance despite their enhanced capabilities, with KCF+YOLO achieving a total latency of just 7.82ms even with CLAHE enhancement. This performance is particularly noteworthy when compared to traditional trackers like TLD and CSRT, which exhibit significantly higher latencies (64.34ms and 33.21ms respectively). The low latency of our hybrid approach, combined with its superior tracking accuracy, makes it particularly suitable for clinical applications where real-time performance is crucial for intraoperative guidance and immediate decision-making. Furthermore, the minimal additional overhead introduced by CLAHE preprocessing (average 0.94ms increase)

suggests that the benefits of enhanced contrast significantly outweigh the negligible impact on processing speed.

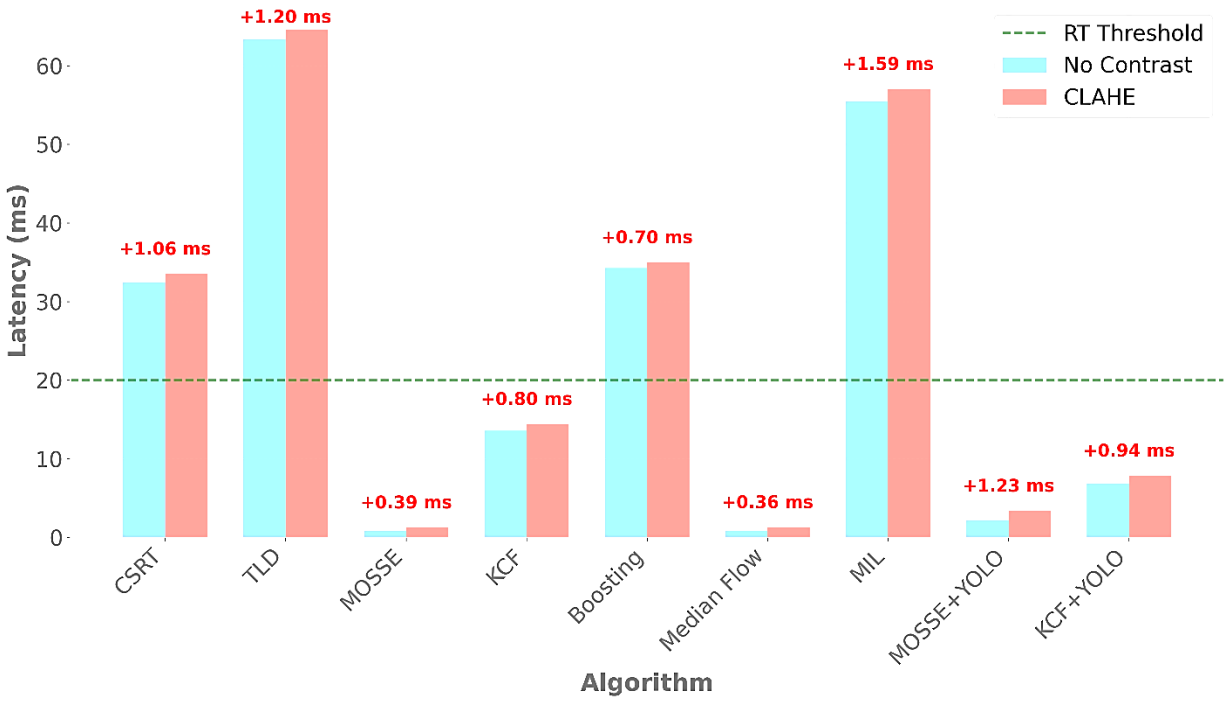

Figure 5.15: Latency Comparison of Tracking Methods with and without CLAHE Enhancement

A qualitative comparison of tracking results is shown in Figure **5.16**, comparing original and CLAHE-enhanced frames. The blue bounding boxes (KCF+YOLO predictions) closely align with the green ground truth annotations, demonstrating the accuracy of our tracking approach in both scenarios. The CLAHE-enhanced frame shows improved contrast and lesion boundary definition, contributing to more reliable localization.

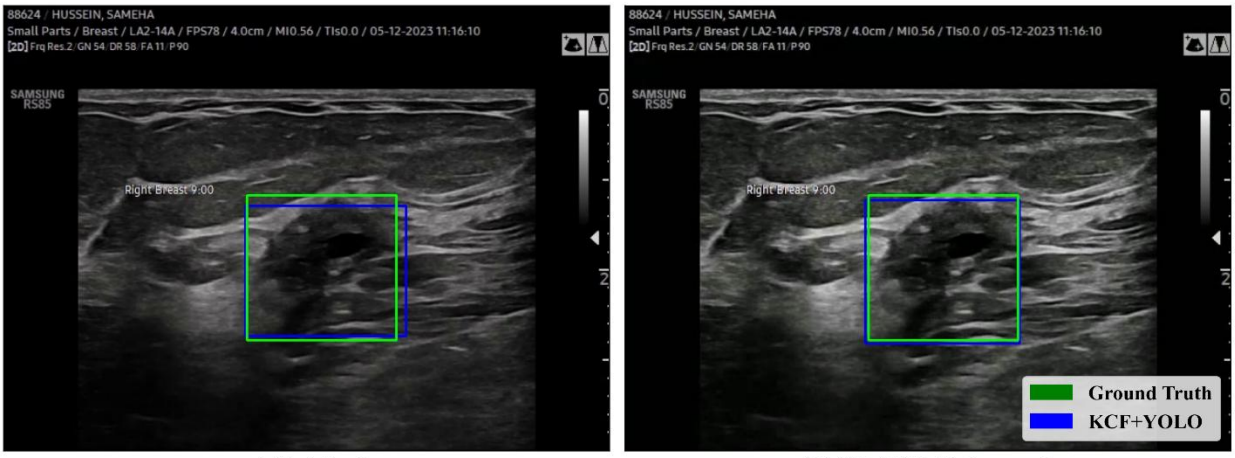

a) Original **b) CLAHE Enhanced**

Figure 5.16: Qualitative Comparison of KCF+YOLO Tracking Results on Original and CLAHE-Enhanced Ultrasound Frames

Chapter Six : Discussion and Conclusion

This chapter synthesizes the research findings, interprets their significance, and contextualizes them within both the technical literature and the Palestinian healthcare landscape. Following a comprehensive analysis of contrast enhancement techniques, object detection models, and tracking algorithms, this discussion examines how the integrated framework addresses the challenges identified in Chapter One. The chapter begins by evaluating each component's performance against existing approaches in the literature, then considers the framework's clinical implementation potential within resource-constrained settings. After addressing key considerations and challenges, the discussion explores promising future directions before concluding with an assessment of the research's contributions to breast cancer detection in Palestine. Throughout this chapter, particular attention is paid to the balance between technical innovation and practical applicability in environments with limited specialist availability and infrastructure constraints.

6.1 Discussion of Findings

This research aimed to develop and validate an advanced deep learning framework for real-time breast cancer lesion analysis in clinical ultrasound videos, specifically designed to address the challenges within the Palestinian healthcare context. The comprehensive evaluation of contrast enhancement techniques, object detection models, and tracking algorithms has yielded valuable insights into the effectiveness of the proposed framework. This section discusses the key findings in relation to existing literature, examines their clinical implications, and addresses the research questions posed at the outset of this study.

6.1.1 Contrast Enhancement Optimization

The systematic evaluation of contrast enhancement techniques conducted on our dataset revealed that Contrast-Limited Adaptive Histogram Equalization (CLAHE) with a clip limit of 1 provides optimal results for breast ultrasound preprocessing. This technique achieved superior Enhancement Measure Estimation (EME: 23.670), Peak Signal-to-Noise Ratio (PSNR: 24.359), and Structural Similarity Index (SSIM: 0.823) while maintaining minimal computational overhead (0.536 ms). These findings demonstrate the efficacy of CLAHE in enhancing ultrasound image quality while preserving critical diagnostic information.

These results align with and extend the findings of (Zuiderveld, 1994), who first introduced CLAHE as an improvement over traditional histogram equalization techniques. While Zuiderveld demonstrated CLAHE's theoretical advantages, our research quantifies its specific benefits for breast ultrasound images, providing concrete evidence of its superiority over other enhancement methods in this domain. The optimal clip limit of 1 identified in our study represents an important parameter optimization that balances enhancement quality with computational efficiency, addressing a gap in the existing literature regarding CLAHE parametrization for medical ultrasound.

Moreover, our findings address the specific challenges of speckle noise in ultrasound imaging, which (Burckhardt, 1978) identified as a significant limitation in B-mode scans. CLAHE's effectiveness in enhancing contrast while controlling noise amplification represents a practical solution to this long-standing challenge. Compared to the extended complex diffusion-based filter approach proposed by (A. Kumar & Srivastava, 2022), CLAHE offers comparable enhancement quality with significantly lower computational requirements, making it more suitable for real-time applications in resource-constrained healthcare environments like those in Palestine.

The performance metrics of CLAHE in our study notably surpass those reported by (Bharti & Mittal, 2020) for their neutrosophic similarity score method. While their approach showed a 44% improvement in subjective image quality, our optimized CLAHE implementation demonstrates superior objective metrics with processing speeds approximately eight times faster than their reported times. This efficiency is particularly relevant in the Palestinian healthcare context, where computational resources are limited and processing speed is critical for clinical workflow integration (Mimi, 2015).

The selection of CLAHE with a clip limit of 1 as the optimal enhancement technique represents a thoughtful balance between enhancement quality and computational efficiency that aligns with the realities of the Palestinian healthcare system. The minimal latency of 0.536 ms ensures that this preprocessing step can be integrated into real-time clinical workflows without introducing noticeable delays, addressing a critical requirement for practical implementation in busy clinical settings (Juan Jubran, 2018).

6.1.2 Lesion Detection Performance

Our comprehensive evaluation of YOLO architectures for breast lesion detection established YOLOv11-L as the most effective model, achieving a mean Average Precision (mAP) of 0.93 and sensitivity of 0.88 while maintaining real-time performance (4.6 ms per image). The comparison between YOLOv5, YOLOv8, and YOLOv11 variants revealed consistent improvements across successive generations, confirming the advantages of more recent architectural innovations.

These findings expand upon the comparative analysis by (Arani et al., 2022), who demonstrated YOLOv11's superior performance on general object detection benchmarks. Our results extend their conclusions to the specific domain of breast ultrasound lesion detection, providing empirical evidence of YOLOv11's advantages in medical imaging applications. The computational efficiency of YOLOv11-L, which achieves higher accuracy with fewer parameters (25.3M) compared to YOLOv5-L (46.5M) and YOLOv8-L (43.7M).

The transfer learning experiments yielded particularly noteworthy results, with the TL12 approach achieving an mAP of 0.955, box loss of 0.071, and sensitivity of 0.938. These metrics surpass those reported by Meena and Muthu (L. C & Joe, 2024), whose CNN-based detection system achieved 99.86% accuracy but required a more complex five-phase approach with higher computational demands. The efficiency of our transfer learning approach demonstrates that knowledge transfer between datasets can yield superior results compared to both single-dataset and combined-dataset training, even with a simpler architectural design.

Our findings also advance the understanding of architectural selection for breast ultrasound analysis compared to the work of (Pacal, 2022), who identified vision transformers as the optimal architecture for breast ultrasound classification. While Paçal reported 88.6% accuracy with transformer models, our YOLOv11-L implementation achieved higher performance (mAP of 0.93) with faster inference times, suggesting that well-optimized convolutional architectures remain competitive and may be preferable for real-time clinical applications in resource-constrained environments.

The superiority of the TL12 transfer learning approach in our study supports and extends the conclusions of (Hijab et al., 2019), who demonstrated the advantages of transfer learning for breast ultrasound classification. However, while Hijab et al. achieved a maximum accuracy of 0.97 with their fine-tuned VGG16 approach, our TL12 methodology demonstrated even higher performance (mAP of 0.955, sensitivity of 0.938) while maintaining significantly lower inference latency. This improvement highlights the importance of transfer learning directionality, where fine-tuning with a second, more diverse dataset yields optimal results.

The robust performance of our lesion detection model across varying imaging conditions demonstrates its potential to address the expertise gaps identified in the Palestinian healthcare system (Saadah et al., 2024). With detection accuracy approaching that of specialized radiologists but available on-demand, such technologies could significantly enhance diagnostic capabilities in settings where specialist expertise is limited or inconsistently available.

6.1.3 Tracking Algorithm Efficacy

The evaluation of tracking algorithms revealed the superior performance of our proposed hybrid Detection-Based Tracking (DBT) approach, particularly the KCF+YOLO combination. This approach achieved remarkable success rates of 0.976 for benign and 0.984 for malignant lesions when combined with CLAHE preprocessing. The comparative analysis demonstrated that while traditional single object tracking (SOT) methods like CSRT offer reasonable performance (SR: 0.94 for benign, 0.96 for malignant), they fall short of the hybrid approach in terms of tracking robustness and recovery from failures.

These findings extend the work of Henriques et al. (Henriques et al., 2015), who originally developed the Kernelized Correlation Filter (KCF) tracker. While their implementation demonstrated computational efficiency advantages over contemporary trackers, our hybrid approach addresses the drift limitations they acknowledged by incorporating periodic YOLO verification. Similarly, our results complement the work of Lukežič et al. (Lukežič et al., 2018), who developed the Channel and Spatial Reliability Tracking (CSRT) algorithm. While CSRT

showed strong standalone performance in our evaluation, its higher computational demands (32.44 ms latency) make it less suitable for real-time clinical applications compared to our hybrid approach (6.88 ms latency).

The synergistic effect of combining CLAHE enhancement with our hybrid tracking approach represents a significant advancement over previous real-time tracking methods for ultrasound. Mendizabal et al. reported tracking speeds approximately 100 times faster than traditional biomechanical models, but their approach required extensive pre-training on synthetic data. In contrast, our methodology achieves comparable tracking accuracy without requiring synthetic training data, while maintaining processing speeds suitable for real-time clinical applications (54 FPS).

Our hybrid tracking approach also addresses the limitations identified by Tagliabue et al. (Tagliabue et al., 2019), whose position-based modeling approach for tracking lesion displacement during ultrasound-guided breast biopsy achieved a mean tracking error below 11 mm. Our KCF+YOLO combination demonstrates substantially lower error rates while maintaining higher processing speeds, representing a significant improvement in tracking precision and efficiency.

The detection-based recovery mechanism in our hybrid approach builds upon the concepts introduced by Wang et al. (Wang et al., 2018) and Zhang et al. (Zhang et al., 2018), who developed verification networks for long-term visual tracking. However, while their approaches were designed for general object tracking, our implementation is specifically optimized for breast ultrasound characteristics, addressing the unique challenges of ultrasound imaging such as speckle noise, tissue deformation, and probe movement. The resulting performance improvements (Success Rate > 0.97) demonstrate the efficacy of domain-specific optimization in medical tracking applications.

The clinical significance of these tracking improvements becomes apparent when considering the Palestinian healthcare context. As documented by the Palestinian Ministry of Health (Palestinian Ministry of Health, 2022) and Jubran et al. (Juan Jubran, 2018), the shortage of specialized breast radiologists in Palestine creates a critical need for assistive technologies that can enhance the capabilities of general practitioners and sonographers. Our tracking system's ability to maintain lesion identity across ultrasound video frames with high reliability (SR > 0.97) could significantly improve the consistency of examinations performed by less experienced operators, potentially addressing some of the expertise gaps identified in the literature (Giacaman et al., 2009; Saadah et al., 2024).

6.1.4 Clinical Implementation Potential

The integration of optimized contrast enhancement, efficient lesion detection, and robust tracking into a unified framework represents a significant contribution to breast ultrasound analysis with direct clinical implications. The complete pipeline maintained real-time processing capability (approximately 54 frames per second) while achieving high accuracy in lesion detection and tracking, confirming its potential for practical implementation in clinical settings.

This performance level directly addresses the specific challenges faced by the Palestinian healthcare system, where limited radiologist availability, restricted access to advanced imaging modalities, and resource constraints create substantial barriers to effective breast cancer detection (Giacaman et al., 2009; Hamdan & Defever, 2003). By providing automated assistance for breast ultrasound interpretation, the framework creates an opportunity to bridge critical expertise gaps and improve diagnostic consistency across diverse healthcare settings. The demonstrated performance suggests considerable value as a clinical decision support tool, particularly for radiologists with varying levels of experience in breast ultrasound interpretation who may benefit from additional guidance in lesion identification and characterization. This assistance could potentially improve early detection rates, addressing the concerning statistic that 52% of breast cancer cases in Palestine are diagnosed at advanced stages (AlWaheidi et al., 2024).

The framework's ability to maintain consistent performance across varying imaging conditions demonstrates its robustness to differences in equipment quality and radiologist technique. This adaptability is particularly valuable in the fragmented Palestinian healthcare system, where standardization of equipment and training remains challenging (Falah et al., 2020.; Mimi, 2015). By providing reliable performance despite these variations, the system could help establish more consistent diagnostic standards across different healthcare facilities, potentially reducing the disparities in care quality between urban centers and rural regions documented by (Juan Jubran, 2018).

The real-time performance of our framework takes on particular significance when considered against Mimi's findings (Mimi, 2015) regarding digital infrastructure limitations in Palestinian healthcare facilities. Since reliable high-speed internet access is severely limited among healthcare facilities, cloud-based processing solutions would face insurmountable implementation barriers. Our framework's ability to operate efficiently on standard computing hardware without requiring internet connectivity makes it suitable for deployment even in facilities with limited digital infrastructure. The computational efficiency, which maintains real-time performance on modest hardware, addresses a critical consideration for technology deployment in Palestinian healthcare facilities, where advanced computing resources may be limited (Mimi, 2015). These minimal hardware requirements could facilitate wider adoption across different levels of the healthcare system, from tertiary hospitals to primary care centers.

Moreover, the framework's design as an assistive tool rather than a replacement for human expertise aligns with the needs and realities of the Palestinian healthcare workforce. By augmenting rather than replacing radiologist judgment, the system could help address the shortage of specialized radiologists (Saadah et al., 2024) while supporting the continued development of local expertise through guided interpretation. It is important to note that implementation of this system would still require qualified radiologists to perform the ultrasound procedures, as per Palestinian Physician Society regulations that restrict ultrasound practice to radiologists only. The AI framework serves as a decision support tool to enhance radiologist efficiency and diagnostic accuracy rather than replacing the need for specialist involvement. This approach acknowledges the importance of building local capacity rather than creating technology dependencies, a consideration emphasized by (Giacaman et al., 2009) as critical for sustainable healthcare improvements in Palestine.

The comprehensive evaluation using ultrasound video sequences with confirmatory biopsy results validated the clinical applicability of the framework. This validation approach addresses concerns raised by (Saadah et al., 2024) regarding the "lack of skilled experts able to accurately interpret mammograms" by demonstrating that AI-assisted interpretation can maintain high accuracy levels across diverse imaging conditions. Such capabilities could be particularly valuable in rural and underserved areas of Palestine, where (AL-Tell, 2019) documented significant barriers to accessing specialized imaging services. However, successful implementation would require ensuring adequate radiologist coverage in these underserved areas, as the system cannot address the fundamental requirement for qualified radiologists to perform the procedures.

Furthermore, the use of locally collected data in system development ensures its relevance to the Palestinian patient population. This approach addresses potential concerns about the applicability of systems trained primarily on Western populations, which (Najjar & Easson, 2010) identified as potentially problematic given the different age profiles and clinical presentations of breast cancer in Arab women. By developing and validating the system using data from Palestinian healthcare facilities, the framework is inherently adapted to the specific characteristics of breast cancer presentation in this population, where diagnosis occurs approximately ten years earlier than in Western countries (Najjar & Easson, 2010).

For successful implementation in the Palestinian healthcare system, the following considerations must be addressed: 1) ensuring adequate radiologist training on the AI-assisted system, 2) maintaining compliance with Palestinian Physician Society regulations requiring radiologist-performed procedures, 3) developing strategies to optimize radiologist workflow efficiency through AI assistance, 4) establishing protocols for quality assurance and system maintenance within the existing radiologist-centered framework, and 5) exploring integration directly into ultrasound equipment manufacturers' systems to provide seamless, real-time AI assistance during the scanning process itself.

A particularly promising implementation approach would involve partnering with ultrasound equipment manufacturers to embed the AI framework directly into the screening devices. This integration would allow the lesion detection and tracking algorithms to operate in real-time during the examination, providing immediate visual feedback to radiologists as they perform the scan. Such embedded solutions could display detection overlays, measurement assistance, and diagnostic suggestions directly on the ultrasound console, streamlining the workflow without requiring separate computer systems or additional hardware setup. This approach would also ensure consistent availability of the AI assistance across different healthcare facilities while maintaining the radiologist-centered practice requirements of the Palestinian healthcare system.

6.3 Considerations and Challenges

Despite the promising results, several important considerations and challenges must be acknowledged for accurate interpretation of this research. The dataset used in this study, while substantial (17,903 ultrasound cases), was collected from only two healthcare facilities in Palestine. This geographical constraint may limit the generalizability of the findings to other healthcare settings with different patient populations, equipment characteristics, or examination protocols. This consideration is particularly relevant given the diversity of healthcare providers

and facilities across the Palestinian territories, as documented by (Palestinian Ministry of Health, 2022).

The evaluation approach in this research focused predominantly on the technical performance of the framework rather than its impact on clinical outcomes or decision-making processes. While the system demonstrated high accuracy in lesion detection and tracking under controlled evaluation conditions, this does not automatically translate to improved diagnostic accuracy or patient outcomes in clinical practice. As emphasized by (Giacaman et al., 2009), technological interventions in the Palestinian healthcare system must demonstrate tangible improvements in care delivery to justify their implementation. Therefore, further research is needed to assess the framework's effect on real-world clinical metrics such as diagnostic accuracy, time to diagnosis, and appropriate referral rates.

A technical limitation of the current implementation lies in its focus on single lesion tracking rather than multiple object tracking capabilities. This constraint, while aligned with typical clinical practice where radiologists often focus on one suspicious finding at a time during ultrasound examination, may restrict the system's utility in cases with multiple lesions requiring simultaneous monitoring. This limitation becomes particularly relevant in screening contexts where multiple suspicious findings may be present, requiring comprehensive assessment and documentation.

Additionally, the framework was evaluated exclusively on 2D B-mode ultrasound images, which represent the most commonly available technology in Palestinian healthcare facilities as noted by (Juan Jubran, 2018). However, this approach does not leverage the additional diagnostic information that could be provided by more advanced techniques such as Doppler, elastography, or 3D ultrasound. While this limitation reflects the current technological reality in many Palestinian healthcare settings, it also represents a constraint on the system's diagnostic capabilities compared to more advanced imaging approaches available in better-resourced environments.

Moreover, while the system demonstrated robust performance across the available dataset, its ability to handle rare or atypical presentations of breast cancer remains uncertain. The relatively small number of malignant cases in the dataset, reflecting the general prevalence of malignancy in screening populations, limits the system's exposure to uncommon manifestations of breast cancer that might be encountered in clinical practice. This concern is particularly relevant given (Najjar & Easson, 2010) findings regarding the unique characteristics of breast cancer presentation in Arab women, which may differ from the patterns typically documented in Western medical literature.

6.4 Future Directions

Building upon the findings and addressing the considerations identified in this research, several promising avenues for future work emerge. Expanding the dataset to include cases from a wider range of healthcare facilities across Palestine represents an essential next step to enhance the generalizability of the findings and improve the system's performance across diverse clinical settings. This expansion would allow the framework to learn from the variety of equipment, operator techniques, and patient demographics encountered throughout the Palestinian healthcare system, potentially addressing some of the geographical constraints noted by (Palestinian Ministry of Health, 2022) in their annual report. Additionally, evaluating our model on internationally

available breast ultrasound datasets would provide crucial insights into its generalizability beyond the Palestinian context. Testing on diverse datasets from different populations, equipment manufacturers, and clinical protocols would strengthen the evidence for the framework's robustness and potentially identify areas requiring further optimization for broader clinical adoption.

To overcome the current technical limitations, implementing multiple objects tracking capabilities would significantly extend the framework's clinical utility, particularly for cases with multiple lesions requiring simultaneous monitoring. This enhancement would necessitate adaptations to the current tracking approach to maintain identity and location information for multiple targets while preserving real-time performance. Such capability would more closely mirror the comprehensive assessment performed by experienced radiologists, who routinely monitor multiple regions of interest during a single examination.

From a technological perspective, exploring the integration of additional ultrasound modalities such as Doppler, elastography, and 3D ultrasound could substantially enhance the diagnostic capabilities of the framework. These modalities provide complementary information about tissue vascularity, stiffness, and three-dimensional structure that could improve the accuracy of lesion characterization. As noted by (AL-Tell, 2019), even limited access to advanced imaging techniques can significantly impact diagnostic accuracy, suggesting that such enhancements could yield meaningful clinical benefits even if implemented selectively in regional centers.

To rigorously validate the clinical impact of the framework, conducting prospective clinical studies would be invaluable for evaluating its effect on diagnostic accuracy, workflow efficiency, and clinical decision-making processes. Such studies should include diverse healthcare providers, from specialists to general practitioners, to assess the system's effectiveness across different levels of expertise. This approach would address (Saadah et al., 2024) concerns regarding diagnostic consistency while providing concrete evidence of the framework's utility in real-world clinical scenarios rather than controlled research environments.

Recognizing the educational challenges documented by (Juan Jubran, 2018), developing training components to accompany the framework could transform it from a diagnostic aid into a comprehensive educational tool for healthcare providers. By explaining the rationale behind its detections and providing annotated reference cases, the system could contribute to building local expertise in breast ultrasound interpretation. This educational dimension could be particularly valuable in addressing the systemic shortage of specialized training opportunities highlighted by (Mimi, 2015) in the Palestinian healthcare workforce.

Beyond breast imaging, extending the framework to other medical imaging applications relevant to the Palestinian healthcare context could maximize its impact on public health. The methodological approach developed in this research—combining optimized preprocessing, efficient detection, and robust tracking—could be adapted to other imaging modalities and anatomical regions where similar expertise gaps exist. This expansion would align with (Giacaman et al., 2009) call for integrated approaches to healthcare improvement in Palestine, where technological innovations address multiple interrelated challenges rather than isolated issues.

6.5 Conclusion

This research developed and validated an advanced deep learning framework for real-time breast cancer lesion analysis in clinical ultrasound videos, specifically designed to address the challenges within the Palestinian healthcare context. The framework integrates optimized contrast enhancement using CLAHE, efficient lesion detection with YOLOv11-L, and robust tracking through a hybrid KCF+YOLO approach, achieving high performance in all components while maintaining real-time processing capability.

The findings demonstrate that deep learning approaches can effectively enhance breast ultrasound interpretation capabilities in resource-constrained healthcare environments. By providing automated assistance for lesion detection and tracking, the framework has the potential to complement limited specialized expertise, improve diagnostic consistency, and enhance early detection capabilities in settings where traditional approaches to capacity building face significant barriers.

The methodological approach established in this research offers a blueprint for developing context-specific AI systems for medical imaging in resource-constrained environments. By carefully considering both technical performance and implementation feasibility, this approach ensures that technological innovations address the practical realities of healthcare delivery in challenging contexts.

In conclusion, this research represents a significant contribution to addressing breast cancer detection challenges in Palestine by providing a computationally efficient, clinically applicable framework that complements limited specialized expertise. While further research is needed to evaluate its impact on clinical outcomes and decision-making, the demonstrated technical performance suggests considerable potential for enhancing breast cancer detection capabilities in the Palestinian healthcare system.

References

Abadi, M., Agarwal, A., Barham, P., Brevdo, E., Chen, Z., Citro, C., Corrado, G. S., Davis, A., Dean, J., Devin, M., Ghemawat, S., Goodfellow, I., Harp, A., Irving, G., Isard, M., Jia, Y., Jozefowicz, R., Kaiser, L., Kudlur, M., … Research, G. (2016). *TensorFlow: Large-Scale Machine Learning on Heterogeneous Distributed Systems*. https://arxiv.org/abs/1603.04467v2

Abd-Elmoniem, K. Z., Youssef, A. B. M., & Kadah, Y. M. (2002). Real-time speckle reduction and coherence enhancement in ultrasound imaging via nonlinear anisotropic diffusion. *IEEE Transactions on Biomedical Engineering*, *49*(9), 997–1014. https://doi.org/10.1109/TBME.2002.1028423

Adabi, S., Ghavami, S., Fatemi, M., & Alizad, A. (2019). Non-Local Based Denoising Framework for In Vivo Contrast-Free Ultrasound Microvessel Imaging. *Sensors 2019, Vol. 19, Page 245*, *19*(2), 245. https://doi.org/10.3390/S19020245

Ahn, J. S., Shin, S., Yang, S. A., Park, E. K., Kim, K. H., Cho, S. I., Ock, C. Y., & Kim, S. (2023). Artificial Intelligence in Breast Cancer Diagnosis and Personalized Medicine. *Journal of Breast Cancer*, *26*(5), 405. https://doi.org/10.4048/JBC.2023.26.E45

Ajmal, S., & Ajmal, S. (2021). Contrast-Enhanced Ultrasonography: Review and Applications. *Cureus*, *13*(9). https://doi.org/10.7759/CUREUS.18243

Albukhari, M. ;, Chen, C.-H., Chi, L., Wu, J., Pan, S., Li, L., Ragab, M., Albukhari, A., Alyami, J., & Mansour, R. F. (2022). Ensemble Deep-Learning-Enabled Clinical Decision Support System for Breast Cancer Diagnosis and Classification on Ultrasound Images. *Biology 2022, Vol. 11, Page 439*, *11*(3), 439. https://doi.org/10.3390/BIOLOGY11030439

Al-Dhabyani, W., Fahmy, A., Gomaa, M., & Khaled, H. (2019). Deep Learning Approaches for Data Augmentation and Classification of Breast Masses using Ultrasound Images. *International Journal of Advanced Computer Science and Applications*, *10*(5), 618–627. https://doi.org/10.14569/IJACSA.2019.0100579

Almuhtaseb, M. I. A., & Alby, F. (2021). Socio-cultural factors and late breast cancer detection in arab-palestinian women. *TPM - Testing, Psychometrics, Methodology in Applied Psychology*, *28*(3), 275–285. https://doi.org/10.4473/TPM28.3.1

AL-Tell Nihal Natour Dina Younes, M. (2019). Barriers to Breast Cancer Screening among Palestinian Women in Nablus Region, North-ern West Bank. *Palestinian Medical and Pharmaceutical Journal*, *5*. https://doi.org/10.59049/2790-0231.1061

AlWaheidi, S., Sullivan, R., & Davies, E. A. (2024). Breast Cancer in Women in Gaza: A Review of Clinical Characteristics and Short-Term Survival. *JCO Global Oncology*, *10*. https://doi.org/10.1200/GO.23.00170/ASSET/CAD46AFF-F017-43E4-9A42-CDD962631024/ASSETS/IMAGES/LARGE/GO.23.00170F3.JPG

Aly, G. H., Marey, M., El-Sayed, S. A., & Tolba, M. F. (2021). YOLO Based Breast Masses Detection and Classification in Full-Field Digital Mammograms. *Computer Methods and Programs in Biomedicine*, *200*, 105823. https://doi.org/10.1016/J.CMPB.2020.105823

Anaconda Documentation - Anaconda. Retrieved March 13, 2025, from https://www.anaconda.com/docs/main

Anthwal, S., & Ganotra, D. (2019). Optical Flow Estimation in Synthetic Image Sequences Using Farneback Algorithm. *Lecture Notes in Electrical Engineering*, *526*, 363–371. https://doi.org/10.1007/978-981-13-2553-3_35

Arani, E., Gowda, S., Mukherjee, R., Magdy, O., Kathiresan, S., & Zonooz, B. (2022). *A Comprehensive Study of Real-Time Object Detection Networks Across Multiple Domains: A Survey*. https://arxiv.org/abs/2208.10895v2

Ardila, D., Kiraly, A. P., Bharadwaj, S., Choi, B., Reicher, J. J., Peng, L., Tse, D., Etemadi, M., Ye, W., Corrado, G., Naidich, D. P., & Shetty, S. (2019). End-to-end lung cancer screening with three-dimensional deep learning on low-dose chest computed tomography. *Nature Medicine 2019 25:6*, *25*(6), 954–961. https://doi.org/10.1038/s41591-019-0447-x

Ayana, G., Dese, K., & Choe, S. W. (2021). Transfer Learning in Breast Cancer Diagnoses via Ultrasound Imaging. *Cancers 2021, Vol. 13, Page 738*, *13*(4), 738. https://doi.org/10.3390/CANCERS13040738

Babenko, B., Yang, M. H., & Belongie, S. (2011). Robust object tracking with online multiple instance learning. *IEEE Transactions on Pattern Analysis and Machine Intelligence*, *33*(8), 1619–1632. https://doi.org/10.1109/TPAMI.2010.226

BeCkeR, A. O. S., MuelleR, M. C. A., StOFFel, elin A., MARCOn, Ma. DA, ghAFOOR, So., & Boss, A. Dr. A. (2018). Classification of breast cancer in ultrasound imaging using a generic deep learning analysis software: a pilot study. *British Journal of Radiology*, *91*(1083). https://doi.org/10.1259/BJR.20170576/7491127

Berg, W. A., Blume, J. D., Cormack, J. B., Mendelson, E. B., Lehrer, D., Böhm-Vélez, M., Pisano, E. D., Jong, R. A., Evans, W. P., Morton, M. J., Mahoney, M. C., Larsen, L. H., Barr, R. G., Farria, D. M., Marques, H. S., & Boparai, K. (2008). Combined Screening With Ultrasound and Mammography vs Mammography Alone in Women at Elevated Risk of Breast Cancer. *JAMA*, *299*(18), 2151–2163. https://doi.org/10.1001/JAMA.299.18.2151

Bertinetto, L., Valmadre, J., Henriques, J. F., Vedaldi, A., & Torr, P. H. S. (2016). Fully-Convolutional Siamese Networks for Object Tracking. *Lecture Notes in Computer Science (Including Subseries Lecture Notes in Artificial Intelligence and Lecture Notes in Bioinformatics)*, *9914 LNCS*, 850–865. https://doi.org/10.1007/978-3-319-48881-3_56

Bharti, P., & Mittal, D. (2020). An Ultrasound Image Enhancement Method Using Neutrosophic Similarity Score. *Ultrasonic Imaging*, *42*(6), 271–283. https://doi.org/10.1177/0161734620961005

Bhateja, V., Srivastava, A., Singh, G., & Singh, J. (2014). A Modified Speckle Suppression Algorithm for Breast Ultrasound Images Using Directional Filters. *Advances in Intelligent Systems and Computing*, *249 VOLUME II*, 219–226. https://doi.org/10.1007/978-3-319-03095-1_24

Bolme, D. S., Beveridge, J. R., Draper, B. A., & Lui, Y. M. (2010). Visual object tracking using adaptive correlation filters. *Proceedings of the IEEE Computer Society Conference on Computer Vision and Pattern Recognition*, 2544–2550. https://doi.org/10.1109/CVPR.2010.5539960

Brem, R. F., Lenihan, M. J., Lieberman, J., & Torrente, J. (2015). Screening breast ultrasound: Past, present, and future. *American Journal of Roentgenology*, *204*(2), 234–240. https://doi.org/10.2214/AJR.13.12072/ASSET/IMAGES/LARGE/02_13_12072_02D.JPEG

Burckhardt, C. B. (1978). Speckle in Ultrasound B-Mode Scans. *IEEE Transactions on Sonics and Ultrasonics*, *25*(1), 1–6. https://doi.org/10.1109/T-SU.1978.30978

Buslaev, A., Iglovikov, V. I., Khvedchenya, E., Parinov, A., Druzhinin, M., & Kalinin, A. A. (2020). Albumentations: Fast and Flexible Image Augmentations. *Information 2020, Vol. 11, Page 125*, *11*(2), 125. https://doi.org/10.3390/INFO11020125

Byra, M., Galperin, M., Ojeda-Fournier, H., Olson, L., O'Boyle, M., Comstock, C., & Andre, M. (2019). Breast mass classification in sonography with transfer learning using a deep convolutional neural network and color conversion. *Medical Physics*, *46*(2), 746–755. https://doi.org/10.1002/MP.13361

Cario, J., & Oelze, M. L. (2022). Design of an electronic radiological clip for improved breast cancer imaging with ultrasound. *The Journal of the Acoustical Society of America*, *151*(4_Supplement), A245–A245. https://doi.org/10.1121/10.0011207

Çelebi, F., Tuncer, O., Oral, M., Duymaz, T., Orhan, T., & Ertaş, G. (2025). Artificial Intelligence in Diagnostic Breast Ultrasound: A Comparative Analysis of Decision Support Among Radiologists With Various Levels of Expertise. *European Journal of Breast Health*, *21*(1), 33. https://doi.org/10.4274/EJBH.GALENOS.2024.2024-9-7

Chan, H. P., Samala, R. K., Hadjiiski, L. M., & Zhou, C. (2020). Deep Learning in Medical Image Analysis. *Advances in Experimental Medicine and Biology*, *1213*, 3–21. https://doi.org/10.1007/978-3-030-33128-3_1

Chaudhury, S., & Sau, K. (2023). Classification of Breast Masses Using Ultrasound Images by Approaching GAN, Transfer Learning, and Deep Learning Techniques. *Journal of Artificial Intelligence and Technology*, *3*(4), 142–153. https://doi.org/10.37965/JAIT.2023.0175

Chen, C., Wang, Y., Niu, J., Liu, X., Li, Q., & Gong, X. (2021). Domain Knowledge Powered Deep Learning for Breast Cancer Diagnosis Based on Contrast-Enhanced Ultrasound Videos. *IEEE Transactions on Medical Imaging*, *40*(9), 2439–2451. https://doi.org/10.1109/TMI.2021.3078370

Cheng, H. D., Shan, J., Ju, W., Guo, Y., & Zhang, L. (2010). Automated breast cancer detection and classification using ultrasound images: A survey. *Pattern Recognition*, *43*(1), 299–317. https://doi.org/10.1016/J.PATCOG.2009.05.012

Cheng, J. Z., Ni, D., Chou, Y. H., Qin, J., Tiu, C. M., Chang, Y. C., Huang, C. S., Shen, D., & Chen, C. M. (2016). Computer-Aided Diagnosis with Deep Learning Architecture: Applications to Breast Lesions in US Images and Pulmonary Nodules in CT Scans. *Scientific Reports 2016 6:1*, *6*(1), 1–13. https://doi.org/10.1038/srep24454

Chiao, J. Y., Chen, K. Y., Ken Ying-Kai Liao, Hsieh, P. H., Zhang, G., & Huang, T. C. (2019). Detection and classification the breast tumors using mask R-CNN on sonograms. *Medicine (United States)*, *98*(19). https://doi.org/10.1097/MD.0000000000015200

Comaniciu, D., & Meer, P. (2002). Mean shift: A robust approach toward feature space analysis. *IEEE Transactions on Pattern Analysis and Machine Intelligence*, *24*(5), 603–619. https://doi.org/10.1109/34.1000236

Dabass, J., & Dabass, M. (2021). Denoising, Edge Correction, and Enhancement of Breast Cancer Ultrasound Images. *Lecture Notes in Electrical Engineering*, *668*, 1153–1172. https://doi.org/10.1007/978-981-15-5341-7_88

Dai, Q., Lin, J., Li, W., & Wang, L. (2024). A Real-Time Network for Fast Breast Lesion Detection in Ultrasound Videos. *Lecture Notes in Computer Science (Including Subseries Lecture Notes in Artificial Intelligence and Lecture Notes in Bioinformatics)*, *14437 LNCS*, 40–50. https://doi.org/10.1007/978-981-99-8558-6_4

Dai, T., Lu, W., Wang, W., Wang, J., & Xia, S. T. (2017). Entropy-based bilateral filtering with a new range kernel. *Signal Processing*, *137*, 223–234. https://doi.org/10.1016/J.SIGPRO.2017.02.005

Dalal, N., & Triggs, B. (2005). Histograms of oriented gradients for human detection. *Proceedings - 2005 IEEE Computer Society Conference on Computer Vision and Pattern Recognition, CVPR 2005*, *I*, 886–893. https://doi.org/10.1109/CVPR.2005.177

Dang, A., Kupelian, P. A., Cao, M., Agazaryan, N., & Kishan, A. U. (2018). Image-guided radiotherapy for prostate cancer. *Translational Andrology and Urology*, *7*(3), 308. https://doi.org/10.21037/TAU.2017.12.37

Daoud, N., Alfayumi-Zeadna, S., & Jabareen, Y. T. (2018). Barriers to Health Care Services Among Palestinian Women Denied Family Unification in Israel. *International Journal of Health Services : Planning, Administration, Evaluation*, *48*(4), 776–797. https://doi.org/10.1177/0020731418783912

Dietrich, C. F., Nolsøe, C. P., Barr, R. G., Berzigotti, A., Burns, P. N., Cantisani, V., Chammas, M. C., Chaubal, N., Choi, B. I., Clevert, D. A., Cui, X., Dong, Y., D'Onofrio, M., Fowlkes, J. B., Gilja, O. H., Huang, P., Ignee, A., Jenssen, C., Kono, Y., … Zheng, R. (2020). Guidelines and Good Clinical Practice Recommendations for Contrast-Enhanced Ultrasound (CEUS) in the Liver–Update 2020 WFUMB in Cooperation with EFSUMB, AFSUMB, AIUM, and FLAUS. *Ultrasound in Medicine and Biology*, *46*(10), 2579–2604. https://doi.org/10.1016/J.ULTRASMEDBIO.2020.04.030/ASSET/0B1068F9-2B62-4EA5-9347-D751E56CEAD0/MAIN.ASSETS/GR1.JPG

Dinesh, M. (2012). Classification of Mass in Breast Ultrasound Images using Image Processing Techniques. *International Journal of Computer Applications*, *42*(10), 975–8887.

Dutt, V., & Greenleaf, J. F. (1996). Adaptive speckle reduction filter for log-compressed B-scan images. *IEEE Transactions on Medical Imaging*, *15*(6), 802–813. https://doi.org/10.1109/42.544498

Dyer, O. (2008). Power cut to hospitals in Gaza for 8-12 hours a day. *BMJ : British Medical Journal*, *336*(7644), 580. https://doi.org/10.1136/BMJ.39517.403947.DB

Elawady, M., Sadek, I., El, A., Shabayek, R., Pons, G., Ganau, S., Sergi, G., & Pons, G. (2016). *Automatic Nonlinear Filtering and Segmentation for Breast Ultrasound Images*. 978. https://doi.org/10.1007/978-3-319-41501-7_24ï

Enquobahrie, A., Gobbi, D., Turek, M. W., Cheng, P., Yaniv, Z., Lindseth, F., & Cleary, K. (2008). Designing tracking software for image-guided surgery applications: IGSTK experience. *International Journal of Computer Assisted Radiology and Surgery*, *3*(5), 395–403. https://doi.org/10.1007/S11548-008-0243-4/METRICS

Esteva, A., Chou, K., Yeung, S., Naik, N., Madani, A., Mottaghi, A., Liu, Y., Topol, E., Dean, J., & Socher, R. (2021). Deep learning-enabled medical computer vision. *Npj Digital Medicine 2021 4:1*, *4*(1), 1–9. https://doi.org/10.1038/s41746-020-00376-2

Falah, B., Meshal, J., & Betawi, W. (2020). *Palestinian Health Sector Assessment: Macro-Analytical Study*.

Fleury, E. F. C., & Marcomini, K. (2020). Breast elastography: diagnostic performance of computer-aided diagnosis software and interobserver agreement. *Radiologia Brasileira*, *53*(1), 27–33. https://doi.org/10.1590/0100-3984.2019.0035

Flores, W. G., & Pereira, W. C. de A. (2017). A contrast enhancement method for improving the segmentation of breast lesions on ultrasonography. *Computers in Biology and Medicine*, *80*, 14–23. https://doi.org/10.1016/J.COMPBIOMED.2016.11.005

Gao, Z., Li, Y., Sun, Y., Yang, J., Xiong, H., Zhang, H., Liu, X., Wu, W., Liang, D., & Li, S. (2018). Motion Tracking of the Carotid Artery Wall from Ultrasound Image Sequences: A Nonlinear State-Space Approach. *IEEE Transactions on Medical Imaging*, *37*(1), 273–283. https://doi.org/10.1109/TMI.2017.2746879

GeForce RTX 4070 Family Graphics Cards | NVIDIA. Retrieved March 13, 2025, from https://www.nvidia.com/en-eu/geforce/graphics-cards/40-series/rtx-4070-family/

Gheflati, B., & Rivaz, H. (2021). *Vision Transformer for Classification of Breast Ultrasound Images*. http://arxiv.org/abs/2110.14731

Giacaman, R., Khatib, R., Shabaneh, L., Ramlawi, A., Sabri, B., Sabatinelli, G., Khawaja, M., & Laurance, T. (2009). Health status and health services in the occupied Palestinian territory. *The Lancet*, *373*(9666), 837–849. https://doi.org/10.1016/S0140-6736(09)60107-0

Glenn Jocher et al. *Yolov11*. Retrieved March 13, 2025, from https://github.com/ultralytics/ultralytics

Gonzalez, R. C., & Woods, R. E. (2018). Digital Image Processing, Global Edition. *Person Education*, 19–44.

Grabner, H., Grabner, M., & Bischof, H. (2006). *Real-Time Tracking via On-line Boosting* (pp. 47–56). . https://graz.elsevierpure.com/en/publications/real-time-tracking-via-on-line-boosting

Hamdan, M., & Defever, M. (2003). Human resources for health in Palestine: a policy analysis: Part I: Current situation and recent developments. *Health Policy*, *64*(2), 243–259. https://doi.org/10.1016/S0168-8510(03)00004-6

Han, S., Kang, H. K., Jeong, J. Y., Park, M. H., Kim, W., Bang, W. C., & Seong, Y. K. (2017). A deep learning framework for supporting the classification of breast lesions in ultrasound images. *Physics in Medicine & Biology*, *62*(19), 7714. https://doi.org/10.1088/1361-6560/AA82EC

Hansen, H. H. G., de Jong, L., Mann, R., Siepel, F., Nikolaev, A., Tagliabue, E., Maris, B., Groenhuis, V., Caballo, M., Sechopoulos, I., & de Korte, C. L. (2019). *Ultrasound-guided breast biopsy of ultrasound occult lesions using multimodality image co-registration and tissue displacement tracking*. 109550W. https://doi.org/10.1117/12.2513630

Harris, C. R., Millman, K. J., van der Walt, S. J., Gommers, R., Virtanen, P., Cournapeau, D., Wieser, E., Taylor, J., Berg, S., Smith, N. J., Kern, R., Picus, M., Hoyer, S., van Kerkwijk, M. H., Brett, M., Haldane, A., del Río, J. F., Wiebe, M., Peterson, P., … Oliphant, T. E. (2020). Array programming

with NumPy. *Nature 2020 585:7825*, *585*(7825), 357–362. https://doi.org/10.1038/s41586-020-2649-2

Henriques, J. F., Caseiro, R., Martins, P., & Batista, J. (2015). High-speed tracking with kernelized correlation filters. *IEEE Transactions on Pattern Analysis and Machine Intelligence*, *37*(3), 583–596. https://doi.org/10.1109/TPAMI.2014.2345390

Hijab, A., Rushdi, M. A., Gomaa, M. M., & Eldeib, A. (2019). Breast Cancer Classification in Ultrasound Images using Transfer Learning. *International Conference on Advances in Biomedical Engineering, ICABME*, *2019-October*. https://doi.org/10.1109/ICABME47164.2019.8940291

Hiremath, P. S., Akkasaligar, P. T., Badiger, S., Hiremath, P. S., Akkasaligar, P. T., & Badiger, S. (2013). Speckle Noise Reduction in Medical Ultrasound Images. *Advancements and Breakthroughs in Ultrasound Imaging*. https://doi.org/10.5772/56519

Hong, Y. T., Yu, Z. H., & Chou, C. P. (2025). Comparative Study of AI Modes in Ultrasound Diagnosis of Breast Lesions. *Diagnostics 2025, Vol. 15, Page 560*, *15*(5), 560. https://doi.org/10.3390/DIAGNOSTICS15050560

Hosny, A., Parmar, C., Quackenbush, J., Schwartz, L. H., & Aerts, H. J. W. L. (2018). Artificial intelligence in radiology. *Nature Reviews Cancer 2018 18:8*, *18*(8), 500–510. https://doi.org/10.1038/s41568-018-0016-5

Hua, Y., Alahari, K., & Schmid Inria, C. (2015). *Online Object Tracking with Proposal Selection*.

Huang, Q., Zhang, F., & Li, X. (2018). Machine Learning in Ultrasound Computer-Aided Diagnostic Systems: A Survey. *BioMed Research International*, *2018*(1), 5137904. https://doi.org/10.1155/2018/5137904

Hunter, J. D. (2007). Matplotlib: A 2D graphics environment. *Computing in Science and Engineering*, *9*(3), 90–95. https://doi.org/10.1109/MCSE.2007.55

Intel® Core™ i7-12700K Processor. Retrieved March 13, 2025, from https://www.intel.com/content/www/us/en/products/sku/134594/intel-core-i712700k-processor-25m-cache-up-to-5-00-ghz/specifications.html

Jabeen, K., Khan, M. A., Alhaisoni, M., Tariq, U., Zhang, Y. D., Hamza, A., Mickus, A., & Damaševičius, R. (2022). Breast Cancer Classification from Ultrasound Images Using Probability-Based Optimal Deep Learning Feature Fusion. *Sensors 2022, Vol. 22, Page 807*, *22*(3), 807. https://doi.org/10.3390/S22030807

Juan Jubran, A. S. (2018). *UNFPA Palestine | Pathway to Survival - the Story of Breast Cancer in Palestine*. https://palestine.unfpa.org/en/publications/pathway-survival-story-breast-cancer-palestine

Kalal, Z., Mikolajczyk, K., & Matas, J. (2010). Forward-backward error: Automatic detection of tracking failures. *Proceedings - International Conference on Pattern Recognition*, 2756–2759. https://doi.org/10.1109/ICPR.2010.675

Kalal, Z., Mikolajczyk, K., & Matas, J. (2012). Tracking-learning-detection. *IEEE Transactions on Pattern Analysis and Machine Intelligence*, *34*(7), 1409–1422. https://doi.org/10.1109/TPAMI.2011.239

Kariri, M., Jalambo, M. O., Kanou, B., Deqes, S., Younis, S., Zabut, B., & Balawi, U. (2017). Risk Factors for Breast Cancer in Gaza Strip, Palestine: a Case-Control Study. *Clinical Nutrition Research*, *6*(3), 161–171. https://doi.org/10.7762/CNR.2017.6.3.161

Khaled, R., Vidal, J., Vilanova, J. C., & Martí, R. (2022). A U-Net Ensemble for breast lesion segmentation in DCE MRI. *Computers in Biology and Medicine*, *140*, 105093. https://doi.org/10.1016/J.COMPBIOMED.2021.105093

Khanam, R., & Hussain, M. (2024). *YOLOv11: An Overview of the Key Architectural Enhancements*. https://arxiv.org/abs/2410.17725v1

Khatib, R., Giacaman, R., Khammash, U., & Yusuf, S. (2017). Challenges to conducting epidemiology research in chronic conflict areas: examples from PURE- Palestine. *Conflict and Health*, *10*(1). https://doi.org/10.1186/S13031-016-0101-X

Kluyver, T., Ragan-Kelley, B., Pérez, F., Granger, B., Bussonnier, M., Frederic, J., Kelley, K., Hamrick, J., Grout, J., Corlay, S., Ivanov, P., Avila, D., Abdalla, S., & Willing, C. (2016). Jupyter Notebooks – a publishing format for reproducible computational workflows. *Positioning and Power in Academic Publishing: Players, Agents and Agendas - Proceedings of the 20th International Conference on Electronic Publishing, ELPUB 2016*, 87–90. https://doi.org/10.3233/978-1-61499-649-1-87

Kucukkaya, F., Aribal, E., Tureli, D., Altas, H., & Kaya, H. (2016). Use of a volume navigation technique for combining real-time ultrasound and contrast-enhanced MRI: Accuracy and feasibility of a novel technique for locating breast lesions fikret kucukkaya1. *American Journal of Roentgenology*, *206*(1), 217–225. https://doi.org/10.2214/AJR.14.14101/ASSET/IMAGES/LARGE/01_14_14101_07B.JPEG

Kumar, A., & Srivastava, S. (2022). Restoration and enhancement of breast ultrasound images using extended complex diffusion based unsharp masking. *Proceedings of the Institution of Mechanical Engineers, Part H: Journal of Engineering in Medicine*, *236*(1), 12–29. https://doi.org/10.1177/09544119211039317

Kumar, A., & Srivastava, S. (2023). A Qualitative and Quantitative Comparative Study of Different Denoising and Enhancement Techniques for Breast Mammograms, Ultrasound and Magnetic Resonance Images. *IET Conference Proceedings*, *2023*(5), 162–169. https://doi.org/10.1049/ICP.2023.1484

Kumar, V., Webb, J. M., Gregory, A., Denis, M., Meixner, D. D., Bayat, M., Whaley, D. H., Fatemi, M., & Alizad, A. (2018). Automated and real-time segmentation of suspicious breast masses using convolutional neural network. *PLOS ONE*, *13*(5), e0195816. https://doi.org/10.1371/JOURNAL.PONE.0195816

L. C, M., & Joe, J. P. (2024). An optimal deep learning approach for breast cancer detection and classification with pre-trained CNN-based feature learning mechanism. *Journal of Biomolecular Structure and Dynamics*. https://doi.org/10.1080/07391102.2024.2430454

Labcharoenwongs, P., Vonganansup, S., Chunhapran, O., Noolek, D., & Yampaka, T. (2023). An Automatic Breast Tumor Detection and Classification including Automatic Tumor Volume Estimation Using Deep Learning Technique. *Asian Pacific Journal of Cancer Prevention*, *24*(3), 1081–1088. https://doi.org/10.31557/APJCP.2023.24.3.1081

Latif, G., Butt, M. O., Yousif Al Anezi, F., & Alghazo, J. (2020a). Ultrasound Image Despeckling and detection of Breast Cancer using Deep CNN. *Proceedings - 2020 RIVF International Conference on Computing and Communication Technologies, RIVF 2020*. https://doi.org/10.1109/RIVF48685.2020.9140767

Latif, G., Butt, M. O., Yousif Al Anezi, F., & Alghazo, J. (2020b). Ultrasound Image Despeckling and detection of Breast Cancer using Deep CNN. *Proceedings - 2020 RIVF International Conference on Computing and Communication Technologies, RIVF 2020*. https://doi.org/10.1109/RIVF48685.2020.9140767

Lee, J., & Cheng Tsui-Fen, F. (2024). Clinical application of novel mobile AI solution for real-time detection and differential diagnosis in breast ultrasound: The first prospective feasibility study. *Journal of Clinical Oncology*, *42*(16_suppl), 574–574. https://doi.org/10.1200/JCO.2024.42.16_SUPPL.574

Li, Y., Xie, S., Chen, X., Dollar, P., He, K., & Girshick, R. (2021). *Benchmarking Detection Transfer Learning with Vision Transformers*. https://arxiv.org/abs/2111.11429v1

Litjens, G., Kooi, T., Bejnordi, B. E., Setio, A. A. A., Ciompi, F., Ghafoorian, M., van der Laak, J. A. W. M., van Ginneken, B., & Sánchez, C. I. (2017). A survey on deep learning in medical image analysis. *Medical Image Analysis*, *42*, 60–88. https://doi.org/10.1016/J.MEDIA.2017.07.005

Liu, S., Lu, Q., & Dai, S. (2025). Adaptive histogram equalization framework based on new visual prior and optimization model. *Signal Processing: Image Communication*, *132*, 117246. https://doi.org/10.1016/J.IMAGE.2024.117246

Liu, S., Wang, Y., Yang, X., Lei, B., Liu, L., Li, S. X., Ni, D., & Wang, T. (2019). Deep Learning in Medical Ultrasound Analysis: A Review. *Engineering*, *5*(2), 261–275. https://doi.org/10.1016/J.ENG.2018.11.020

Liu, W., Anguelov, D., Erhan, D., Szegedy, C., Reed, S., Fu, C. Y., & Berg, A. C. (2016). SSD: Single shot multibox detector. *Lecture Notes in Computer Science (Including Subseries Lecture Notes in Artificial Intelligence and Lecture Notes in Bioinformatics)*, *9905 LNCS*, 21–37. https://doi.org/10.1007/978-3-319-46448-0_2/FIGURES/5

Lucas, B. D., & Kanade, T. (2018). *An Iterative Image Registration Technique with an Application to Stereo Vision*.

Lukežič, A., Vojíř, T., Čehovin Zajc, L., Matas, J., & Kristan, M. (2018). Discriminative Correlation Filter Tracker with Channel and Spatial Reliability. *International Journal of Computer Vision*, *126*(7), 671–688. https://doi.org/10.1007/S11263-017-1061-3/METRICS

Makandar, A., & Halalli, B. (2015). Breast Cancer Image Enhancement using Median Filter and CLAHE. *International Journal of Scientific & Engineering Research*, *6*(4). http://www.ijser.org

Makwana, G., Yadav, R. N., & Gupta, L. (2022). Analysis of Various Noise Reduction Techniques for Breast Ultrasound Image Enhancement. *Lecture Notes in Electrical Engineering*, *825*, 303–313. https://doi.org/10.1007/978-981-16-7637-6_27

Mallat, S. G. (1989). A Theory for Multiresolution Signal Decomposition: The Wavelet Representation. *IEEE Transactions on Pattern Analysis and Machine Intelligence*, *11*(7), 674–693. https://doi.org/10.1109/34.192463

Mango, V. L., Sun, M., Wynn, R. T., & Ha, R. (2020). Should we ignore, follow, or biopsy? Impact of artificial intelligence decision support on breast ultrasound lesion assessment. *American Journal of Roentgenology*, *214*(6), 1445–1452. https://doi.org/10.2214/AJR.19.21872/ASSET/IMAGES/LARGE/06_19_21872_06_CMYK.JPEG

Marvasti-Zadeh, S. M., Cheng, L., Ghanei-Yakhdan, H., & Kasaei, S. (2019). Deep Learning for Visual Tracking: A Comprehensive Survey. *IEEE Transactions on Intelligent Transportation Systems*, *23*(5), 3943–3968. https://doi.org/10.1109/TITS.2020.3046478

McKinney, S. M., Sieniek, M., Godbole, V., Godwin, J., Antropova, N., Ashrafian, H., Back, T., Chesus, M., Corrado, G. C., Darzi, A., Etemadi, M., Garcia-Vicente, F., Gilbert, F. J., Halling-Brown, M., Hassabis, D., Jansen, S., Karthikesalingam, A., Kelly, C. J., King, D., … Shetty, S. (2020). International evaluation of an AI system for breast cancer screening. *Nature 2020 577:7788*, *577*(7788), 89–94. https://doi.org/10.1038/s41586-019-1799-6

McKinney, W. (2010). Data Structures for Statistical Computing in Python. *Scipy*, 56–61. https://doi.org/10.25080/MAJORA-92BF1922-00A

Mendizabal, A., Tagliabue, E., Brunet, J.-N., Dall'alba, D., Fiorini, P., Cotin, S., Mendizabal, * A, & Tagliabue, E. *Physics-based Deep Neural Network for Real-Time Lesion Tracking in Ultrasound-guided Breast Biopsy*. Retrieved April 2, 2025, from https://inria.hal.science/hal-02311277v1

Mimi, Y. (2015). *The Routine Health Information System in Palestine: Determinants and Performance*.

Mohammed, A., Razek, M. A., El-dosuky, M., & Sobhi, A. (2023). *Breast Cancer Detection Using Deep Learning Technique Based On Ultrasound Image*.

Najjar, H., & Easson, A. (2010). Age at diagnosis of breast cancer in Arab nations. *International Journal of Surgery*, *8*(6), 448–452. https://doi.org/10.1016/J.IJSU.2010.05.012

Nissan, A., Spira, R. M., Hamburger, T., Badrriyah, M., Prus, D., Cohen, T., Hubert, A., Freund, H. R., & Peretz, T. (2004). Clinical profile of breast cancer in Arab and Jewish women in the Jerusalem area. *American Journal of Surgery*, *188*(1), 62–67. https://doi.org/10.1016/j.amjsurg.2003.11.039

Njeh, I., Sassi, O. B., Chtourou, K., & Ben Ha Mida, A. (2011). *Speckle noise reduction in breast ultrasound images: SMU (SRAD median unsharp) approch*. 1–6. https://doi.org/10.1109/SSD.2011.5981429

Noble, J. A., & Boukerroui, D. (2006). Ultrasound image segmentation: A survey. *IEEE Transactions on Medical Imaging*, *25*(8), 987–1010. https://doi.org/10.1109/TMI.2006.877092

Ortmaier, T., Vitrani, M.-A., Morel, G., & Pinault, S. (2005). Robust real-time instrument tracking in ultrasound images. *Https://Doi.Org/10.1117/12.594109*, *5750*, 170–177. https://doi.org/10.1117/12.594109

Pacal, İ. (2022). Deep Learning Approaches for Classification of Breast Cancer in Ultrasound (US) Images. *Journal of the Institute of Science and Technology*, *12*(4), 1917–1927. https://doi.org/10.21597/JIST.1183679

Palestinian Ministry of Health. (2022). *Annual Health Report*. https://site.moh.ps/Content/Books/qEbwa3OkFYRzxTPkZMgjNqwMUHxyrrY2NPBl5lui4Fu5kUPtNtDIva_jdAtJuL53McCo1cwhdKheWcMLNwVMRo2a7EJhCs7LE5jQklgULmBUj.pdf

Paszke, A., Gross, S., Massa, F., Lerer, A., Bradbury Google, J., Chanan, G., Killeen, T., Lin, Z., Gimelshein, N., Antiga, L., Desmaison, A., Xamla, A. K., Yang, E., Devito, Z., Raison Nabla, M., Tejani, A., Chilamkurthy, S., Ai, Q., Steiner, B., … Chintala, S. (2019). PyTorch: An Imperative Style, High-Performance Deep Learning Library. *Advances in Neural Information Processing Systems*, *32*.

Peralta, L., Christensen-Jeffries, K., Caius, M., & Samani, A. (2023). Comparative Study of Ultrasound Tissue Motion Tracking Techniques for Effective Breast Ultrasound Elastography. *Applied Sciences 2023, Vol. 13, Page 11912*, *13*(21), 11912. https://doi.org/10.3390/APP132111912

Perona, P., & Malik, J. (1990). Scale-Space and Edge Detection Using Anisotropic Diffusion. *IEEE Transactions on Pattern Analysis and Machine Intelligence*, *12*(7), 629–639. https://doi.org/10.1109/34.56205

Pesteie, M., Abolmaesumi, P., Ashab, H. A. D., Lessoway, V. A., Massey, S., Gunka, V., & Rohling, R. N. (2015). Real-time ultrasound image classification for spine anesthesia using local directional Hadamard features. *International Journal of Computer Assisted Radiology and Surgery*, *10*(6), 901–912. https://doi.org/10.1007/S11548-015-1202-5

Phelps, M. E., Cherry, S. R., & Dahlbom, M. (2006). PET: Physics, instrumentation, and scanners. *PET: Physics, Instrumentation, and Scanners*, 1–130. https://doi.org/10.1007/0-387-34946-4/COVER

Pizer, S. M., Amburn, E. P., Austin, J. D., Cromartie, R., Geselowitz, A., Greer, T., ter Haar Romeny, B., Zimmerman, J. B., & Zuiderveld, K. (1987). Adaptive histogram equalization and its variations. *Computer Vision, Graphics, and Image Processing*, *39*(3), 355–368. https://doi.org/10.1016/S0734-189X(87)80186-X

Pluim, J. P. W., Maintz, J. B. A. A., & Viergever, M. A. (2003). Mutual-information-based registration of medical images: a survey. *IEEE Transactions on Medical Imaging*, *22*(8), 986–1004. https://doi.org/10.1109/TMI.2003.815867

Qasrawi, R., Daraghmeh, O., Qdaih, I., Thwib, S., Vicuna Polo, S., Owienah, H., Abu Al-Halawa, D., & Atari, S. (2024). Hybrid ensemble deep learning model for advancing breast cancer detection and classification in clinical applications. *Heliyon*, *10*(19). https://doi.org/10.1016/J.HELIYON.2024.E38374/ASSET/593AD600-CDEA-41EC-9A2B-FF1503331473/MAIN.ASSETS/GR5.JPG

Qasrawi, R., Daraghmeh, O., Thwib, S., Qdaih, I., Issa, G., Polo, S. V., Owienah, H., Al-Halawa, D. A., & Atari, S. (2025). Advancing breast cancer detection in ultrasound images using a novel hybrid ensemble deep learning model. *Intelligence-Based Medicine*, *11*, 100222. https://doi.org/10.1016/J.IBMED.2025.100222

Qi, X., Zhang, L., Chen, Y., Pi, Y., Chen, Y., Lv, Q., & Yi, Z. (2019). Automated diagnosis of breast ultrasonography images using deep neural networks. *Medical Image Analysis*, *52*, 185–198. https://doi.org/10.1016/J.MEDIA.2018.12.006

Quellec, G., Cazuguel, G., Cochener, B., & Lamard, M. (2017). Multiple-Instance Learning for Medical Image and Video Analysis. *IEEE Reviews in Biomedical Engineering*, *10*, 213–234. https://doi.org/10.1109/RBME.2017.2651164

Radhi, E. A., & Kamil, M. Y. (2024). Anisotropic Diffusion Method for Speckle Noise Reduction in Breast Ultrasound Images. *International Journal of Intelligent Engineering and Systems*, *17*(2). https://doi.org/10.22266/ijies2024.0430.50

Ragab, M., Albukhari, A., Alyami, J., & Mansour, R. F. (2022). Ensemble Deep-Learning-Enabled Clinical Decision Support System for Breast Cancer Diagnosis and Classification on Ultrasound Images. *Biology*, *11*(3), 439. https://doi.org/10.3390/BIOLOGY11030439

Rahman, S., Rahman, M. M., Abdullah-Al-Wadud, M., Al-Quaderi, G. D., & Shoyaib, M. (2016). An adaptive gamma correction for image enhancement. *Eurasip Journal on Image and Video Processing*, *2016*(1), 1–13. https://doi.org/10.1186/S13640-016-0138-1/TABLES/4

Raza, A., Ullah, N., Khan, J. A., Assam, M., Guzzo, A., & Aljuaid, H. (2023). DeepBreastCancerNet: A Novel Deep Learning Model for Breast Cancer Detection Using Ultrasound Images. *Applied Sciences 2023, Vol. 13, Page 2082*, *13*(4), 2082. https://doi.org/10.3390/APP13042082

Reddy, K., Gharde, P., Tayade, H., Patil, M., Reddy, L. S., Surya, D., Reddy, K., Gharde, P., Tayade, H., Patil, M., Reddy, L. srivani, & Surya, D. (2023). Advancements in Robotic Surgery: A Comprehensive Overview of Current Utilizations and Upcoming Frontiers. *Cureus*, *15*(12). https://doi.org/10.7759/CUREUS.50415

Redmon, J., Divvala, S., Girshick, R., & Farhadi, A. (2015). You Only Look Once: Unified, Real-Time Object Detection. *Proceedings of the IEEE Computer Society Conference on Computer Vision and Pattern Recognition*, *2016-December*, 779–788. https://doi.org/10.1109/CVPR.2016.91

Ren, S., He, K., Girshick, R., & Sun, J. (2015). Faster R-CNN: Towards Real-Time Object Detection with Region Proposal Networks. *IEEE Transactions on Pattern Analysis and Machine Intelligence*, *39*(6), 1137–1149. https://doi.org/10.1109/TPAMI.2016.2577031

Riboldi, M., Orecchia, R., & Baroni, G. (2012). Real-time tumour tracking in particle therapy: Technological developments and future perspectives. *The Lancet Oncology*, *13*(9), e383–e391. https://doi.org/10.1016/S1470-2045(12)70243-7/ASSET/BB9E047D-CD13-4D42-953D-7FF50B093981/MAIN.ASSETS/GR2.SML

Richa, R., Balicki, M., Meisner, E., Sznitman, R., Taylor, R., & Hager, G. (2011). Visual Tracking of Surgical Tools for Proximity Detection in Retinal Surgery. *Lecture Notes in Computer Science (Including Subseries Lecture Notes in Artificial Intelligence and Lecture Notes in Bioinformatics)*, *6689 LNCS*, 55–66. https://doi.org/10.1007/978-3-642-21504-9_6

Roboflow: Computer vision tools for developers and enterprises. Retrieved March 13, 2025, from https://roboflow.com/

Rodriguez-Cristerna, A., Guerrero-Cedillo, C. P., Donati-Olvera, G. A., Gomez-Flores, W., & Pereira, W. C. A. (2017). Study of the impact of image preprocessing approaches on the segmentation and classification of breast lesions on ultrasound. *2017 14th International Conference on Electrical Engineering, Computing Science and Automatic Control, CCE 2017*. https://doi.org/10.1109/ICEEE.2017.8108826

Rodríguez-Ruiz, A., Krupinski, E., Mordang, J. J., Schilling, K., Heywang-Köbrunner, S. H., Sechopoulos, I., & Mann, R. M. (2019). Detection of breast cancer with mammography: Effect of an artificial intelligence support system. *Radiology*, *290*(3), 305–314.

https://doi.org/10.1148/RADIOL.2018181371/ASSET/IMAGES/LARGE/RADIOL.2018181371.FIG6B.JPEG

Royer, L., Krupa, A., Dardenne, G., Le Bras, A., Marchand, E., & Marchal, M. (2017). Real-time target tracking of soft tissues in 3D ultrasound images based on robust visual information and mechanical simulation. *Medical Image Analysis*, *35*, 582–598. https://doi.org/10.1016/J.MEDIA.2016.09.004

Saadah, H., Owda, A. Y., & Owda, M. (2024). Convolutional neural networks breast cancer classification using Palestinian mammogram dataset. *Indonesian Journal of Electrical Engineering and Computer Science*, *36*(2), 1149–1162. https://doi.org/10.11591/ijeecs.v36.i2.pp1149-1162

Samanta, P. K., Basuli, A., Rout, N. K., & Panda, G. (2023). Improved Breast Cancer Detection from Ultrasound Images Using YOLOv8 Model. *2023 IEEE 3rd International Conference on Applied Electromagnetics, Signal Processing, and Communication, AESPC 2023*. https://doi.org/10.1109/AESPC59761.2023.10390341

Schlemper, J., Oktay, O., Schaap, M., Heinrich, M., Kainz, B., Glocker, B., & Rueckert, D. (2019). Attention gated networks: Learning to leverage salient regions in medical images. *Medical Image Analysis*, *53*, 197–207. https://doi.org/10.1016/J.MEDIA.2019.01.012

Sellami, L., Sassi, O. Ben, Chtourou, K., & Hamida, A. Ben. (2015). Breast Cancer Ultrasound Images' Sequence Exploration Using BI-RADS Features' Extraction: Towards an Advanced Clinical Aided Tool for Precise Lesion Characterization. *IEEE Transactions on Nanobioscience*, *14*(7), 740–745. https://doi.org/10.1109/TNB.2015.2486621

Sharma, A., Gonzalez, E. A., Ambinder, E., Myers, K., Oluyemi, E., & Bell, M. A. L. (2023). Real-time coherence imaging of suspicious breast masses recommended for aspiration or biopsy. *IEEE International Ultrasonics Symposium, IUS*. https://doi.org/10.1109/IUS51837.2023.10307040

Shaw, C. J., Ter Haar, G. R., Rivens, I. H., Giussani, D. A., & Lees, C. C. (2014). Pathophysiological mechanisms of high-intensity focused ultrasound-mediated vascular occlusion and relevance to non-invasive fetal surgery. *Journal of the Royal Society Interface*, *11*(95), 20140029. https://doi.org/10.1098/RSIF.2014.0029

Shen, L., Margolies, L. R., Rothstein, J. H., Fluder, E., McBride, R., & Sieh, W. (2019). Deep Learning to Improve Breast Cancer Detection on Screening Mammography. *Scientific Reports 2019 9:1*, *9*(1), 1–12. https://doi.org/10.1038/s41598-019-48995-4

Shen, Y., Shamout, F. E., Oliver, J. R., Witowski, J., Kannan, K., Park, J., Wu, N., Huddleston, C., Wolfson, S., Millet, A., Ehrenpreis, R., Awal, D., Tyma, C., Samreen, N., Gao, Y., Chhor, C., Gandhi, S., Lee, C., Kumari-Subaiya, S., … Geras, K. J. (2021). Artificial intelligence system reduces false-positive findings in the interpretation of breast ultrasound exams. *Nature Communications 2021 12:1*, *12*(1), 1–13. https://doi.org/10.1038/s41467-021-26023-2

Singh, K., & Kapoor, R. (2014). Image enhancement using Exposure based Sub Image Histogram Equalization. *Pattern Recognition Letters*, *36*(1), 10–14. https://doi.org/10.1016/J.PATREC.2013.08.024

Sohan, M., Sai Ram, T., & Rami Reddy, Ch. V. (2024). *A Review on YOLOv8 and Its Advancements*. 529–545. https://doi.org/10.1007/978-981-99-7962-2_39

Stark, J. A. (2000). Adaptive image contrast enhancement using generalizations of histogram equalization. *IEEE Transactions on Image Processing*, *9*(5), 889–896. https://doi.org/10.1109/83.841534

State of Palestine Palestinian Central Bureau of Statistics Palestine in Figures. (2023). http://www.pcbs.gov.ps

Suganyadevi, S., Seethalakshmi, V., & Balasamy, K. (2021). A review on deep learning in medical image analysis. *International Journal of Multimedia Information Retrieval 2021 11:1*, *11*(1), 19–38. https://doi.org/10.1007/S13735-021-00218-1

Sun, L., Legood, R., Dos-Santos-Silva, I., Gaiha, S. M., & Sadique, Z. (2018). Global treatment costs of breast cancer by stage: A systematic review. *PLoS ONE*, *13*(11), e0207993. https://doi.org/10.1371/JOURNAL.PONE.0207993

Tagliabue, E., Dall'Alba, D., Magnabosco, E., Tenga, C., Peterlik, I., & Fiorini, P. (2019). Position-based modeling of lesion displacement in ultrasound-guided breast biopsy. *International Journal of Computer Assisted Radiology and Surgery*, *14*(8), 1329–1339. https://doi.org/10.1007/S11548-019-01997-Z/FIGURES/7

Tan, J., Li, J., Li, Y., Li, B., Leng, Y., Rong, Y., & Fu, C. (2024). Autonomous Trajectory Planning for Ultrasound-Guided Real-Time Tracking of Suspicious Breast Tumor Targets. *IEEE Transactions on Automation Science and Engineering*, *21*(3), 2478–2493. https://doi.org/10.1109/TASE.2023.3262844

Tay, P. C., Garson, C. D., Acton, S. T., & Hossack, J. A. (2010). Ultrasound despeckling for contrast enhancement. *IEEE Transactions on Image Processing*, *19*(7), 1847–1860. https://doi.org/10.1109/TIP.2010.2044962

TensorBoard | TensorFlow. Retrieved March 13, 2025, from https://www.tensorflow.org/tensorboard

Teuwen, J., Moriakov, N., Fedon, C., Caballo, M., Reiser, I., Bakic, P., García, E., Diaz, O., Michielsen, K., & Sechopoulos, I. (2021). Deep learning reconstruction of digital breast tomosynthesis images for accurate breast density and patient-specific radiation dose estimation. *Medical Image Analysis*, *71*, 102061. https://doi.org/10.1016/J.MEDIA.2021.102061

The OpenCV Library | Dr Dobb's. Retrieved March 13, 2025, from https://www.drdobbs.com/open-source/the-opencv-library/184404319

Ultrasound System RS85 Prestige | Samsung Healthcare Global. Retrieved March 14, 2025, from https://previous.samsunghealthcare.com/en/products/UltrasoundSystem/RS85%20Prestige/General%20Imaging/benefit

Uniyal, N., Eskandari, H., Abolmaesumi, P., Sojoudi, S., Gordon, P., Warren, L., Rohling, R. N., Salcudean, S. E., & Moradi, M. (2015). Ultrasound RF time series for classification of breast lesions. *IEEE Transactions on Medical Imaging*, *34*(2), 652–661. https://doi.org/10.1109/TMI.2014.2365030

UNRWA. (2022). *Annual Report 2022-Department of Health*. https://www.unrwa.org/resources/reports/annual-report-2022-department-health

User Guide — nsight-systems 2025.1 documentation. Retrieved March 13, 2025, from https://docs.nvidia.com/nsight-systems/UserGuide/index.html

Van Rossum, G., & Drake, F. L. (2009). Python 3 Reference Manual; CreateSpace. *Scotts Valley, CA*, 242. https://www.python.org/

Varghese, R., & Sambath, M. (2024). YOLOv8: A Novel Object Detection Algorithm with Enhanced Performance and Robustness. *2024 International Conference on Advances in Data Engineering and Intelligent Computing Systems, ADICS 2024*. https://doi.org/10.1109/ADICS58448.2024.10533619

Vimala, B. B., Srinivasan, S., Mathivanan, S. K., Muthukumaran, V., Babu, J. C., Herencsar, N., & Vilcekova, L. (2023). Image Noise Removal in Ultrasound Breast Images Based on Hybrid Deep Learning Technique. *Sensors 2023, Vol. 23, Page 1167*, *23*(3), 1167. https://doi.org/10.3390/S23031167

Wang, Q., Zhang, L., Bertinetto, L., Hu, W., & Torr, P. H. S. (2018). Fast Online Object Tracking and Segmentation: A Unifying Approach. *Proceedings of the IEEE Computer Society Conference on Computer Vision and Pattern Recognition*, *2019-June*, 1328–1338. https://doi.org/10.1109/CVPR.2019.00142

Waskom, M. L. (2021). seaborn: statistical data visualization. *Journal of Open Source Software*, *6*(60), 3021. https://doi.org/10.21105/JOSS.03021

Wiputra, H., Chan, W. X., Foo, Y. Y., Ho, S., & Yap, C. H. (2020). Cardiac motion estimation from medical images: a regularisation framework applied on pairwise image registration displacement fields. *Scientific Reports 2020 10:1*, *10*(1), 1–14. https://doi.org/10.1038/s41598-020-75525-4

World Health Organization. (2022). Breast cancer fact sheet. In *Global Cancer Observatory*. https://gco.iarc.who.int/media/globocan/factsheets/cancers/20-breast-fact-sheet.pdf

World Health Organization. Regional Office for the Eastern Mediterranean. (2023). *Understanding the private health sector: in the occupied Palestinian territory*. https://iris.who.int/handle/10665/375666

Xue, G., Zhang, J., Wang, K., Ma, D., Chen, P., Hu, S., Yang, Z., & Liu, T. (2024). Application of YOLOv7-tiny in the detection of steel surface defects. *ACM International Conference Proceeding Series*, 718–723. https://doi.org/10.1145/3672758.3672878

Yala, A., Mikhael, P. G., Strand, F., Lin, G., Smith, K., Wan, Y. L., Lamb, L., Hughes, K., Lehman, C., & Barzilay, R. (2021). Toward robust mammography-based models for breast cancer risk. *Science Translational Medicine*, *13*(578). https://doi.org/10.1126/SCITRANSLMED.ABA4373/SUPPL_FILE/ABA4373_SM.PDF

Yap, M. H., Pons, G., Martí, J., Ganau, S., Sentís, M., Zwiggelaar, R., Davison, A. K., & Martí, R. (2018). Automated Breast Ultrasound Lesions Detection Using Convolutional Neural Networks. *IEEE Journal of Biomedical and Health Informatics*, *22*(4), 1218–1226. https://doi.org/10.1109/JBHI.2017.2731873

Yarney, J., Ohene Oti, N. O., Calys-Tagoe, B. N. L., Gyasi, R. K., Agyeman Duah, I., Akoto-Aidoo, C., McGuire, V., Hsing, J. C., Parkin, M., Tettey, Y., & Hsing, A. W. (2020). Establishing a Cancer Registry in a Resource-Constrained Region: Process Experience From Ghana. *JCO Global Oncology*, *6*, 610–616. https://doi.org/10.1200/JGO.19.00387/SUPPL_FILE/DS_JGO.19.00387.PDF

Zachiu, C., Ries, M., Ramaekers, P., Guey, J. L., Moonen, C. T. W., & De Senneville, B. D. (2017). Real-time non-rigid target tracking for ultrasound-guided clinical interventions. *Physics in Medicine & Biology*, *62*(20), 8154. https://doi.org/10.1088/1361-6560/AA8C66

Zakaria, R., Abdelmajid, H., & Zitouni, D. (2022). Deep Learning in Medical Imaging: A Review. *Applications of Machine Intelligence in Engineering*, 131–144. https://doi.org/10.1201/9781003269793-15

Zhang, Y., Cheng, H. D., Tian, J., & Huang, J. (2010). A novel speckle reduction and contrast enhancement method based on fuzzy anisotropic diffusion. *Proceedings - International Conference on Image Processing, ICIP*, 4161–4164. https://doi.org/10.1109/ICIP.2010.5649132

Zhang, Y., Wang, D., Wang, L., Qi, J., & Lu, H. (2018). *Learning regression and verification networks for long-term visual tracking*. https://arxiv.org/abs/1809.04320v2

Zheng, J., Lin, D., Gao, Z., Wang, S., He, M., & Fan, J. (2020). Deep Learning Assisted Efficient AdaBoost Algorithm for Breast Cancer Detection and Early Diagnosis. *IEEE Access*, *8*, 96946–96954. https://doi.org/10.1109/ACCESS.2020.2993536

Zhou, Y., Shi, C., Lai, B., & Jimenez, G. (2019). Contrast enhancement of medical images using a new version of the World Cup Optimization algorithm. *Quantitative Imaging in Medicine and Surgery*, *9*(9), 1528547–1521547. https://doi.org/10.21037/QIMS.2019.08.19

Zuiderveld, K. (1994). Contrast Limited Adaptive Histogram Equalization. *Graphics Gems*, 474–485. https://doi.org/10.1016/B978-0-12-336156-1.50061-6

الملخص

يشكل سرطان الثدي تحدياً صحياً كبيراً في فلسطين، حيث يمثل نحو ثلث حالات السرطان لدى النساء الفلسطينيات، مع تشخيص أكثر من نصف الحالات في مراحل متأخرة. ويزيد من تفاقم هذا التحدي النقص الحاد في أخصائيي الأشعة والتصوير الطبي، إضافة إلى ضعف البنية التحتية الرقمية والعوائق الاجتماعية والاقتصادية التي تحول دون الوصول للخدمات الصحية المتخصصة.

في ضوء هذه التحديات، يقدم هذا البحث إطاراً متكاملاً يعتمد على تقنيات التعلم العميق لتحليل صور وفيديوهات الموجات فوق الصوتية للثدي في الوقت الحقيقي، بهدف تعزيز قدرات الكشف المبكر عن سرطان الثدي بما يتناسب مع الواقع الصحي الفلسطيني. ولضمان ملاءمة النظام للبيئة المحلية، قمنا بتجميع قاعدة بيانات واسعة من مؤسستين صحيتين فلسطينيتين رائدتين: مركز دنيا لأورام النساء ومستشفى أوغستا فكتوريا، حيث شملت أكثر من 17 ألف حالة، بعضها موثق بنتائج خزعة تأكيدية.

يرتكز نظامنا المقترح على ثلاثة ابتكارات تقنية رئيسية متكاملة تشكل معاً حلاً شاملاً. بدايةً، أجرينا مقارنة منهجية لتقنيات تحسين التباين وتوصلنا إلى أن تقنية CLAHE بمعامل قطع مُحدد (قيمته 1) هي الأنسب لصور الموجات فوق الصوتية للثدي، حيث حققت نتائج متفوقة في مقاييس جودة الصورة مع زمن معالجة منخفض يناسب التطبيقات في الوقت الحقيقي. وبالاعتماد على هذه النتائج، طورنا نظام كشف آلي يستخدم خوارزميةYOLOv11-L ، والتي أثبتت كفاءتها في تحديد موقع وتصنيف الآفات المشتبه بها بدقة عالية، مع الحفاظ على سرعة معالجة مناسبة للتطبيقات السريرية. ولاستكمال منظومة التحليل، ابتكرنا نهجاً هجيناً للتتبع يجمع بين خوارزمية KCF وآلية التحقق باستخدامYOLO ، مما مكّننا من تتبع الآفات عبر مقاطع الفيديو بكفاءة عالية، محققاً معدلات نجاح تجاوزت 97% للآفات الحميدة والخبيثة على حد سواء.

وقد أكدت اختباراتنا الشاملة على مقاطع فيديو حقيقية مرفقة بنتائج خزعة تأكيدية فعالية النظام المقترح في البيئة السريرية، حيث تمكن من معالجة نحو 54 إطاراً في الثانية مع الحفاظ على دقة عالية في الكشف والتتبع. هذه النتائج المشجعة تدل على إمكانية توظيف تقنيات التعلم العميق لتحسين تفسير صور الموجات فوق الصوتية للثدي في البيئات الصحية محدودة الموارد، مما يساهم في سد الفجوة الناتجة عن نقص الخبرات الطبية المتخصصة.

تكمن أهمية هذا البحث في تقديمه حلاً عملياً لتحدي الكشف المبكر عن سرطان الثدي في فلسطين، من خلال نظام فعال حسابياً ومناسب للتطبيق السريري. علاوة على ذلك، تقدم المنهجية المتبعة في تطوير هذا النظام نموذجاً يمكن تكييفه مع تحديات صحية أخرى في بيئات مماثلة. ونأمل أن تتوسع الأبحاث المستقبلية لتشمل تطوير قدرات تتبع آفات متعددة في آنٍ واحد، واستكشاف إمكانات التحليل الثلاثي الأبعاد للموجات فوق الصوتية، إضافة إلى إجراء دراسات تحقّق سريرية أوسع نطاقاً في مراكز متعددة.